SRNS-STI-2008-00050 Revision 1

Key Words: Saltstone PA
Concrete Degradation
Concrete Properties
Saltstone Properties

Retention: Permanent

EVALUATION OF SULFATE ATTACK ON SALTSTONE VAULT CONCRETE AND SALTSTONE

SIMCO TECHNOLOGIES, INC.
PART I: FINAL REPORT

SIMCO TECHNOLOGIES, INC.
SUBCONTRACT SIMCORD08009 ORDER AC48992N (U)

Christine A. Langton

August 28, 2009

Savannah River National Laboratory
Savannah River Nuclear Solutions, LLC
Aiken, SC 29808

Prepared for the U.S. Department of Energy
Under Contract No. DE- AC09-08SR22470

SRNL
SAVANNAH RIVER NATIONAL LABORATORY
TM

DISCLAIMER

This document was prepared in conjunction with work accomplished under Contract No. DE-AC09-08SR22470 with the U.S. Department of Energy.

Printed in the United States of America

Prepared For
U.S. Department of Energy

SRNS-STI-2008-00050 Revision 1

Key Words: Saltstone PA
Concrete Degradation
Concrete Properties
Saltstone Properties

Retention: Permanent

EVALUATION OF SULFATE ATTACK ON SALTSTONE VAULT CONCRETE AND SALTSTONE

SIMCO TECHNOLOGIES, INC.
PART I: FINAL REPORT

SIMCO TECHNOLOGIES, INC.
SUBCONTRACT SIMCORD08009 ORDER AC48992N (U)

Christine A. Langton

August 28, 2009

Savannah River National Laboratory
Savannah River Nuclear Solutions, LLC
Aiken, SC 29808

Prepared for the U.S. Department of Energy
Under Contract No. DE- AC09-08SR22470

SRNL
SAVANNAH RIVER NATIONAL LABORATORY
TM

REVIEWS AND APPROVALS

Authors:

C. A. Langton, SRNL / E&CPT — 8-28-09 Date

Technical Reviewer:

G. P. Flach, SRNL / Geo-Modeling — 8/28/09 Date

SRNL Management Approvals:

H. H. Burns, Project Manager, SRNL / E&CPT — 8/31/09 Date

A. B. Barnes, Manager, SRNL / E&CPT — 09/03/09 Date

S. L. Marra, Manager, SRNL / E&CPT — Allan B. Barnes FOR S.L. MARRA 09/03/09 Date

Customer Approvals:

T. C. Robinson, SRR / WASTE DETERMINATION — for TC Robinson 09/04/09 Date

TABLE OF CONTENTS

LIST OF TABLES

LIST OF FIGURES

LIST OF ACRONYMS

ASR	Alkali Silica Reaction
ASTM	American Society for Testing & Materials
C3A	Tricalcium aluminate
cm	centimeters
C-S-H	Calcium silicate hydrate (non to poorly crystalline solid)
CV	coefficient of varience
d	Days of time
DCR	Document Control Register
E&CPT	Engineering and Chemical Process Technology
ICP	Inductively Coupled Plasma spectrometry
MCU	Modular Caustic Side Solvent Extraction Unit
Mol/L	Moles per liter
MPa	Mega Pascals
PA	Performance Assessment
pH	Measure of the hydrogen ion concentration in an aqueous solution (acidic solutions, pH from 0–6; basic solutions, pH > 7; and neutral solutions, pH = 7)
PS&E	Process Science and Engineering
Psig	Pound-force per square inch gauge (pressure relative to the surrounding atmosphere
s	Seconds
SIMCO	SIMCO Technologies, Inc.
SQRT	Square Root of Time
SRNL	Savannah River National Laboratory
SRNS	Savannah River Nuclear Solutions
SRR	Savannah River Remediation
SRS	Savannah River Site
STR	Subcontract Technical Representatives
TTR	Technical Task Request
WSRC	Washington Savannah River Company
yr	Year

BLANK PAGE

1.0 REVISION SUMMARY

Cured property measurements presented in Section 6 were updated to include one-year data. A Progress Report from SIMCO, Technologies, Inc. documenting these new data is included in Attachment 5.

Exposure testing for Vault 1 / 4 and Disposal Unit 2 concretes cured for 56 days to simulated saltstone pore solution indicated no penetration or damage to the concrete. The STADIUM® code predicted phase changes to a depth of up to 6 mm from the exposed surface, but these changes were not observed.

The surrogate data used in the model predictions for 5000 year performance were conservative compared to actual data. This indicates that for comparable sulfate concentrations in the corrosive solution, the rate of sulfate diffusion into the Vault 1 / 4 and Disposal Unit 2 concretes will be slower than that predicted in the STADIUM® simulations. (The relationships between the concentration of sulfate in 1) saltstone feed solution, 2) pore solution extracted from simulated MCU saltstone, and 3) the corrosive solution / leachate in the durability analysis in the saltstone PA are provided in SRNS-STI-2009-00447 Rev 0.)

Additional characterization of the exposed samples is necessary to identify the consequences of sulfate ingress into the exposed concrete samples. This information will be generated over the next three months. This report will be revised to include new data.

In addition, a brief discussion of possible synergistic effects due to other degradation mechanisms was added in Section 3.3.

2.0 EXECUTIVE SUMMARY

This report summarizes 1) characterization results for Saltstone Vault 1 /4 and Disposal Unit 2 concretes cured for up to 365 days at 100% relative humidity and 2) results of exposure to sulfate solutions for up to 90 days (exposure / ponding tests). A comparison of the sulfur profiles generated from the simulated and actual saltstone vault concretes indicate that the modeled results using the surrogate concrete data were conservative.

The sulfate diffusion modeling provides the following information on two concrete mixes that will be used to support the Saltstone PA:

- Relationship between the rate of advancement of the sulfate front (depth of sulfate ion penetration into the concrete) and the rate of change of the concrete permeability and diffusivity.
- Relationship between the sulfate ion concentration in the corrosive leachate and the rate of the sulfate front progression.
- Equation describing the change in hydraulic properties (hydraulic conductivity and diffusivity) as a function of sulfate ion concentration in the corrosive leachate.

These results were incorporated into the current Saltstone PA analysis (Flach, 2008).

SIMCO Technologies, Inc. prepared samples of the Saltstone Vaults 1 / 4 and Disposal Unit 2 concretes and characterized the hydraulic and physical properties of the samples after curing for up to one year at 100% relative humidity at 75°F. The results indicate that the values used in the service life predictions were conservative and that the rate of sulfate front advancement for the actual vault concrete will be less than that indicated using the surrogate property data. The modeled results were validated by 90-day chloride solution and sulfate solution exposure tests.

Simulations based on transport properties evaluated on two concrete mixtures with a water to binder ratio of 0.35 were performed to estimate the long-term durability of material exposed to saltstone waste leachate for an extended period of time. The simulations showed that the presence of sulfate in the leachate is responsible for the penetration of an ettringite front in the structure. No other sulfate-bearing minerals were predicted, including gypsum. According to the simulations, the exposure level (concentration of sulfate ions in the aggressive solution) is the parameter that has the strongest influence on the penetration kinetic.

The SIMCO modeling of sulfate penetration depth was performed for three concentrations of sulfate which were based on pore solution results for a saltstone mix characterized in early screening studies [Langton 1987]. The high sulfate concentration, 0.21 mol/L, used in the STADIUM® simulation was 1.5x higher than the concentration of sulfate in the pore solution extracted from SIMCO simulated saltstone sample, 0.14 mol/L [Langton 2009]. The boundary conditions for the STADIUM® simulations and the exposure testing were assumed to be conservative. However, pore solution results determined by SIMCO Technologies, Inc. indicate sulfate is 2.7x more concentration in the pore solution compared to the saltstone make up solution (feed solution). Additional pore solution data are required.

The effects of cracks due to the formation of ettringite cannot be taken into account in STADIUM®. The simulations thus represent an optimistic situation where ettringite actually reduces the porosity of the material and reduces the rate of ingress of sulfate. In the presence of cracks, the rate of sulfate ingress could increase depending on the nature of the crack network. Consequently, the rate of degradation could be faster than what was predicted by the model.

It was assumed that the other face of the concrete slab was exposed to pure water in the soil. According to the model, this particular boundary condition caused the decalcification of C-S-H, which could potentially affect the structural integrity of the reinforced concrete. According to the simulations, the degradation could reach 4 cm after 10,000 years of exposure.

This report also provides information in Section 3.3 on microbial degradation of concrete and the effect of radiation on the stability of concrete. The consequences of synergistic concrete degradation processes, e.g., simultaneous exposure to sulfate plus microbial attack and exposure to radiation are unknown although the effect of radiation is expected to be negligible. The consequences of synergistic concrete degradation process, e.g. simultaneous exposure to sulfate plus other chemicals, such as alkalis and hydroxide, will be obtained from the exposure testing. At this time, exposure testing has resulted in negligible damage because of the high quality of the concrete.

3.0 INTRODUCTION

3.1 Objective

The objective of this report is to provide information on the durability of the concrete vaults and disposal units used to contain the saltstone waste form. Sulfate attack resulting from exposure to sulfate ions originating in the saltstone waste form was determined to be the most aggressive form of degradation anticipated [Flach, 2008]. This report summarizes results of a durability analysis performed by SIMCO Technologies Inc. to assess the effects of sulfate attack on Saltstone Vaults 1 / 4 and Disposal Unit 2 concrete. In addition microbial degradation and radiation effects on concrete are briefly addressed.

This work was originally requested by J. L. Newman, REGULATORY INTEGRATION & BUISINESS MANAGEMENT, and T. C. Robinson Jr., WASTE DETERMINATIONS. Since initiation of this work, Savannah River Remediation (SRR) has assumed responsibility for the liquid waste operations contract at the Savannah River Site. This work was coordinated through H. H. Burns, Engineering and Chemical Process Technology / Savannah River National Laboratory (E&CPT / SRNL) and will support the Saltstone Performance Analysis (PA) Revision.

Input on concrete vault degradation required for the Saltstone PA includes:

- Relationship between the rate of advancement of the sulfate front (depth of sulfate ion penetration into the concrete) and the rate of change of the concrete permeability and diffusivity
- Relationship between the sulfate ion concentration in the corrosive leachate and the rate of the sulfate front progression.
- Equation describing the change in hydraulic properties (hydraulic conductivity and diffusivity) as a function of sulfate ion concentration in the corrosive leachate.

3.2 Approach

The STADIUM® code and data from two surrogate concretes, which are similar to the Vaults 1 / 4 and Disposal Unit 2 concretes,[1] were initially used in the preliminary durability analysis reported in SRNS-STI-2008-00050 Revision 0. Laboratory samples of the saltstone concrete vault mixes were also prepared and cured for up to one year. These samples were characterized and used in sulfate solution exposure studies to validate the modeled results. (These results are provided in this report.) The STADIUM® code was re-run using transport properties measured for the SRS Vaults 1 / 4 and Disposal Unit 2 concrete samples after SIMCO personnel completed characterization testing on samples of these materials.

Exposure testing to validate the predicted results for SRS vault concretes involved: 1) exposing samples of the two concretes to the three highly alkaline, sulfate containing solutions (compositions provided by SRNL) for several months, and then 2) characterizing the samples

[1] The surrogate concrete were selected from the SIMCO Technologies Inc. database on the basis of water to binder ratios and binder to aggregate ratios.

with respect to chemistry, mineralogy, damage as a function of distance from the solution-concrete interface. Validation of the predicted results for the surrogate concretes is complete. The long exposure times are a consequence of the high quality of the concrete used in the SRS saltstone vaults.

3.3 Background

The saltstone waste form contains high concentrations of more or less soluble sulfate and aluminate. The waste form is cast as a slurry into concrete vaults which isolate the cured waste form from the environment.[2] The performance of the waste form over the long time (10,000 years) is required for disposal of long lived radionuclides in the near surface environment.

The ability of the concrete vault to serve as a barrier between the environment (water in the environment) and source of mobile, water soluble radionuclides depends on how aging and exposure changes the permeability and water, gas and contaminant diffusivities of the concrete vault. The vaults are part of a large landfill that will be covered by an engineered barrier that will limit infiltration of water during a portion of the performance time.

A subcontract was awarded to SIMCO Technologies, Inc., to use existing expertise including a validated simulation code (STADIUM®) and characterization methodology to predict the effects of sulfate exposure (from saltstone, a cement waste form) on reinforced concrete and more specifically on SRS Saltstone Vaults 1 / 4 and Disposal Unit 2 concretes, over 10,000 years. A summary of the requirements in the Statement of Work are provided in Attachment 1 [Contract SIMCORD08009, 2008].

Results of the study will be used as input to the Saltstone Performance Assessment, which predicts transport of radionuclides from the saltstone waste form into the surrounding environment and water table.

3.3.1 Potential Synergistic Degradation Mechanisms

The effects of degradation process other than those associated with sulfate attack may also contribute to the rate and consequences of sulfate-concrete reactions. Episodic events, structural settlement or collapse will result in through wall-structure-monolith cracking. This type of cracking will impact moisture, contaminant, and corrodent (sulfate) transport. The synergistic consequences of exposure to sulfate ions under these conditions will be specific to the scenario encountered.

The consequences of synergistic concrete degradation processes, e.g., exposure to sulfate and other chemicals, such as alkali and hydroxide in saltstone, are being evaluated. Detailed concrete characterization results from extended exposure experiments currently underway at SIMCO Technologies, Inc. are in progress on samples cured for up to one year. Results will be reported in a revision to this report.

Acid leaching due to exposure to acidic soil pore water and carbonation reactions modify the pore structure of concrete. The concrete surfaces exposed to these processes are not the surfaces exposed to sulfate and alkalis. The STADIUM® simulations address this situation for the case of neutral soil pore water.

[2] Portions of the Vault 1 / 4 concrete interior surfaces are in direct contact with the saltstone. Disposal Unit 2 will have a coating between the saltstone and the vault concrete.

Two additional concrete exposure conditions, microbial degradation and exposure to radiation, are discussed below. The impacts of these mechanisms on the saltstone vault concrete degradation are unknown for long performance periods. For short term performance (50 to 100 years) the effects are expected to be negligible based on observation of the current exposed surface condition of the vaults.

Testing is recommended to determine the consequences of microbial interaction with concrete containing sulfur / sulfate and nitrate since these chemical species will be present in concrete exposed to saltstone pore solution.

3.3.1.1 Microbial Influenced Concrete Degradation

Concrete degradation due to microbial activity is thought to occur when microorganisms present in the environment produce mineral or organic acids that dissolve or disintegrate the concrete matrix [Rogers, et. al, 1993]. While the mechanism of attack is the same as that described for acid attack, some evidence exists that the presence of microorganisms greatly magnifies the intensity of attack.

Three groups of bacteria are known to destroy concrete integrity [Rogers, et. al, 1993]. Thiobacillus, sulfur-oxidizing bacteria, are most often associated with microbial deterioration of concrete structures (most often sewers). They metabolize reduced sulfur compounds and produce sulfuric acid as a waste product. Nitrobacillus, nitrifying bacteria, obtain energy required for cell synthesis by oxidizing inorganic nitrogen compounds to nitrite and nitrate. The formation of nitrite and nitrate is accompanied by the release of hydrogen ions, forming nitrous and nitric acids. Heterotrophs include a variety of fungi as well as anaerobic and aerobic bacteria that obtain energy by assimilating organic carbon sources. Many species of heterotrophs generate organic acids as metabolic byproducts, including lactic, citric, gluconic, and malic acids.

Many of these bacteria are ubiquitous in the environment and can lie dormant until favourable conditions arise for growth. *T. thiooxidans* as well as other acid producing bacteria have been isolated from soils at disposal sites for solidified low level radioactive waste (LLW) [Rogers, et. al, 1993]. Subsequent exposure of solidified LLW samples to these bacteria under favorable laboratory conditions demonstrated very rapid dissolution and contaminant release.

3.3.1.2 Radiation Stability of Concrete

Radiation can affect concrete by two mechanisms [Fillmore, 2004]:

- Breaking bonds in the paste and or aggregate that results in embrittlement.
- Localized heating of the concrete caused by absorption of radiation energy.

Low doses or radiation, $<10^{10}$ neutron/cm2 or 10^{10} GY gamma, over periods of less than 50 years have no significant effect on concrete. Longer doses have not been studied.

Since the radiation dose anticipated for the saltstone vault concrete is less than $<10^{10}$ neutron/cm2 or 10^{10} GY gamma, no synergistic effect is expected on sulfate attack.

4.0 STADIUM® MODEL and SULFATE ATTACK SIMULATION METHODOLOGY

4.1 STADIUM® Model Description

STADIUM® is a multi ionic one dimensional transport model based on a sequential split operator approach that separates ionic movement and chemical reactions. The ionic transport module in STADIUM® is based on the extended Nernst-Planck equation applied to unsaturated and non-isotherm materials. The equation accounts for electrical coupling as well as the chemical activity between ionic fluxes, transport due to water content gradient and temperature: See Equation 1.

Equation 4-1.

$$\frac{\partial(wc_i)}{\partial t} - \operatorname{div}\left(D_i w \operatorname{grad}(c_i) + \frac{D_i z_i F}{RT} w c_i \operatorname{grad}(\psi) + D_i w c_i \operatorname{grad}(\ln \gamma_i) + \frac{D_i c_i \ln(\gamma_i c_i)}{T} w \operatorname{grad}(T) + c_i D_w \operatorname{grad}(w) \right) = 0$$

Where:
- c_i = Ion concentration [mmol/L]
- w = Water content [m^3/m^3]
- D_i = Diffusion coefficient [m^2/s]
- z_i = Valence number of the ionic species *i*
- F = Faraday constant [96488.46 C/mol]
- ψ = Electrodiffusion potential [V]
- R = Ideal gas constant [8.3143 J/mol/°K]
- T = Temperature [°K]
- γ_I = Activity coefficient
- D_w = Water diffusivity [m^2/s].

For the evaluation of sulfate attack on the Saltstone vault concrete, eight ionic species were considered: OH^-, Na^+, K^+, SO_4^{2-}, Ca^{2+}, $Al(OH)_4^-$, NO_2^-, and NO_3^-. The activity coefficients used in the model were evaluated on the basis of the Harvie, Moller and Weare implementation of Pitzer's ion interaction model. Details are provided in Attachment 2 and in references supplied in Attachment 2.

The second module in STADIUM® consists of a chemical equilibrium code. Following the transport step, the chemical equilibrium module verifies equilibrium conditions between the ion concentrations in the pore solution and the solid phases of the hydrated cement paste, i.e., calcium hydroxide, calcium silicate hydrates, ettringite, and mono-sulfate phases.[3] This is done

[3] Mono-sulfate phases are calcium alumina ferrites that contain one mole of anhydrite, $CaSO_4$, in the chemical formula. Formation of Friedel's salt, a chloride-containing calcium alumina–sulfate solid phase that forms as the result of exposure of concrete to chloride, from monosulfate was modeled as an ion-exchange/substitution mechanism.

at each node of the finite element mesh. Details of are provided in Attachment 2 and in references supplied in Attachment 2.

4.2 STADIUM®® Input Parameters

The following concrete properties are required as input to the STADIUM® code:

- Porosity: Measured using ASTM C-642 standard method for concrete.
- Ionic Diffusivities: Determined by determining the tortuosity of the pore structure from data generated by a modified chloride ASTM C-1202 rapid chloride penetration test. The test method and calculations are described in SRNS-STI-2008-00052.
- Water Diffusivity: A and B coefficients in Equation 2 and the equilibrium water content are determined from a Sorption – Desorption Test described in SRNS-STI-2008-00052.

  Equation 4-2. $$D_w = A\exp(Bw)$$

  Where: D_w = Water diffusivity (nonlinear)
  w = Volumetric water content
  A = Experimentally determined parameters
  B = Experimentally determined parameter (positive)

- Initial Pore Solution Composition: Determined by extraction of pore solution under 345 MPa (50,000 psi) pressure and analyzed by ICP techniques. The solution is typically analyzed for OH^-, Na^+, K^+, SO_4^{2-}, Ca^{2+}, $Al(OH)^{-4}$. However, for the saltstone materials it will also be analyzed for NO_2^- and NO_3^-.
- Initial Mineralogy: The initial solid phases in the hydrated cement paste are estimated from the cement and admixture chemical compositions.

4.2.1 Selection of Surrogate Concrete Samples for Early Results

Two concrete mix designs similar to the Saltstone Vaults 1 / 4 and Disposal Unit 2 mixes were selected for the initial modeling effort in order to provide an early indication of the effect of sulfate exposure to the saltstone vault concrete. The surrogate concretes are similar to the actual Vaults 1 / 4 and Disposal Unit 2 concrete mixes. Consequently the surrogate data can be used in the initial SRNL PorFlow® runs required to meet the Saltstone Disposal Facility PA schedule.

STADIUM® results using data for the Saltstone Vaults 1 / 4 and Disposal Unit 2 concrete samples prepared at SIMCO Technologies, Inc., are expected to be available and will be provided in a revision to the final report due at the end of the 2009 calendar year. Due to the low porosities and permeabilities and high degree of sulfate resistance of the Saltstone Vaults 1 / 4 and Disposal Unit 2 concretes, validation of the model results is not expected for several months after the final report is issued. Validation test results will be provided as revisions to the final

report as they become available. Validation consists of exposing samples of the vault concretes to the corrosive solutions and characterizing the depth of penetration of the various chemical and mineralogical fronts in addition to other chemical and physical effects.

The mix designs for the Vaults 1 / 4 and Disposal Unit 2 concretes and the surrogate concretes are provided in Table 4-1. Oxide compositions and additional characterization data for the surrogate concrete mixes are provided in Attachment 2.

4.2.2 Compositions of Hypothetical Corrosive Solutions for Three Exposure Scenarios

Compositions for three corrosive solutions containing high concentrations of sulfate were constructed by G. Flach, M. Phifer, and M. Denham, SRNL, from potential scenarios related to leaching of the saltstone [Flach, et al., 2008.]. The bases for these high sulfate solutions are provided below:

Case 1 - Saltstone pore water, undiluted
This case is intended to be a surrogate for concrete in diffusional contact with saltstone at early times. Determine composition of saltstone pore water by analyzing water squeezed from a sufficiently cured saltstone sample. Exposure vault concrete to a simulant of this water (no dilution).

Case 2 - Saltstone pore water, diluted 10:1
This case is intended to be a surrogate for concrete in diffusional contact with saltstone at later times, after saltstone pore water near the saltstone/concrete interface has been diluted through diffusion. Same as Case 1, except that the Case 1 simulant is diluted 10:1 with a simulant of ground water that has equilibrated with vault concrete (defined below and used as a permeant in recent saltstone permeability testing, WSRC-STI-2007-00649).

Case 3 - Leached saltstone pore water at 10:1 dilution
This case is intended to be a surrogate for infiltrating soil moisture that flows through saltstone before contacting concrete.
Equilibrate ground water simulant in Case 2 with crushed saltstone at 10:1 dilution. That is, the volume of groundwater simulant should be 10x the volume of pore water in the saltstone sample assuming 60% porosity.

The pore solution extracted from a saltstone formulation cured for 28 days was used as the Case 1 (most aggressive) solution. The Case 2 and 3 solutions are 10:1 and 100:1 dilutions of the Case 1 solutions in equilibrium with $Ca(OH)_2$. The composition of saltstone pores solutions at various curing times is provided in Table 4-2. The compositions of the three hypothetical saltstone leachates used in the STADIUM® simulation to evaluate the durability of the surrogate Vaults 1 / 4 and Disposal Unit 2 concretes are provided in Table 4-3.

NOTE: The sulfate concentration in pore solution extracted from SIMCO simulated saltstone samples after curing for123 days (SO_4^{2-} = 0.14 moles/L) is lower by a factor of 1.5 than the high value used in the SIMCO Technologies, Inc. model simulations (SO_4^{2-} = 0.21 moles/L) [Langton, 2009]. Consequently the results of the exposure testing are conservative with respect to concentration of the corrosive sulfate fluid extracted from the SIMCO saltstone samples.

Table 4-1. Vault Concrete and Surrogate Concrete Mix Designs.

Ingredient	Vaults 1 / 4 Concrete (1)	Surrogate Binary Concrete	Disposal Unit 2 Concrete (2)	Surrogate Ternary Concrete
	(kg/m3) *(lbs/cu yd)*		(kg/m3) *(lbs/cu yd)*	
Cement Type I	0 *0*	276 *465*	0 *0*	0 *0*
Cement Type I/II	239 *419*	0 *0*	0 *0*	0 *0*
Cement Type V (Lehigh)	0 *0*	0 *0*	116 *201*	0 *0*
Ternary Blended Cement (3)	0 0	0 0	0 *0*	425 *716*
Slag	158 *278*	149 *251*	153 *268*	0 *0*
Silica Fume	0 *0*	0 *0*	25.5 *44.7*	Included in ternary blend
Fly Ash Class F	0 *0*	0 *0*	89 *156.3*	Included in ternary blend
Water	152 *268*	149 *251*	145 *255*	149 *251*
Coarse Aggregate ¾ in.	1025 *1798*	925 *1559*	1055 *1850*	910 *1534*
Fine Aggregate (quartz sand)	646 *1133*	815 *1374*	519 *911*	800 *1348*
Unit Weight (kg/m^3) (lbs/yd^3)	 2220 3896	 2314 *3900*	 2103 3626	 2284 *3850*
Density	2.31	2.31	2.19	2.29
Water to total cementitious material ratio	0.385	0.35	0.38	0.35

(1) Vaults 1 / 4 concrete mix design is representative of the concrete mixes for the Vault 1 and Vault 4 floor and wall concrete shown in Tables 4-5 and 4-6 of Phifer et al., 2006.

(2) Disposal Unit 2 concrete mix design is representative of the concrete mixes being proposed for the future disposal cells indicated in Table 4-7 of Phifer et al., 2006.

(3) Ternary blended cement that included a Type I portland cement equivalent (CSA Type 10).

Table 4-2 Approximate Saltstone Pore Solution Compositions [Langton, 1987].

(mg/L)	7d	28d	56d	90d
AlO_2^-	17.7	6.3	26.9	1.33
Ca^{+2}	9.0	29	94.6	92.05
Fe^{+3}*	1.6	3.5	1.74	2.21
K^+	6,000	7,000	7,400	6,500
Mg^{+2}*	0.1	1.2	11.5	1.96
Na^+	77,000	85,000	91,000	60,000
SiO_3^{-2}*	203.6	230.7	169.6	76.6
CO_3^{-2}	800	1,000	675	736.5
Cl^-	1170	1380	661	739
NO_2^-	42,000	43,000	33,800	27,000
PO_4^{-3}	<150	<150	<150	<150
NO_3^-	175,000	205,000	177,000	122,700
SO_4^{-2}	26,000	25,000	25,500	24,000
OH^-[a]	14,258	16,315	227	3,794
pH	13.8	13.98	12.13	13.3

a = Calculated values.

Table 4-3. Saltstone Leachate Compositions Used for the STADIUM®® Simulations.[4] (Boundary conditions at *x*=0)

Ionic species	Concentrations (mmol/L)		
	High level	Mid level	Low level
OH^-	769.0	76.9	7.69
Na^+	4366.0	436.6	43.66
K^+	215.0	21.5	2.15
SO_4^{2-}	208.0	20.8	2.08
Ca^{2+}	1.0	0.1	0.01
NO_3^-	2649.0	264.9	26.49
NO_2^-	749.0	74.9	7.49

[4] The concentrations listed in Table 4-2 are about 20 % lower than the concentrations in the pore solution extracted from a cement - slag – fly ash samples cured for 28 days [Langton, 1987]. Since the concentrations decrease with curing time, this discrepancy is not expected to inpact the overall conclusions.

4.2.3 Equilibrium Mineral Assemblages

The hydrated mineral assemblage considered in the durability analysis for the surrogate concretes exposed to the Case 1 corrosive solution (saltstone pore solution) is shown in Table 4-4. For the simulations it was assumed that the NO_3^- and NO_2^- did not react with other species to form additional phases or solid solutions. A more detailed discussion of the equilibrium mineral assemblage is provided in Attachment 2.

Table 4-4. Mineral Phases Considered for the Calculations

Minerals	Composition	log(*K*) @ 25°C
Portlandite	$Ca(OH)_2$	-5.15
C-S-H (portlandite fraction)	$Ca(OH)_2$	-6.2
Monosulfates	$3CaO.Al_2O_3.CaSO_4.12H_2O$	-29.4
Ettringite	$3CaO.Al_2O_3.3CaSO_4.26H_2O$	-44.0
Glauberite	$Na_2Ca(SO_4)_2$	-5.18
Gypsum	$CaSO_4.2H_2O$	-4.58
Mirabilite	Na2SO4.10H2O	-1.4
Syngenite	$K_2Ca(SO_4)_2.H_2O$	-7.45
Glaserite	$NaK_3(SO_4)_2$	-3.8

4.3 Saltstone Vaults 1 / 4 and Disposal Unit 2 Service Life Simulations

Service life simulations were performed on a 1-D case illustrated in Figure 4-1 using the STADIUM® code. The simulations were performed using a 90 element finite element mesh for a 20 cm thick slab (L = 20 cm, Disposal Unit 2 concrete was assumed to be 20 cm thick) and 154 elements for a 46 cm slab (L = 46 cm, Vaults 1 / 4 concrete was assumed to be 46 cm thick) and were refined near the domain boundaries.

The time steps were increased progressively to reduce the calculation time. Details are provided in Attachment 2. The temperature was set at 15°C and the concrete was assumed to be saturated with the water content at x = 0. The volume of water in the concrete corresponded to the volume of pores (porosity) that transmits fluid. The concrete surface at the concrete-corrosive solution interface was assumed to always be saturated. The concrete surface in contact with the soil (x = L cm) was assumed to be at 100 % relative humidity. This boundary condition corresponds to saturated concrete with water content equal to the porosity of the concrete.

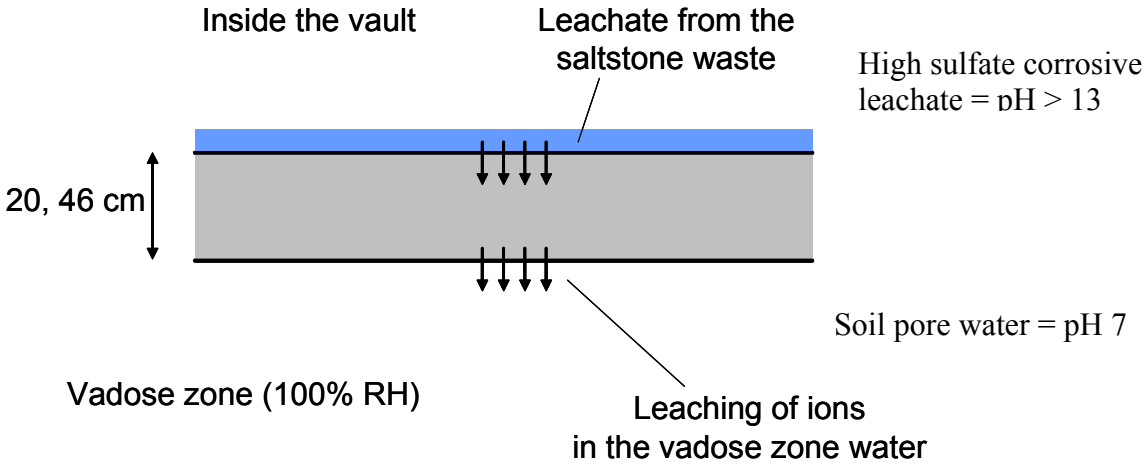

Figure 4-1. Simulation Case for Surrogate Vault Concretes.

5.0 SALTSTONE VAULT CONCRETE SERVICE LIFE PREDICTIONS

5.1 Simulation Results for Disposal Unit 2 Concrete Exposed to Case 2 Corrosive Solution

The surrogate Disposal Unit 2 concrete (20 cm thick) exposed to the Case 2 corrosive solution (10:1 dilution of the saltstone pores solution) was used to illustrate the STADIUM®® out put for a 2000 year exposure simulation. The concentrations of eight ionic species in the pore solution as a function of position in the sample (penetration depth) are plotted after 2000 years exposure. See Figure 5-1. The corresponding solid phases in equilibrium with the calculated pore solutions were also calculated and plotted in Figure 5-2.

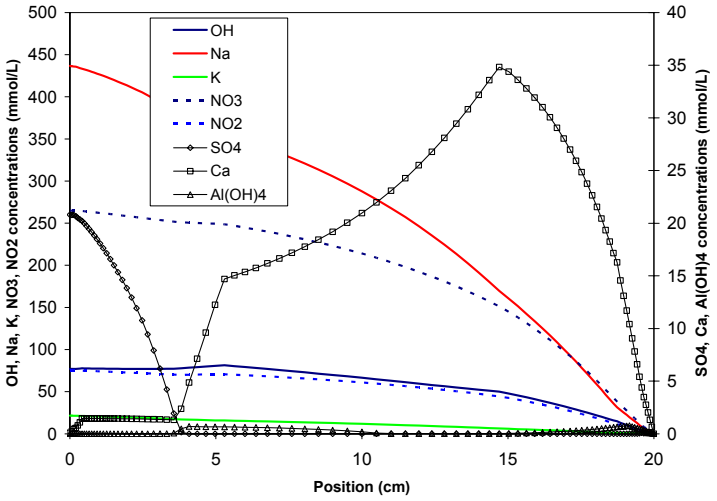

Figure 5-1. Ionic Species in the Pore solution for the Surrogate Disposal Unit 2 Concrete after Exposure to Case 2 Corrosive Solution for 2000 years.

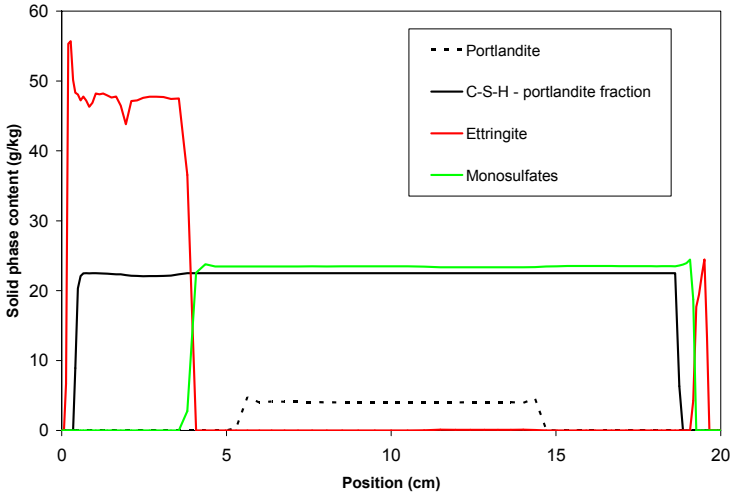

Figure 5-2. Solid phases in the Hydrated Cement Paste for the Surrogate Disposal Unit 2 Concrete after Exposure to Case 2 Corrosive Solution for 2000 Years.

Simulation results presented in Figures 5-1 and 5-2 that pertain to the corrosive leachate – concrete interface can be summarized as follows:

- Ettringite formation begins at the surface exposed to the corrosive high sulfate leachate.
- Since ettringite formation also requires additional calcium, portlandite initially present in the concrete paste will dissolve as the ettringite is formed.
- However, the high pH, (high OH^-) and high concentration of sulfate in the corrosive leachate at the leachate – concrete interface limits decalcification of the poorly crystalline calcium silicate hydrate phase, C-S-H. (This condition is outside the conditions encountered in typical sulfate attack.)
- Ettringite is the only sulfate containing phase predicted to form. Gypsum is not predicted as an equilibrium phase in the highly alkaline pore solution predicted for the exposed concrete.[5]
- The rate at which the ettringite front progresses depends on the transport properties of the material and on the initial amount of hydrated monosulfate phase (source of aluminate) in the cement paste since ettringite formation requires dissolution of monosulfate (assuming no other source of aluminate.)
- For concretes with comparable transport properties, the ettringite front will penetrate the concrete more rapidly for a cement paste with a lower tricalcium aluminate (C3A) content compared to a concrete with a paste with a higher C3A content.

Simulation results pertaining to the soil – concrete interface can be summarized as follows:

- A dissolution front progresses from the concrete surface in contact with the vadose zone soil inward toward the advancing ettringite front.
- The rate of decalcification is controlled primarily by the transport properties.
- A small ettringite peak is predicted in front of the C-S-H front due to the release of calcium and sulfate in the pore solution upon D-S-H decalcification and monosulfate dissolution.

---

[5] The influence of gypsum formation on the damage caused by sulfate attack is controversial but important. Formation of gypsum as the result of incongruent dissolution of C-S-H is reported to weaken the matrix and contribute to the damaging effects of ettringite formation, i.e., expansion that leads to cracking.

A consequence of the absence of gypsum in the exposed material is that the amount of sulfur bound in the hydrated paste is independent of the external sulfate concentration because the amount of ettringite (g/kg of concrete) is limited by the amount of alumina present in the material. Consequently, the sulfate concentration in a corrosive leachate will only influence the rate of advancement of the ettringite front.

5.2 Simulations Over 10,000 Years

Plots of the progression of the ettringite fronts as a function of time are presented in Figure 5-3 for the two surrogate vault concretes and the three corrosive leachate solutions. The progression is from the corrosive leachate – concrete contact into the concrete. The results of these simulations can be summarized as follows:

- The rate of advancement of the ettringite front depends on the concentration of sulfate in the corrosive solution in contact with the concrete.
- Small differences in material properties do not significantly affect the rate of the ettringite front advancement.
- If the exposure conditions are continuous over the service life of the Disposal Unit 2 (20 cm thick), the ettringite front will completely penetrate the walls in about 5000 years for the Case 1 corrosive solution. The reduction in advancement of the ettringite front after 5000 + years is due to the interaction of this front with the decalcification front advancing from the opposite direction (soil-concrete interface).
- If microcracks form as the ettringite front advances, the rate of ingress of the ettringite front will increase.

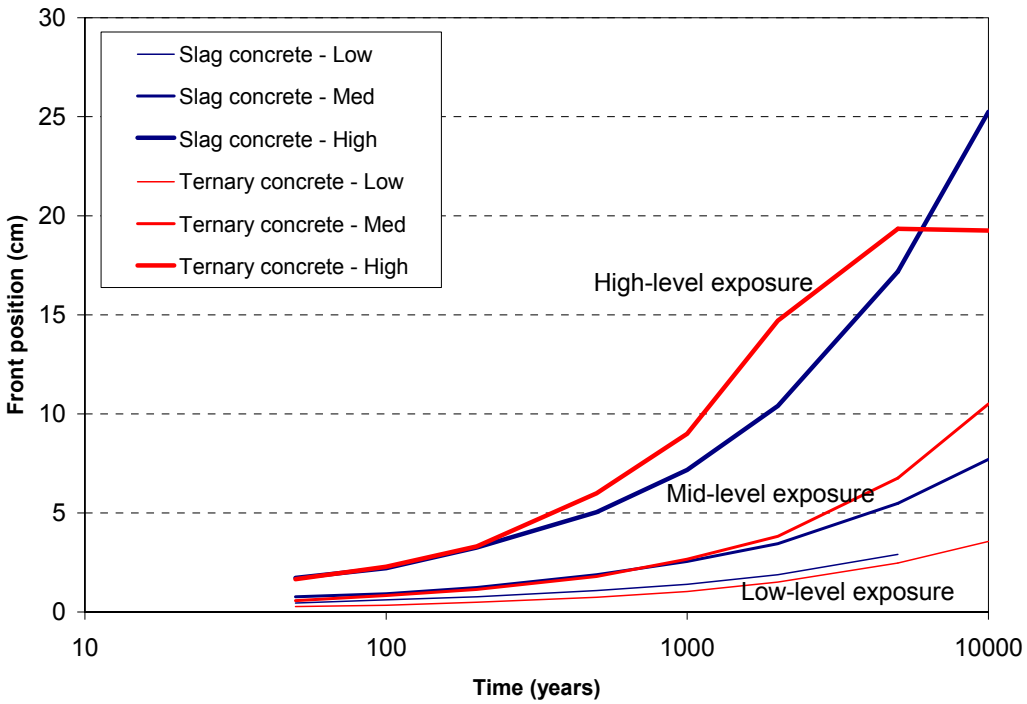

Figure 5-3. Simulated Progression of the Ettringite Front as a Function of Time.

Plots of the advancement of the decalcification fronts as a function of time are presented in Figure 5-4 for the two surrogate vault concretes and the three corrosive leachate solutions. The progression of the decalcification front is from the soil – concrete interface into the concrete). The results of these simulations can be summarized as follows:

- For the first 500 years, the rates of decalcification for the six cases are similar.
- After about 500 years, the penetration of OH^- from the advancing corrosive leachate front on the other side of the element tends to slow the decalcification process.
- Consequently the advancement of the decalcification front is lessened for the cases exposed to the most corrosive alkaline, sulfate leachates on the opposite side.
- The STADIUM® code predicts that the decalcified degraded zone should not exceed 4 cm after 10,000 years.

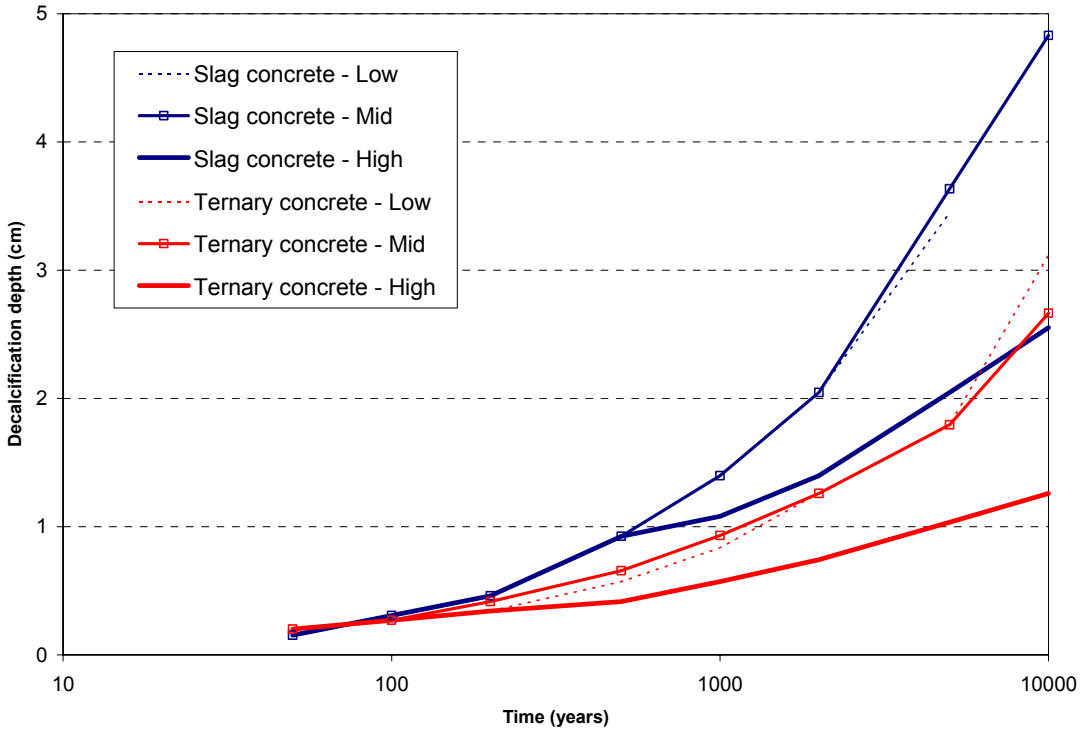

Figure 5-4. Progression of the Decalcification Front from the Soil – Concrete Interface.

5.3 Discussion of Concrete Damage Mechanisms Based on Simulated Results

For the concrete at the soil – concrete interface, decalcification of the C-S-H resulted in a calculated increase in porosity from 10 volume percent to 15 volume percent which results in doubling the rate of degradation of the material at this interface.

Ettringite is the only sulfate phase predicted to form at the concrete – corrosive solution interface. This is due to the high pH of the corrosive leachate solutions. Lack of a gypsum front between the ettringite front and the exposed surface is atypical. This finding is significant because the gypsum – decalcified C-S-H – calcium hydroxide absent zone is where the cracks, associated with sulfate attack, are formed. (Replacement of C-S-H by gypsum is known to weaken the matrix and make it more vulnerable to cracking parallel to the exposed surface caused by expansive reactions.)

The simulation results account for dissolution and precipitation of phases which locally modifies the porosity of the material and thereby affects the transport properties. In the absence of cracking, the formation of ettringite will reduce the porosity. However, if cracking does occur, the rate of advancement for the ettringite will increase.

Although considerable research has been done on damage associated with sulfate attack, little work has been performed under controlled conditions relevant to the cases analyzed. Related research work at SIMCO Technologies, Inc. has shown that micro cracks (less than about 100μm) have little effect (about a 50 % increase) on diffusion and drying rates (related to moisture diffusivity). Macro cracks (greater than about 100μm) in concrete result in saturated diffusion coefficients corresponding to those reported for free water which represents about a 50 times increase.

Observations are required to determine how exposure to highly alkaline high sulfate solutions affects the saltstone vault concrete. The approach to more completely addressing damage under the conditions provided for this study is to perform exposure tests to validate the model and characterize the consequences of exposure with respect to cracking and porosity.

6.0 VAULTS 1 / 4 and DISPOSAL UNIT 2 CONCRETE PROPERTIES

Saltstone Vault 1 / 4 and Disposal Unit 2 concrete properties were measured on samples prepared and cured by SIMCO Technologies Inc. for up to one year. Results are presented in Table 6-1 and Table 6-2. The Vault 1 / 4 concrete gained 92.8% of the 365 day strength at 28 days. The Disposal Unit 2 concrete gained 75% of the 365 day strength after curing for 28 days at 100 % relative humidity.

The porosity of the Vault 1 / 4 concrete ranged from 10.0 to 10.5 for measurements taken at 28, 91, and 365 days per the ASTM C 642 method. Porosity measurements for the Disposal Unit 2 concrete samples increased from 10.3 to 10.6 to 13.1 for samples cured 28, 91, and 365 days, respectively.

Porosities were also determined on thin samples using the SIMCO desorption / adsorption test methodology. This method produces higher porosities than those estimated by ASTM C 642. The values determined using the desorption / adsorption method for the Vault 1 / 4 concrete and Disposal Unit 2 concrete were 12 and 13 volume percent, respectively.

Intrinsic diffusion coefficients as a function of curing time up to 365 days are listed in Table 6-1 and were determined for the two concrete mixes using the SIMCO migration test which is an extension / modification of ASTM C1202: Standard Test Method for Electrical Indication of Concrete's Ability to Resist Chloride Ion Penetration. For comparison, the saturated effective diffusion coefficient value used in the Saltstone PA for all ions is 5E-08 cm^2/s.[6]

Table 6-1. Intrinsic Diffusion Coefficients as a Function of Curing Time for Saltstone Vault 1 / 4 Concrete and Disposal Unit 2 Concrete.

Species	Diffusion coefficients (E-11 m^2/s)					
	Saltstone Vault 1/4			Saltstone Vault 2		
	28d	91d	365d	28d	91d	365d
OH^-	3.63	3.71	3.50	1.40	1.20	0.40
Na^+	0.92	0.94	0.89	0.35	0.30	0.10
K^+	1.35	1.38	1.30	0.52	0.45	0.15
SO_4^{2-}	0.73	0.75	0.71	0.28	0.24	0.08
Ca^{2+}	0.55	0.56	0.53	0.21	0.18	0.06
$Al(OH)_4^-$	0.37	0.38	0.36	0.14	0.12	0.06
Cl^-	1.40	1.43	1.35	0.54	0.46	0.15

[6] The Savannah River Site PA and the key supporting documents, such as WSRC-TR-2006-00198, refer to the free / molecular ion diffusion coefficient divided by the tortuosity as an effective diffusion coefficient rather that using the intrinsic diffusion coefficient terminology used by SIMCO Technologies, Inc. Authors of SRNL reports related to PAs, such as WSRC-STI-2006-00198, apply the term intrinsic diffusion coefficient to the free / molecular ion diffusion coefficient divided the tortuosity and multiplied by porosity.

The ASTM C1202 test was used to determine the tortuosity. The tortuosity values for each concrete were then used to calculate the intrinsic diffusion coefficient for each ion of interest using Equation 6-1.

Equation 6-1. $$D_i = \tau^s D_i^o$$

Where: D_i = Intrinsic diffusion coefficient of species *i*
τ^s = Intrinsic tortuosity of the material
D_i^0 = Diffusion coefficient of the i^{th} *species* in free water

For the Vault 1 / 4 concrete samples, the tortuosity and hence the intrinsic diffusion coefficient for each ion are relatively constant for samples cured between 28 and 365 day. In contrast, the tortuosity and hence the diffusion coefficients for the disposal unit 2 concrete sample decrease by about 14% between 28 and 91 days and by about 67% between 91 and 365. The change in tortuosity was attributed to continued hydration of the Disposal Unit 2 mix stored at 100 % relative humidity over the one year period.[7]

Moisture (water) diffusivities were also determined for the two concrete mixes and were based on drying test results. (Equation 6-2) Water loss was modeled according to Richards' model (Equation 6-3) by adjusting *A* and *B* to reproduce the measured mass loss during the drying test. Values for water diffusivity D_w, A and B are listed in Table 6-2.

Equation 6-2. $$D_w = Ae^{Bw}$$

Where: D_w = nonlinear water diffusivity parameter (m^2/s)
w = volumetric water content (m^3/m^3)
A = experimentally determined (m^2/s)
B = experimentally determined (-)

Equation 6-3. $$\frac{\partial w}{\partial t} - \operatorname{div}\left(Ae^{Bw}\operatorname{grad}(w)\right) = 0$$

Where: w = water content (m^3/m^3)
t = *time (s)*
A = (m^2/s)
B = (-)

[7] Changes in the tortuosity / microstructure as a result of the degree of hydration as a function of time are accounted for in the STADIUM®® code.

At saturation, the moisture diffusivity values for the Vault 1 / 4 concrete and the Disposal Unit 2 concrete were similar, which indicates similar resistances to drying and water ingress. Drying test results were also used to estimate the intrinsic permeabilities of both concrete mixes. The mass loss profiles were reproduced using a moisture transport model that accounted for both liquid water and water vapor transport using Darcy's Law and Fick's Law respectively. Details of the calculation are provided in the SIMCO report in Attachment 1 Section 4.5.

Table 6-2. Summary of Physical and Transport Properties of Saltstone Vault 1 / 4 and Disposal Unit 2 Concretes Determined by SIMCO Technologies Inc.

Property (units)	Vault 1 / 4 Concrete	Vault 1 / 4 Concrete [Dixon, 2008]	Disposal Unit 2 Concrete	Disposal Unit 2 Concrete [Dixon, 2008]
Compressive Strength				
7d (MPa)	32.1	--	20.1	--
28d	59.8	60.1	35.2	51.2
91d	63.3	64.9	47.2	60.0
365d	64.4	--	47.0	--
7d (psi)	4656	--	2915	--
28d	8673	8720	5105	7430
91d	9181	9420	6845	9285
365d	9340	--	6817	--
Porosity (vol. %) (ASTM C 642)				
28d	10.0	18.1	10.3	18.4
91d	10.5		10.6	
365d	10.0		13.1	
Porosity by Sorption/Desorption (vol. %) 28d	12	--	13	--
Tortuosity (-)				
28d	0.0069	--	0.0027	--
91d	0.0070	--	0.0023	--
365d	0.0066	--	0.00076	--
Moisture Diffusivity at 28 days, 100 Saturation (m^2/s)	1.4E-10	--	1.1E-10	--
Water Permeability (m^2)	5.0E-22	--	18.0E-22	--
Saturated Hydraulic Conductivity (cm/s)	5.5E-13	1.0E-10	2.0E-12	1.0E-10
A* (10^{-14} m^2/s)	0.02	**	1.20	**
B* (-)	112.0	**	67.6	**

* Parameters in Richards' model (Equation 6-2). ** Parameters were measured but for a different equation [Dixon, 2008].

6.1 Comparison of SIMCO Saltstone Concrete Results to SIMCO Surrogate Data

A comparison between compressive strength and density values obtained from samples of the saltstone vault concretes and the surrogate concrete samples used in the STADIUM® sulfate diffusion simulations are provided in Table 6-3. The surrogate Vault 1 / 4 concrete contained cement and slag in the binder. The surrogate Disposal Unit 2 concrete mix contained cement, fly ash, and silica fume. (Slag was not an ingredient in the surrogate Disposal Unit 2 mix but the water to cementitious ratio was comparable to the Disposal Unit 2 concrete.)

Comparisons of porosity, water diffusivity, tortuosity, and intrinsic diffusivity data for saltstone vault concrete obtained from samples cured for 28 days and the surrogate concretes used in the STADIUM® sulfate diffusion simulations are also provided in Table 6-3 and Table 6-4. The results obtained for the saltstone concrete samples are in reasonable enough agreement with the surrogate concretes to justify use of the surrogate data in the STADIUM® simulations.

Table 6-3. Compressive Strength of Saltstone Vault Concretes at 7 and 28 days.

Cure Time (days)	Properties	Saltstone Vault 1/4			Saltstone Disposal Unit 2		
		Actual		Surrogate	Actual		Surrogate
		average	CV (%)		Average	CV (%)	
7	f_c comp. strength (MPa) (psi)	32.1 4650	13	42.7 6190	20.1(*) 2915	4.5	41.6 6030
	Density (kg/m^3) (lb/ft^3)	2380 148	0.5	-	2250(1) 140	0.7	-
28	f_c comp. strength (MPa) (psi)	59.8 8,670	3.8	54.0 7830	35.2 5,102	2.8	56.7 8220
	Density (kg/m^3) (lb/ft^3)	2,390 149	0.1	-	2,250 140	1.0	-
90	f_c comp. strength (MPa) (psi)	63.3 9,181	15.8	65.3 9,471	47.2 6,846	2.8	62.1 9,007
	Density (kg/m^3) (lb/ft^3)	2,400 150	0.18	-	2,240 140	0.16	-
365	f_c comp. strength (MPa) (psi)	64.4 9,340	4.5	65.7 9,529	47.0 6817	4.8	66.5 9,645
	Density (kg/m^3) (lb/ft^3)	2,395 150	0.27	-	2,240 140	0.28	-

(*) measured at 8 days

Table 6-4. Transport Properties for Saltstone Vault Concretes at 28 Days.

	Saltstone Vaults 1 / 4		Saltstone Disposal Unit 2	
Parameter	**Actual**	**Surrogate**	**Actual**	**Surrogate**
Porosity (%)	10.0	10.0	10.3	10.2
Effective Diffusion Coefficients* (10^{-11} m^2/s)				
OH^-	5.5	13.0	1.3	4.0
Na^+	1.4	3.3	0.3	1.0
K^+	2.0	4.8	0.5	1.5
SO_4^{2+}	1.1	2.6	0.3	0.8
Ca^{2+}	0.8	2.0	0.2	0.6
$Al(OH)_4$	0.6	1.3	0.1	0.4
NO_3	1.9	4.7	0.4	1.4
NO_2	1.9	4.7	0.4	1.4
Water diffusivity (10^{-10} m^2/s)	1.4		1.1	
A (10^{-13} m^2/s)	0.2	4.3	12.0	1.0
B (-)	112.0	80	67.6	80
w @ 50%RH (m^3/m^3)	N/A	0.059	N/A	0.064

* $D_{effective} = D_{molec\ in\ water} \div$ Tortuosity
$D_{intrinsic} = (D_{effective})$(Porosity)

7.0 TRANSPORT PROPERTY VALIDATION

A series of immersion tests were performed in which samples of the saltstone vault concretes cured for 56 days were exposed to the following solutions for 90 days:

- pH 10.5, 0.5N NaCl solution and
- 3 solution that simulate saltstone pore solution with pHs equal to or greater than 14
  - Case 1: Simulated saltstone pore solutions
  - Case 2: Simulated saltstone pore solution diluted 10:1 with a saturated calcium hydroxide solution and
  - Case 3: Simujlated saltstone pore solution diluted 100:1 with saturated calciumhydroxide solution.

Samples were periodically removed from the solutions and analyzed for chloride and sulfur, respectively using a procedure similar to the ASTM C 1152 method. (The solutions were not renewed during the exposure period.)

Both concretes exposed to the NaCl solution exhibited low chloride penetration. The disposal unit 2 had a slower chloride ingress rate that the Vault 1 / 4 concrete. However, the Vault 1 / 4 concrete exhibited about twice the chloride binding capacity than the Disposal Unit 2 concrete, 6 versus 3 g/kg, respectively. This difference is due to the higher amount of monosulfoaluminate phase in the Vault 1 / 4 binder which exchanges with sulfate in the monosulfate phases and forms Friedel's salt, $Ca_2Al(OH)_6(Cl, OH) \cdot 2\ H_2O$.[8] The Vault 1 / 4 concrete also has other calcium alumnate hydrate phases that react with chloride to form Friedel's salt.

Both concretes exposed to the high pH high to medium sulfate saltstone pore solutions exhibited no or negligable sulfate ingress. This result is surprising for the 100 % saltstone pore solution and 10:1 diluted pore solution exposure conditions. The sulfate profiles as a function of distance from the exposed surfaces are flat and the total sulfur content corresponds to the approximate amount of SO_3 in the unhydrated binder. Longer exposure periods are required to determine a sulfate ingress rate for both saltstone vault concrete samples.

7.1 STADIUM® Simulations of the Chloride Exposure Experiments

STADIUM® simulation results for chloride penetration of the Saltstone Vault 1 / 4 and Disposal Unit 2 concretes are shown in Figures 7-1 and 7-2. In both cases, the STADIUM® simulation matched the chloride binding in the concrete (paste) by reproducing the measured chloride contents near the exposed surfaces of the samples. For both materials the model predictions were slightly behind the measured chloride profiles which is probably due to underestimation of the transport properties of the concretes. Longer term exposure testing is required to obtain additional data to support the transport parameter estimates.

[8] Friedel's salt in cement notation = $3CaO{\cdot}Al_2O_3{\cdot}CaCl_2 \cdot 10\ H_2O$.

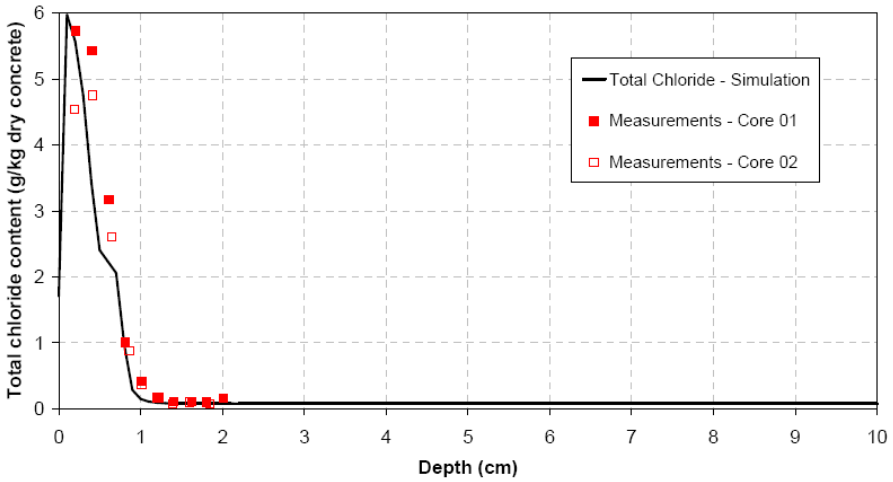

Figure 7-1. Chloride Penetration Results and Simulation Results for Vault 1 / 4 Concrete.

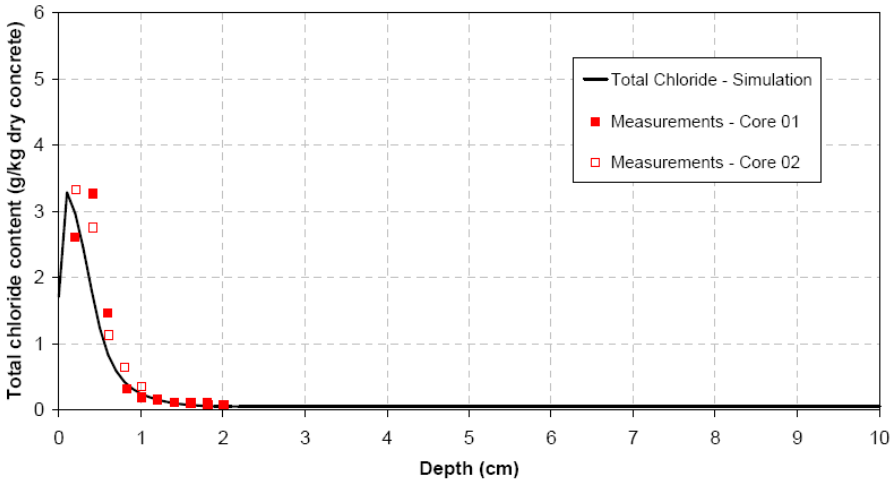

Figure 7-2. Chloride Penetration Results and Simulation Results for Disposal Unit 2 Concrete.

7.2 Simulations of High pH, High Sulfate Pore Solution Exposure Experiments

Simulation results for sulfur as a function of penetration are compared to the experimentally determined profiles for Saltstone Vault 1 / 4 concrete in Figure 7-3. STADIUM® predicts an increase in the level of sulfur between the surface and 6 mm for Case 1, exposure to undiluted saltstone pore solution. This increase was not observed in the exposed samples. For Cases 1 and 2 (10:1 dilution with saturated calcium hydroxide solution) the simulation predicted an ettringite peak near the surface which was not observed in the actual samples. It is possible that the sulfur peak near the surface is too narrow to detect at the short exposure times. Longer exposure could validate the STADIUM® prediction.

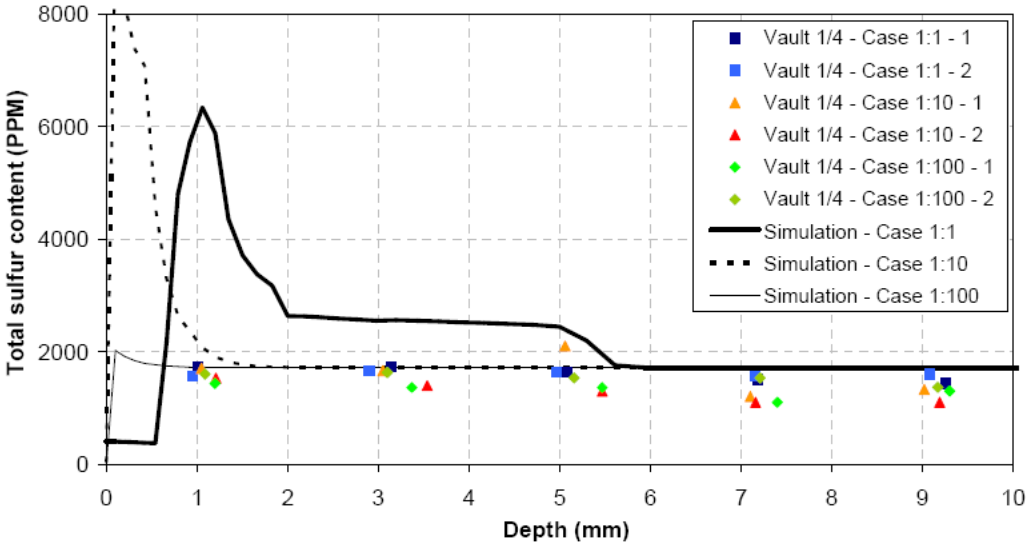

Figure 7-3. Comparison between STADIUM® Simulated and Measured Sulfur Profiles for Vault 1 / 4 Concrete.

Similar results were obtained for the Disposal Unit 2 concrete simulations and actual observations. This is illustrated in Figure 7-4

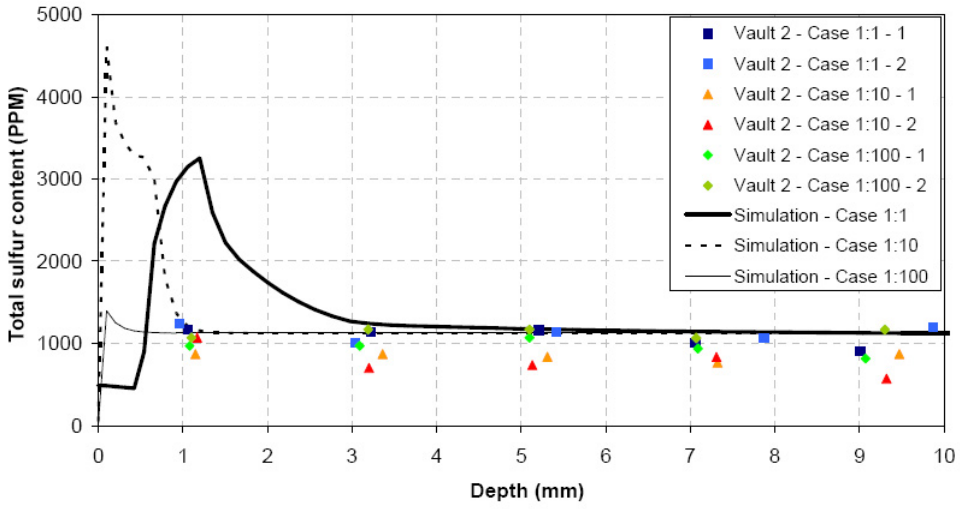

Figure 7-4. Comparison between STADIUM® Simulated and Measured Sulfur Profiles for Disposal Unit 2 Concrete.

8.0 CONCLUSIONS AND RECOMMENDATIONS

STADIUM® simulation results on the durability of Saltstone Vault 1 /4 and Disposal Unit 2 concretes exposed to three corrosive alkaline solutions containing high concentrations of sulfate are summarized in this report. SIMCO Technologies, Inc. used properties from surrogate concretes with similar to the saltstone vault concretes to parameterize their code. Physical, hydraulic, and chemical properties of Saltstone Vault 1 / 4 and Disposal Unit 2 concrete samples cured for up to 365 days were also measured by SIMCO Technologies, Inc. and will be used to update the simulations and predictions. These results will be reported in a revision to this document.

Simulations based on transport properties evaluated on two concrete mixtures with a water to binder ratio of 0.35 were performed to estimate the long-term durability of material exposed to saltstone waste leachate for an extended period of time. The simulations showed that the presence of sulfate in the leachate is responsible for the penetration of an ettringite front in the structure. No other sulfate-bearing minerals were predicted, including gypsum. According to the simulations, the exposure level (concentration of sulfate ions in the aggressive solution) is the parameter that has the strongest influence on the penetration kinetic.

The SIMCO modeling of sulfate penetration depth was performed for three concentrations of sulfate which were based on pore solution results for a saltstone mix characterized in early screening studies [Langton 1987]. The high sulfate concentration, 0.21 mol/L, used in the STADIUM® simulation was 1.5x higher than the concentration of sulfate in the pore solution extracted from SIMCO simulated saltstone sample, 0.14 mol/L [Langton 2009]. The boundary conditions for the STADIUM® simulations and the exposure testing were assumed to be conservative. However, pore solution results determined by SIMCO Technologies, Inc. indicate sulfate is 2.7x more concentration in the pore solution compared to the saltstone make up solution (feed solution). Additional pore solution data are required.

The effects of cracks due to the formation of ettringite cannot be taken into account in STADIUM®. The simulations thus represent an optimistic situation where ettringite actually reduces the porosity of the material and reduces the rate of ingress of sulfate. In the presence of cracks, the rate of sulfate ingress could increase depending on the nature of the crack network. Consequently, the rate of degradation could be faster than what was predicted by the model.

It was assumed that the other face of the concrete slab was exposed to pure water in the soil. According to the model, this particular boundary condition caused the decalcification of C-S-H, which could potentially affect the structural integrity of the reinforced concrete. According to the simulations, the degradation could reach 4 cm after 10,000 years of exposure.

The consequences of synergistic concrete degradation processes, e.g., simultaneous exposure to sulfate plus microbial attack and exposure to radiation are unknown although the effect of radiation is expected to be negligible. The consequences of synergistic concrete degradation process, e.g. simultaneous exposure to sulfate plus other chemicals, such as alkalis and hydroxide, will be obtained from the exposure testing. At this time, exposure testing has resulted in negligible damage because of the high quality of the concrete.

9.0 REFERENCES

Burns, H. H. 2008. "Program Plan for the Science and Modeling Tasks in Support of the Z-Area Saltstone Disposal facility Performance Assessment (U)," SRNL-ECP-2008-00001 Rev. 0, Washington Savannah River Company, Savannah River National Laboratory, Savannah River Site, Aiken, SC 29808.

Contract No. SIMCORD08009, Order No. AC48992N, "Saltstone Vault Sulfate Attack and Saltstone Durability," SIMCO Technologies, Inc., 2008.

Dixon, K. L., J. Harbour, M. Phifer, 2008. Hydraulic and Physical Properties of Saltstone Grouts and Vault Concretes," SRNS-STI-2008-00042, Rev. 0, Savannah River Nuclear Solutions, LLC, Savannah River Site, Aiken, SC, 29808.

Flach G. P., 2008. Personal Communication August 2008.

Flach, G. P., M. A. Phifer, and M. E. Denham, Jr., 2008. Personal communication, March 2008.

Langton, C. A., 2009. "Saltstone Matrix Characterization and STADIUM Simulation Results, SIMCO Technologies Inc., Task 6 Report." SRNL, STI, 2009-00477, Savannah River National Laboratory, Savannah River Site, Aiken, SC, 29808.

Langton, C. A., 1987. Analysis of Saltstone Pore Solutions - PSU Progress Report IV, DPST-87-530, July 7, 1987, E. I. du Pont de Nemours and Company, Aiken, South Carolina, 29808.

Phifer, M. A., Millings, M. R., and G. P. Flach, 2006. "Hydraulic Property Data Package for the E-Area and Z-Area Soils, Cementitious Materials, and Waste Zones," WSRC-STI-2006-00198, September 2006, Washington Savannah River Company, Savannah River Site, Aiken, SC, 29808.

BLANK PAGE

10.0ATTACHMENT 1

Summary of Subcontract No. AC 48992N Work Requirements

BLANK PAGE

SUBCONTRACT No. AC 48992N WORK REQUIREMENTS

Task Descriptions

Task 1. Preliminary estimate of service life.

Predict degradation using literature data for concrete properties using mixes similar to the WSRC mixes or actual data supplied by SRNL for exposure to up to three (3) different corrodent solutions as specified by the STR at a later date.

Use STADIUM® and/or other modeling capabilities to predict the depth of penetration (diffusion front) of corrodents, including sulfate, aluminate, chloride, sodium, etc., in 2 different concretes exposed to 3 different solutions for extended time (up to 10,000 years):

a. Estimates values for the important parameters from data provided by SRNL and by analogy to similar materials previously tested by SIMCO, Inc.
b. Run the STADIUM® code for a rough estimate of depth of penetration.
c. Estimate service life taking into consideration penetration depth, formation of expansive phases, and consequence of formation of expansive phases including effect of reinforcement and post tensioning steel.
d. Estimate the effective transport properties (effective permeability, effective diffusivity coefficient, effective porosity, etc.), according to in-house protocol in addition to providing an estimate assuming the concrete is fully degraded behind the advancing front and intact (not degraded) ahead of the front with respect to computing effective transport properties – if the two approaches are different.

Task 2. Measure relevant properties for SRS mixes.

Measure parameters for 2 concrete mix designs (on samples cured for 28 and/or 90 days) required to support STADIUM® and/or other service life prediction modeling. Up to two (2) different curing times may be requested by the STR.

Task 3. Estimate for SRS mixes.

Run STADIUM® using data on SRS mixes. Predict depth of penetration of the corrodent species using data generated in 3.1.2 for the 2 concrete mix designs.

Estimate the effective transport properties (effective permeability, effective diffusivity, effective porosity, etc.), according to in-house protocol in addition to providing an estimate assuming the concrete is fully degraded behind the advancing front and intact (not degraded) ahead of the front with respect to computing effective transport properties – if the two approaches are different.

Task 4. Confirm short term predictions.

Expose samples for 2 concrete mix designs to up to three (3) different corrodent solutions to support calculated depth of penetration and service life predictions. The exact number of

corrodent solutions and the compositions of those solutions will be specified by the STR at a later date.

Analyze samples for relevant data after exposure for 4 months to compare with model predictions. (A request may be made to continue testing to obtain additional data points.) Monitor volumetric changes due to sulfate reactions with the two different concretes. The corrodent solutions will contain at a minimum sulfate, aluminate, chloride, and sodium.

Task 5. Provide approach and methodology.

The SIMCO, Inc. proposal will document the approach and methodology, identify information and testing required, identify the number of samples and sample geometry required, recommend laboratory prepared samples or actual samples (Vault 4) or test samples (Disposal Unit 2), and include a cost for preparing samples from materials supplied by SRNL. In the event that certain test methods for quantifying advancing fronts of both sulfate (sulfur) and aluminate (aluminum) in concrete (which already contain significant concentrations of S and Al) are determined to involve the use of radio tracers, a joint work scope with SRNL should also be prepared for the proposal.

Task 6. Characterize MCU Saltstone and predict durability.

Prepare MCU saltstone samples and measure properties that are required to run the STADIUM® code. Predict the durability of saltstone exposed to infiltrating water.

Task 7. Final Report.

A draft final report is due on August 15, 2008.
A final reviewed and accepted report is due on September 30, 2008.
Data and modeling runs performed after September 30, 2008 will be submitted in Revisions of the final report within one month after being generated.

11.0 ATTACHMENT 2

STADIUM® Code Predictions: Effects of High Sulfate Alkaline Solutions and SRS Soil Pore Water on Surrogate Saltstone Vault 1/4 and Disposal Unit 2 Concretes

Subcontract No. AC48992N Task 1 Report

BLANK PAGE

Washington Savannah River Company

Subcontract no. AC48992N

Report

Task 1

May 31, 2008

Presented by:

SIMCO Technologies Inc.
203-1400 Boul. du Parc Technologique
Quebec QC G1P 4R7
Canada
(418) 656-0266 tel | (418) 656-6083 fax

LIMITED LIABILITY STATEMENT: THIS REPORT IS FOR THE EXCLUSIVE USE OF SIMCO'S CLIENT AND IS PROVIDED ON AN "AS IS" BASIS WITH NO WARRANTIES, IMPLIED OR EXPRESSED, INCLUDING, BUT NOT LIMITED TO, WARRANTIES OF MERCHANTABILITY AND FITNESS FOR A PARTICULAR PURPOSE, WITH RESPECT TO THE SERVICES PROVIDED. SIMCO ASSUMES NO LIABILITY TO ANY PARTY FOR ANY LOSS, EXPENSE OR DAMAGE OCCASIONED BY THE USE OF THIS REPORT. ONLY THE CLIENT IS AUTHORIZED TO COPY OR DISTRIBUTE THIS REPORT AND THEN ONLY IN ITS ENTIRETY. THE ANALYSIS, RESULTS AND RECOMMENDATIONS CONTAINED IN THIS REPORT REFLECT THE CONDITION OF THE SAMPLES TESTED EXCLUSIVELY, WHICH WERE MANUFACTURED FROM MATERIALS PROVIDED TO SIMCO BY THE CLIENT OR BY THIRD PARTIES. THE REPORT'S OBSERVATIONS AND TEST RESULTS ARE RELEVANT ONLY TO THE SAMPLES TESTED AND ARE BASED ON IDENTICAL TESTING CONDITIONS. FURTHERMORE, THIS REPORT IS INTENDED FOR THE USE OF INDIVIDUALS WHO ARE COMPETENT TO EVALUATE THE SIGNIFICANCE AND LIMITATIONS OF ITS CONTENT AND RECOMMENDATIONS AND WHO ACCEPT RESPONSIBILITY FOR THE APPLICATION OF THE MATERIAL IT CONTAINS.

THE STADIUM®®® MODEL IS A HELPFUL TOOL TO PREDICT THE FUTURE CONDITIONS OF CONCRETE MATERIALS. HOWEVER, ALL DURABILITY-MODELING PARAMETERS HAVE A STATISTICAL RANGE OF ACCEPTABLE RESULTS. THE MODELING USED IN THIS REPORT USES MEAN LABORATORY- OR FIELD-DETERMINED SINGLE VALUES AS INPUT PARAMETERS. THIS PROVIDES A SINGLE RESULT, WHICH PROVIDES A SIMPLE ANALYSIS EVALUATING CORROSION PROTECTION OPTIONS. PREVIOUS CONDITIONS ARE ASSUMED TO CARRY FORWARD IN THE PREDICTION MODEL; THERE ARE NO ASSURANCES THAT THE STRUCTURE WILL BE EXPOSED TO A SIMILAR ENVIRONMENT AS IN THE PAST.

1. OBJECTIVE

The objective of Task 1 was to predict the service life of two concrete mixtures similar to the concrete mixtures used at SRS for radioactive waste storage when exposed to an aggressive sulfate solution for an extended period of time. The composition of the aggressive solution was provided by SRNL. The surrogate concretes identified by SIMCO Technologies were previously tested by SIMCO Technologies as part of their own research activities for transport properties. The selected mixtures were:

A. A concrete with a w/b ratio of 0.35 made with an ASTM Type I cement and 35% slag,
B. A concrete made with a pre-blended ternary binder incorporating CSA Type 10 cement, fly ash and silica fume. Type 10 cement is general use cement and equivalent to ASTM Type 1 cement.

The first mixture (A) was selected as a surrogate for the concrete referred as "Saltstone Vault 1 and 4" concrete. The second mixture (B) was selected as a surrogate for the "Saltstone Disposal Unit 2" concrete.

The report is divided as follow. Section 2 describes the ionic transport model called STADIUM®®® that was used to perform the service life calculations. Section 3 describes the two concrete mixtures that were simulated, along with the tests that were performed to estimate their properties. Section 4 focuses on the simulation. The various hypotheses used for the calculations as well as the analysis of the results are outlined in this section.

2. MODEL DESCRIPTION

STADIUM®®® is a multiionic transport model based on a sequential split operator approach that separates ionic movement and chemical reactions. Details on the paper can be found in papers [1-3]. The present version of the model does not include any coupling with mechanical damages. It does not allow predicting the apparition of cracks resulting from the exposure to an aggressive environment (e.g. sulfate attacks) or internal chemical degradation such as alkali silica reaction (ASR). Given the high alkalinity of the aggressive solution composition provided by SRNL, the risk of ASR should be considered in a more global performance assessment study.

The ionic transport is described by the extended Nernst-Planck equation applied to unsaturated and non-isotherm materials. This equation accounts for the electrical coupling as well as the chemical activity between ionic fluxes, transport due to water content gradient and temperature effects:

$$\frac{\partial(wc_i)}{\partial t} - \operatorname{div}\left(D_i w \operatorname{grad}(c_i) + \frac{D_i z_i F}{RT} w c_i \operatorname{grad}(\psi) + D_i w c_i \operatorname{grad}(\ln \gamma_i) + \frac{D_i c_i \ln(\gamma_i c_i)}{T} w \operatorname{grad}(T) + c_i D_w \operatorname{grad}(w) \right) = 0 \quad (1)$$

where c_i is the concentration [mmol/L], w is the water content [m^3/m^3], D_i is the diffusion coefficient [m^2/s], z_i is the valence number of the ionic species i, F is the Faraday constant [96488.46 C/mol], ψ is the electrodiffusion potential [V], R is the ideal gas constant [8.3143 J/mol/°K], T is the temperature [°K], γ_i is the activity coefficient, and D_w is the water diffusivity [m^2/s]. Eight ionic species were considered for this task: OH^-, Na^+, K^+, SO_4^{2-}, Ca^{2+}, $Al(OH)_4^-$, NO_2^-, and NO_3^-. The activity coefficients in the model are evaluated on the basis of the Harvie, Moller and Weare (HMW) implementation of Pitzer's ion interaction model [4].

The electrodiffusion term in equation (1), involving the potential ψ, is mainly responsible for maintaining the electroneutrality of the pore solution. Its role is to balance each individual ionic mobilities so that there is no net accumulation of charge at any location in the pore solution. It is usually neglected in models dealing with ionic transport in groundwater where the concentration levels can be low. However, in cementitious materials, where pore solution concentrations are high (pH around 13.2), this term can have a significant influence on the ingress rate of contaminants in structures. This was emphasized for the case of sulfate attack in reference [3]. To solve the diffusion potential ψ, the ionic transport equation is coupled to Poisson's equation, which relates the electrodiffusion potential in the material to the ionic profile distributions:

$$\operatorname{div}(\tau w \operatorname{grad} \psi) + \frac{F}{\varepsilon} w \left(\sum_{i=1}^{N} z_i c_i \right) = 0 \quad (2)$$

where ε [C/V/m] is the medium permittivity and N is the number of ions in the pore solution.

To account for water flow in the presence of water content gradients in unsaturated materials, the previous equations are coupled to Richard's equation:

$$\frac{\partial w}{\partial t} - \operatorname{div}\left(D_w \operatorname{grad}(w)\right) = 0 \quad (3)$$

This diffusion-type equation gives the distribution of water content within the material. The water diffusivity parameter is nonlinear and follows an exponential function [5]: $D_w = Ae^{Bw}$ [9]. Finally, the temperature distribution in the material is calculated from the classical heat condition equation:

[9] Work is ongoing at SIMCO to model moisture flow based on a capillary pressure approach. The objective in that case is to use drying test results to estimate the permeability of cementitious materials.

$$\rho C_p \frac{\partial T}{\partial t} - \mathrm{div}\big(\kappa\, \mathrm{grad}(T)\big) = 0 \qquad (4)$$

where ρ is the density of the material [kg/m^3], C_p is the specific heat of the material [J/kg/°C], and k is the heat conductivity [W/m^2/°C].

The key material parameter that determines the rate of ingress of chloride and other contaminants in the structure is the diffusion coefficient D_i (see equation (1)). This parameter is influenced by multiple parameters:

$$D_i = D_i^{\mathrm{ref}} \times S(w) \times G(T) \times H(t) \times M(\phi) \qquad (5)$$

where D_i^{ref} is a reference value measured on sound material samples using the migration test procedure, described later in the report. It usually corresponds to the measurement at 28 days of curing. The various functions affecting the diffusion coefficient are given as:

$$\begin{aligned} S(w) &= \frac{w^{7/3}}{\phi_o^{7/3}} \\ G(T) &= e^{0.028(T-T^{\mathrm{ref}})} \\ H(t) &= \frac{a}{1+(a-1)e^{-\alpha(t-t^{\mathrm{ref}})}} \\ M(\phi) &= \frac{e^{4.3\phi/V_p}}{e^{4.3\phi_o/V_p}} \end{aligned} \qquad (6)$$

where ϕ_o is the initial porosity of the material,ϕ is the porosity at time t and V_p is the volumetric paste content of the cementitious material [m^3/m^3]. The function *S(w)* models the influence of the water content on diffusion. It is based on the relationship derived by Millington and Quirk [6]. The function *G(T)* considers the effect of temperature [2,7] on transport properties, compared to a reference value evaluated at the temperature T^{ref}. The function *H(t)* takes into account the variation of transport properties as a result of the cement hydration process [2]. The transport properties of cementitious materials are generally high at young age but tend to decrease with time, especially when supplementary materials such as fly ash are used in the production of concrete. The reduction rate is determined by the factor α while the ultimate value of $H(t\rightarrow\infty)$, when the hydration process is completed, is given by a.

Finally, the alteration to the material's microstructure caused by the chemical reactions between the external contaminants, such as sulfate, and the cement paste can induce local porosity variations that affect the diffusion coefficients. Alteration of the microstructure can result in one or more of the following consequences, increase or decrease in the porosity of the microstructure, fracturing of the microstructure, or macro fracturing of the structural element. This is taken into account using the function $M(\phi)$, which was established on the basis of porosity and diffusion coefficient measurements performed over a wide range of

cementitious materials [2][10]. A similar approach has been widely used to predict the long-term effect of contaminant transport in soils (see for instance reference [8]).

The porosity variations are calculated by accounting at each node for changes in the solid phase distribution evaluated at the previous time step. The description of the chemical module is given below.

The water diffusivity, which governs the kinetic of the moisture movement in the materials, is affected by the same factors as the diffusion coefficient.

Since eight ionic species are considered in the model, there are 11 variables in the system of equations: $8\times c_i$, ψ, w and T, which are solved using 8 ionic conservation equations (1), coupled with equations (2)-(4). This system of nonlinear equations is solved using the Newton-Raphson method with all equations solved simultaneously. The spatial discretization of this coupled system is based on the finite element approach using the standard Galerkin procedure. An Euler implicit scheme is used to discretize the time-dependent part of the model. The numerical details are given in reference [2].

The second module in STADIUM®®® consists in a chemical equilibrium code. Following the transport step, the chemical equilibrium module verifies, at each node of the mesh, the equilibrium between the concentrations and the solid phases of the hydrated cement paste: calcium hydroxide, calcium silicate hydrates, ettringite, and mono-sulfates. The equilibrium of each phase is modeled according to:

$$K_m = \prod_{i=1}^{N} c_i^{\nu_{mi}} \gamma_j^{\nu_{mi}} \quad \text{with} \quad m = 1, \ldots, M \tag{7}$$

where M is the number of solid phases, N is the number of ions, K_m is the equilibrium constant (or solubility constant) of the solid m, c_i is the concentration of the ionic species i, γ_i is its chemical activity coefficient, and ν_{mi} is the stoechiometric coefficient of the ith ionic species in the mth mineral. If the solution is not in equilibrium with the paste, solid phases are either dissolved or precipitated to restore equilibrium. Solid phases can also be formed when aggressive species penetrate into the porous network of the material, e.g. ettringite, gypsum, hydrated sodium sulfate, and halite.

The penetration of chloride in concrete structures leads to the formation of a chloride-AFm solid compound called the Friedel's salt [9], $3CaO.Al_2O_3.CaCl_2.10H_2O$. The formation of Friedel's salt upon chloride penetration is modeled following an ion-exchange mechanism with monosulfates:

[10] At this time, the STADIUM®®® code does not predict fracturing caused by exposure to external contaminants. In addition to exposure to external contaminants, fracture patterns are a function of element geometry, initial conditions (cracking incurred during construction and curing), and specific loading conditions. Methodology to address fracture damage and consequences of microfracturing caused by exposure to chemical contaminants is included in the SIMCO scope for the CBP CRADA.

$$\text{monosulfate} + 2\text{Cl}^- \leftrightarrow \text{Friedel's salt} + \text{SO}_4^{2-} \quad (8)$$

This reaction obeys the following equilibrium relationship [1]:

$$K_{Cl/SO_4} = \frac{\{\text{Cl}\}^2}{\{\text{SO}_4\}} \frac{[\text{AFm}_{SO4}]}{[\text{AFm}_{Cl}]} \quad (9)$$

where [AF_m] and [FS] are the solid content [mmol/g] in monosulfate and Friedel's salt respectively. The curly brackets {…} correspond to the chemical activity of the ionic species.

Papers describing laboratory validation of the model for different type of exposures can be found in references [1, 3, 10]. Field validation test cases were also performed [11, 12].

3. CONCRETE MIXTURE CHARACTERISTICS

The properties of the concrete mixtures that were used to emulate the Vault 1/4 and Disposal Unit 2 concretes are summarized in Tables 1 and 2. They had a water to binder (total cementitious materials ratio) ratio of 0.35. The Vaults 1 / 4 surrogate concrete was made with ASTM Type I cement and slag cement. The Disposal Unit 2 surrogate concrete was made with a ternary binder (CSA Type 10 cement, Class F fly ash, and silica fume). In both cases, the mixtures were cast in plastic cylinders (10 cm diameter, 20 cm length) and demolded 24 hours later. The cylinders were then placed in a fog room (100% RH) for curing. After selected curing periods (28 days, 90 days, 1 year, and 2 years) cylinders were taken from the chamber and tested for the different transport properties. The tests are described in the following paragraphs.

Porosity: The porosity was evaluated on the basis of the ASTM C642 procedure. This procedure consists in oven-drying a concrete sample and then re-saturating it with water. The mass difference provides the porosity value. Laboratory measurements at different curing age showed no significant effect of the curing age of concrete on the porosity. Accordingly, the porosity is not affected by the hydration in the model.

Diffusivity: The diffusion coefficients were evaluated using the migration test procedure. The migration test is a modified version of the ASTM C1202 standard procedure. It consists in accelerating the transport of ions in a saturated concrete sample by applying an external electrical potential. The experimental set-up is shown in Figure 1. To perform the test, 50-mm thick discs were first cut from the cores and vacuum saturated in a 300 mmol/L NaOH solution for 24 hours.

The lateral surface of the discs was coated with a silicon gel. The discs were then mounted on the migration cells. The cell/disc interface was also coated with silicon to ensure a watertight joint. Both compartments of the cells were filled with approximately 2.5 litres of solution. The test solution on the upstream side of the cell was made of 300 mmol/L of sodium hydroxide (NaOH) and 500 mmol/L of sodium chloride (NaCl). The downstream compartment of the cell was filled with a 300 mmol/L sodium hydroxide solution. During the

test, an external 20 V potential was applied to the cell, and the current passing through the samples was regularly measured over a 200-hour period. Current values were then analyzed following the procedure described in Samson et al. [13] in order to evaluate the diffusion coefficients.

The hydration of cementitious materials leads to a reduction of the diffusion coefficients with time. To account for this, migration tests were performed at different curing age and fitted to the time dependent function *H(t)* reported in equation (6). The hydration function for each material is plotted on Figure 2A and 2B. The hydration parameters are given in Tables 1 and 2.

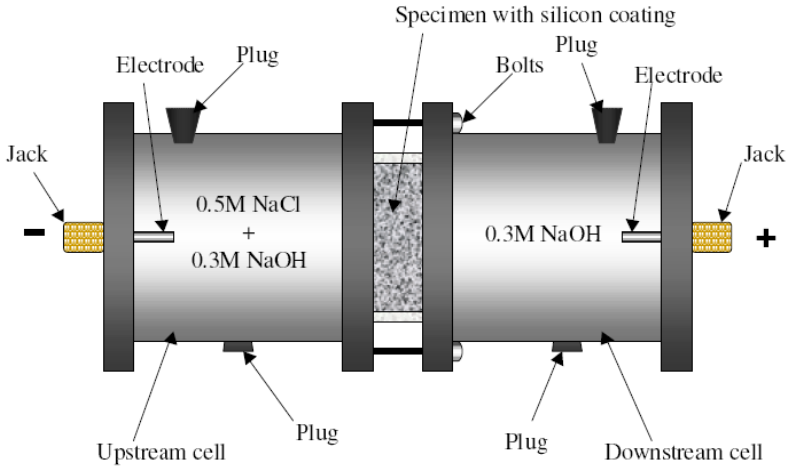

Figure 1 – Migration test setup

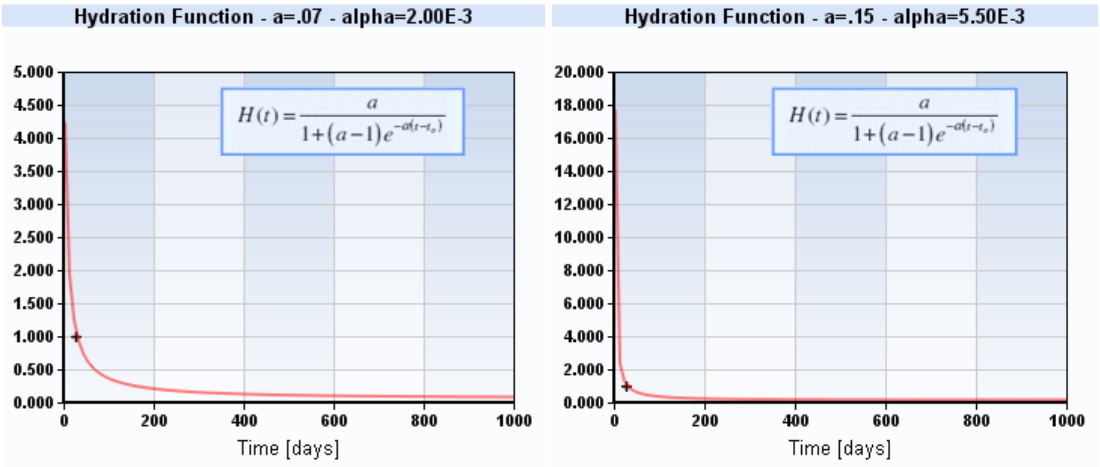

Figure 2 – Hydration functions for the two surrogate concretes. Figure A: slag concrete, Figure B: ternary concrete

Pore Solution Extraction and Analysis: The initial composition of the pore solution was obtained by extracting the solution under an applied external pressure [14]. Prior testing, a concrete sample was broken into pieces and placed in the extraction cell (Figure 3). The pressure was then applied. The solution was collected in a syringe to limit contact with air. It was stored in a refrigerator until the analysis was performed. Before the analysis, the solution was diluted approximately 10 times to get sufficient solution for all the measurements. The

concentrations in OH^- was evaluated by potentiometric titration, and the cation concentrations (Ca^{2+}, Na^+, K^+) were analyzed using ICP. The sulfate concentration was measured using ionic chromatography.

The initial $Al(OH)_4^-$ content was estimated at 0.1 mmol/L since it was too weak to be measured after the solution dilution. Also, due to experimental errors, the extracted solution was not strictly neutral. The solution was balanced to respect the electroneutrality requirement. One set of pore solution extractions was performed on samples directly from the curing room after 28 days for future service life simulations. Those values are reported in Tables 1 and 2. Another series of extraction was performed on samples saturated for 24 hours under vacuum in a 300 mmol/L NaOH solution. These results were used in interpretation of the migration tests.

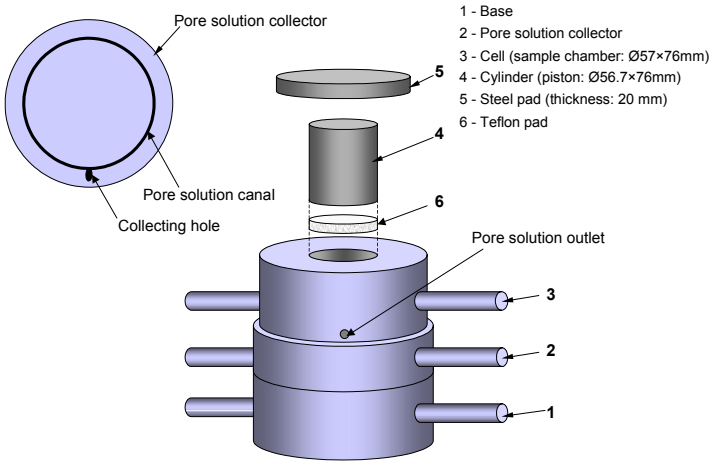

Figure 3 – Pore solution extraction cell

Water Diffusivity Characterization: The water diffusivity is estimated from drying test results. The test procedure consists in drying two series of samples in a 50% RH room. In the first series, the samples were 50 mm thick while they had a 10 mm thickness in the second series. The samples were coated with epoxy on their circular face, which left two flat surfaces open for drying. The saturated samples were placed in a 50% RH room and their weight loss was monitored periodically. When the thin samples reached equilibrium, the test was analyzed by fitting the mass loss curves with Richards' model (equation 3). It is assumed that the water diffusivity is nonlinear and can be expressed as: $D_w = Ae^{Bw}$ [5]. Parameters *A* and *B* were adjusted to fit the model prediction with the experimental mass loss curves. Details on the analysis are provided in reference [15]. Values for *A* and *B* for the surrogate concretes and are listed in Tables 1 and 2.

Initial Mineralogy Characterization: Finally, the initial solid phases of the hydrated cement paste are estimated from the cement and admixtures chemical composition. The calculations are based on a simple mass balance, assuming that the initial paste is made of portlandite, C-S-H, monosulfates, and ettringite. Details on the calculation are provided in reference [2]. It should be noted that only a small amount of portlandite is present initially in

both materials, due to the presence of supplementary cementitious admixtures which favor the formation of C-S-H.

Table 1 – Properties of the slag concrete mixture (Vault 1/4 surrogate)

Properties	Values	Properties	Values
Cement type	ASTM Type I	Porosity	10.0%
w/b	0.35		
		Diffusion coefficients	(E-11 m^2/s)
Mixture proportions	(kg/m^3)	OH^-	13.0
Cement	276	Na^+	3.3
Slag	149	K^+	4.8
Water	149	SO_4^{2-}	2.6
Coarse aggregates	925	Ca^{2+}	2.0
Fine aggregates	815	$Al(OH)_4^-$	1.3
Density	2314	NO3-	4.7
		NO2-	4.7
Cement composition	(% mass)		
CaO	64.5	Water diffusivity	
SiO_2	20.8	A (E-13 m^2/s)	4.3
Al_2O_3	5.3	B (-)	80
SO_3	2.8	*w* @ 50%RH (m^3/m^3)	0.059
Fe_2O_3	2.1		
		Hydration parameters	
Slag composition	(% mass)	a (-)	0.07
CaO	40.1	α (1/s)	2.0E-03
SiO_2	36.8		
Al_2O_3	8.7	Initial pore solution	(mmol/L)
SO_3	2.3	OH^-	217.2
Fe_2O_3	0.7	Na^+	108.7
		K^+	110.4
Bogue cement analysis	(% mass)	SO_4^{2-}	1.9
C_3S	57.9	Ca^{2+}	1.0
C_2S	16.0	$Al(OH)_4^-$	0.1
C_3A	10.5		
C_4AF	6.4	Initial solid phases	(g/kg)
		Portlandite	3.3
Compressive strength	(Mpa)	C-S-H	81.3
7 days	42.7	Monosulfate	29.3
28 days	54.0	Ettringite	2.0
91 days	65.3		
1 year	56.7		
2 years	69.7		

Table 2 – Properties of the ternary concrete mixture (Disposal Unit 2 surrogate)

Properties	Values	Properties	Values
Cement type	CSA Type 10	Diffusion coefficients	(E-11 m^2/s)
w/b	0.35	OH^-	4.0
		Na^+	1.0
Mixture proportions	(kg/m^3)	K^+	1.5
Blended Cement	425	SO_4^{2-}	0.8
Water	149	Ca^{2+}	0.6
Coarse aggregates	910	$Al(OH)_4^-$	0.4
Fine aggregates	800	NO3-	1.4
Density	2284	NO2-	1.4
Blended cement composition	(% mass)	Water diffusivity	
CaO	47.1	A (E-13 m^2/s)	1.0
SiO_2	30.2	B (-)	80
Al_2O_3	5.0	*w* @ 50%RH (m^3/m^3)	0.064
SO_3	3.2		
Fe_2O_3	3.8	Hydration parameters	
		a (-)	0.15
Bogue cement analysis*	(% mass)	α (1/s)	5.5E-03
C_3S	N/A		
C_2S	N/A	Initial pore solution	(mmol/L)
C_3A	N/A	OH^-	204.0
C_4AF	N/A	Na^+	58.8
		K^+	149.9
Compressive strength	(Mpa)	SO_4^{2-}	3.3
7 days	41.6	Ca^{2+}	1.0
28 days	56.7	$Al(OH)_4^-$	0.1
91 days	62.1		
1 year	66.5	Initial solid phases	(g/kg)
2 years	72.8	Portlandite	3.0
		C-S-H	85.2
Porosity	10.2%	Monosulfate	23.4
		Ettringite	2.0

*Bogue analysis is not suited for blended cements

4. SIMULATIONS AND ANALYSIS

Model: The service life simulations were performed on the case illustrated on Figure 4. The 1D simulations were performed on a 20-cm (8 in.) slab[11] for Disposal Unit 2 and 46-cm (18 in.) slab for Vault 1/4. The slabs were exposed on one side (x=0) to the leachate from the saltstone waste and on the other side to groundwater (x=L). It is assumed that the groundwater composition corresponds to pure water at a pH of 7 [12].

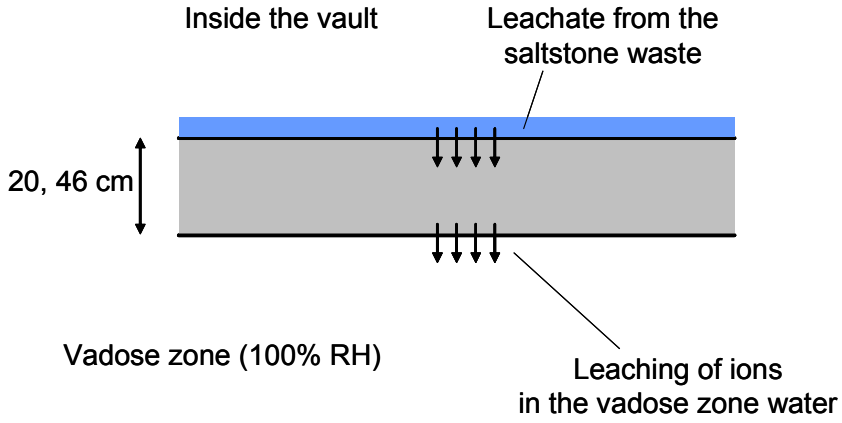

Figure 4 – Test case for the simulations

Composition of Aggressive Solutions: Compositions of three hypothetical saltstone leachates were provided by SNRL. The main species of the leachates are OH^-, NO_2^-, NO_3^-, Na^+, K^+, and SO_4^{2-}. For the purpose of the simulations, the minor species such as AlO_2^-, Fe^{3+}, SiO_3^{2-}, CO_3^{2-}, and PO_4^{3-} were neglected. This is partly due to a lack of data concerning the mineral phases associated with these ions. Also, neglecting these species allow reducing calculation time. If it is estimated that these species cannot be neglected, additional simulations incorporating the associated chemical reactions would be performed.

Following these simplifications, the provided leachate compositions were adjusted to enforce the electroneutrality requirement. The concentrations previously discussed are provided in Table 3 and correspond to the "High level" "worst case" case. Other sets of simulations were performed with the "high (worst) case" solution diluted 10 ("Mid-level" case) and 100 times ("Low-level" case). All solutions are reported in Table 3. The concentrations for all ionic species at x=L cm, corresponding to the material in contact with the vadose water, are set to zero.

[11] The orientation of the slab is irrelevant for the calculations since gravity is a negligible factor for ionic and mass transport. The same results would be obtained with a vertical buried wall.
[12] Actual vadose water pH value is around 6. The present version of STADIUM®®® does not allow considering acid exposure. The slightly acid water would likely increase the degradation rate at x=L. However, the thick slab, combined to the high pH solution inside the vault would likely buffer the acid attack and limit its effect.

Table 3 – Saltstone leachate composition used for the simulations (Boundary conditions at x=0)

Ionic species	Concentrations (mmol/L)		
	High level	Mid level	Low level
OH^-	769.0	76.9	7.69
Na^+	4366.0	436.6	43.66
K^+	215.0	21.5	2.15
SO_4^{2-}	208.0	20.8	2.08
Ca^{2+}	1.0	0.1	0.01
NO_3^-	2649.0	264.9	26.49
NO_2^-	749.0	74.9	7.49

Corrosion: Chloride present in the saltstone leachate was also neglected. As discussed in reference [16], chloride does not have a major impact on the microstructure of the material but is a major concern for structure durability due to its role in the initiation of reinforcement corrosion. However, the amount of Cl^- in the most concentrated leachate (<1500 ppm, or < 44 mmol/L) is too low to trigger the corrosion process [17].

The presence of CO_2 is also a concern for corrosion. This is especially the case for environmental carbonation, where CO_2 enter the material and reacts to form $CaCO_3$. The various steps leading to the formation of calcite requires hydroxide ions, which lowers the pH of the pore solution. When carbonation reaches the rebars, the steel is depassivated due to the drop of pH and will corrode if oxygen and water are available. In the present case, the risks for carbonation-induce corrosion are minimal. The high pH of the leachate will likely prevent the depassivation of steel. For the concrete face exposed to the vadose zone water, poor oxygen availability would in this case prevent the corrosion process, even if CO_3^{2-} and HCO_3^- are dissolved in solution.

Equilibrium Mineral Assemblages: The minerals that were considered for the durability analysis are listed in Table 4. The portlandite, C-S-H, monosulfates, and ettringite were present initially in the hydrated cement paste. The other minerals were considered as possible precipitates due to the presence of SO_4^{2-}. For these simulations, it was assumed that NO_3^- and NO_2^- did not react with other species. However, their strong concentration likely affected the precipitation of other phases due to their impact on the chemical activity calculations (equation (7)).

The chemical equilibrium of C-S-H is modeled on the basis of Berner's approach [17] that assigns separate C/S-dependent equilibrium relationships to the $Ca(OH)_2$ and CaH_2SiO_4 fractions of this hydration product. For the present calculations, this approach is further simplified by considering solely the $Ca(OH)_2$ fraction and an equilibrium constant corresponding to a C/S ratio of approximately 1. This approach has been successfully validated previously for sulfate attack cases [3, 10]. Using this approach allows neglecting the $H_2SiO_4^{2-}$ ion and the CaH_2SiO_4 mineral, which saves calculation time.

Table 4 – Mineral phases considered for the calculations

Minerals	Composition	log(*K*) @ 25°C
Portlandite	$Ca(OH)_2$	-5.15
C-S-H (portlandite fraction)	$Ca(OH)_2$	-6.2
Monosulfates	$3CaO.Al_2O_3.CaSO_4.12H_2O$	-29.4
Ettringite	$3CaO.Al_2O_3.3CaSO_4.26H_2O$	-44.0
Glauberite	$Na_2Ca(SO_4)_2$	-5.18
Gypsum	$CaSO_4.2H_2O$	-4.58
Mirabilite	Na2SO4.10H2O	-1.4
Syngenite	$K_2Ca(SO_4)_2.H_2O$	-7.45
Glaserite	$NaK_3(SO_4)_2$	-3.8

Temperature and Moisture Boundary Conditions: The temperature was set at a constant temperature of 15°C. The boundary condition for the water content at x=0 corresponds to the porosity of the material, assuming that the concrete is always saturated at this interface. For the surface in contact with the soil (x=L cm), simulations were made at 100% relative humidity. This boundary condition corresponds to a water content set at the porosity value.

Finite Element Mesh: The simulations were performed with finite element meshes of 90 elements for L=20 cm and 154 elements for L=46 cm that are refined near the domain boundaries. The time steps were increased progressively to reduce the calculation time: Δt=1 day for t<100 years, Δt=2 days for t<500 years, Δt=5 days for t<2000 years, and Δt=8 days for t=2000+ years.

Simulation Results: Results are shown in Figures 5 and 6 for the ternary concrete (surrogate for Saltstone Disposal Unit 2 concrete) exposed to the mid-level conditions after 2000 years. One of the main features of all simulation results is the formation of ettringite, which was the only SO_4-related mineral predicted by the model for all three exposure conditions. In all cases, an ettringite front begins at the surface exposed to the aggressive leachate, x=0, and penetrates deeper into the slab with time. As will be discussed later, the kinetic of the front progression depends on the transport properties of the materials and on the exposure conditions. It also depends on the initial amount of hydrated monosulfate in the cement paste, since the formation of ettringite requires monosulfate to dissolve. This dissolution provides calcium and alumina and part of the sulfur needed in the formation of ettringite. For comparable transport properties, cement with lower C_3A content will exhibit an ettringite front that penetrates more rapidly in the material.

Since the formation of ettringite not only requires SO_4^{2-} in the solution but also an additional amount of calcium, the small amount of portlandite initially present in the material is

dissolved upon ettringite formation. Similar observations were made on simulations of ordinary concrete mixtures exposed to sodium sulfate [3].

Due to the strong concentration in OH^- at x=0, limited decalcification of C-S-H is predicted at this location. However, the simulation results indicate that the decalcification process is more important at the soil/concrete interface (x = 20 cm for Disposal Unit 2 and x = 46 cm for Vault 1/4 surrogates), where the material is exposed to pure water. On this side of the concrete, a dissolution front moves inward toward the surface in contact with the aggressive leachate and the advancing ettringite front. The kinetic of the decalcification front is mostly controlled by the transport properties. A small ettringite peak (shown in Figure 6) is predicted in front of the C-S-H front. It is caused by the release of calcium and sulfate in the pore solution upon C-S-H decalcification and monosulfate dissolution.

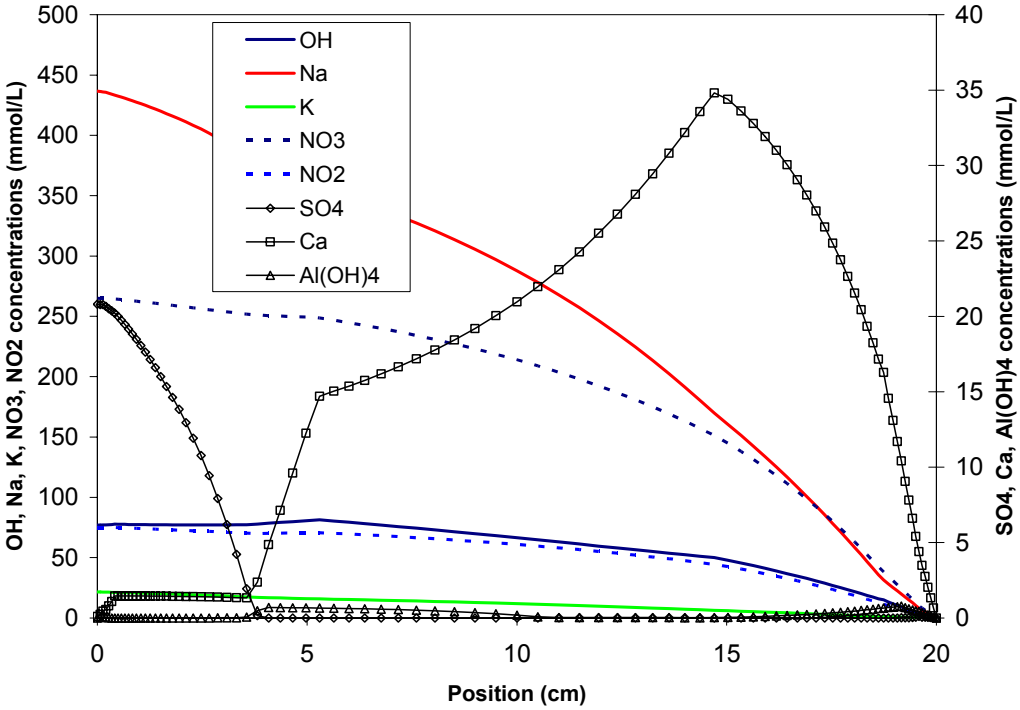

Figure 5 – Ionic species in the pore solution for the ternary concrete exposed to the mid-level conditions after 2000 years

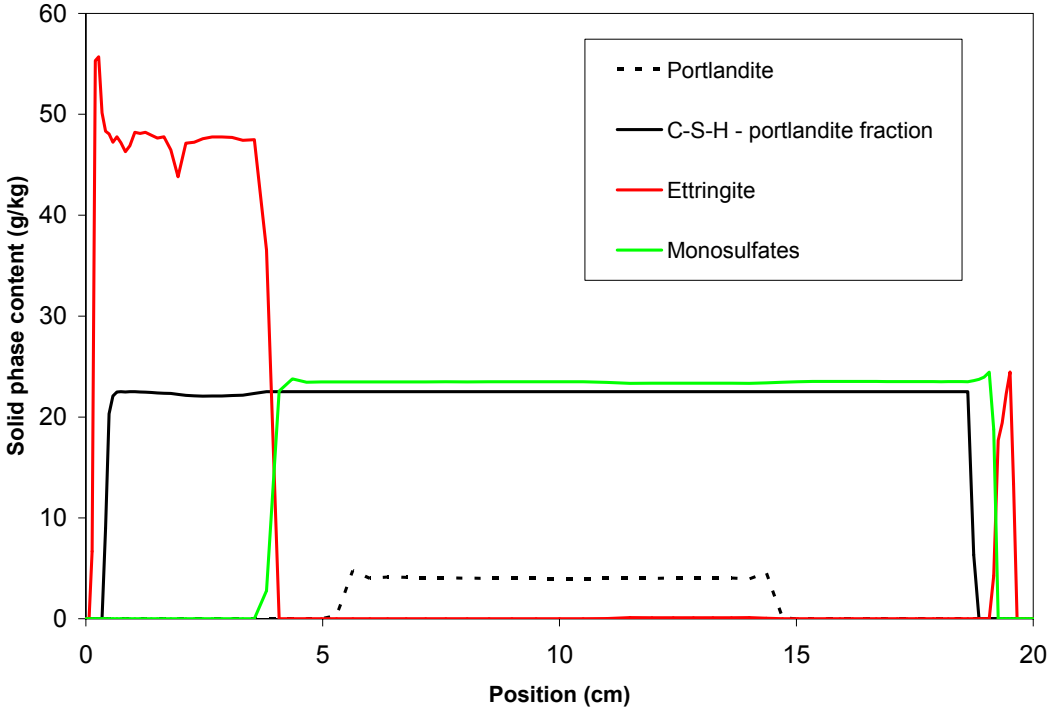

Figure 6 – Solid phases in the hydrated cement paste for the ternary concrete exposed to the mid-level conditions after 2000 years

The results of the six simulations (2 surrogate concretes and 3 sulfate solutions) are summarized in the following figures. Figure 7 shows the progression of the ettringite front from the leachate/concrete interface. The simulation results clearly emphasize that the main driving parameter of the front kinetic is the exposure level in sulfate. The small differences in the material transport properties do not translate into significant differences in the position of the ettringite front.

The simulations show that if the exposure conditions are maintained over the structure service-life, the ettringite is likely to go through the slab after approximately 5000 years for the high-concentration case. The reduction in the penetration rate after 5000+ years is due to the interaction with the decalcification ongoing at the soil/concrete interface. As mentioned previously, it should be remembered that these calculations do not consider the possible formation of microcracks associated with the formation of ettringite. In that case, the rate of ingress of the ettringite front would be increased.

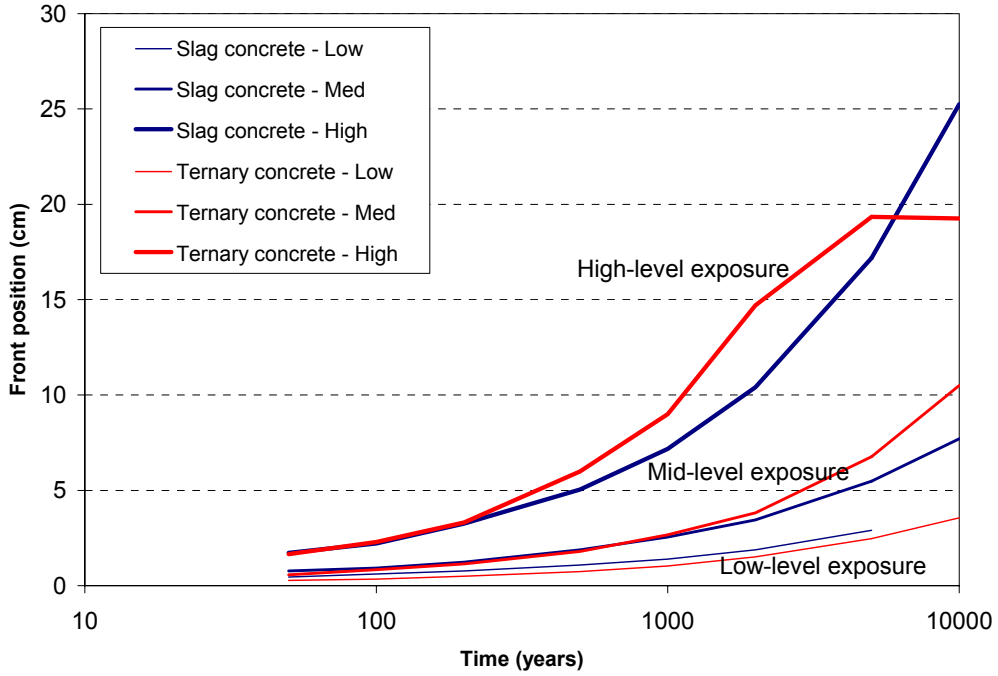

Figure 7 – Progression of the ettringite front from the saltstone leachate / concrete interface.

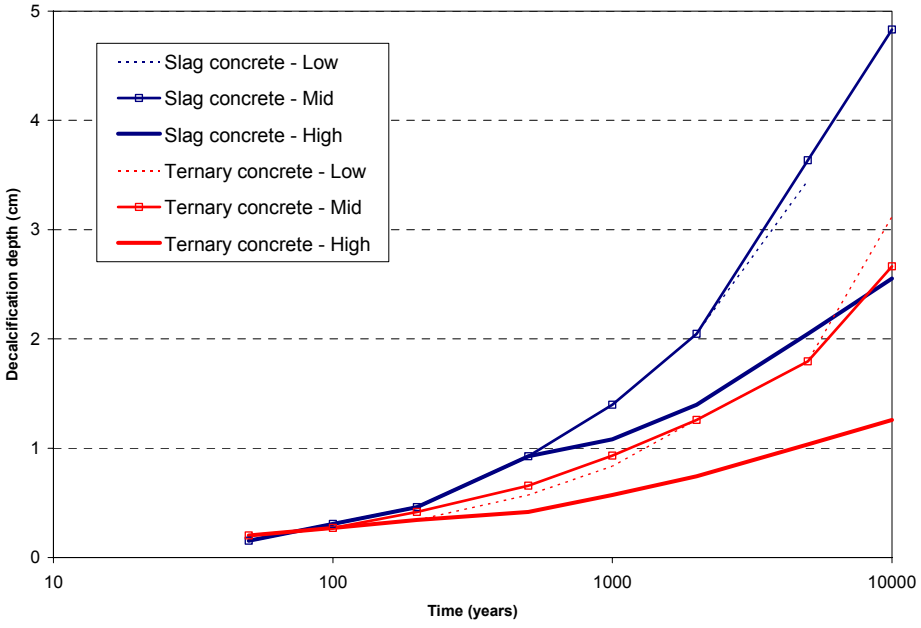

Figure 8 – Progression of the decalcification front from the soil/ concrete interface

The situation for the decalcification front starting at the soil/concrete interface is different (Figure 8). For the first 500 years, the degradation kinetic is very similar for all the simulations cases. After that, the penetration of OH^- present in the leachate on the other side of the slab tends to slow down the decalcification process. Consequently, the decalcification

process is less important (has a lesser impact) for the high-concentration case while the low concentration case exhibits the higher rate of decalcification. In any case, the model predicts that the degraded zone should not exceed 4 cm, which means that if the rebars are deeper than that and the slab is thick enough, the decalcification process is not likely to affect the service life of the structure over its intended period of use.

Discussion of Material Damage: The mechanisms and conditions that cause damage to concrete as the result of exposure to sulfate solutions are topics of hundreds of research papers. Although ettringite formation is associated with expansion and consequent cracking, other conditions (chemical and mineralogical) are characteristic of the sulfate attack process and contribute at least in part to the damage (expansion and cracking) typically related to this type of concrete degradation.

As reported in reference [19], sulfate attacks in natural conditions usually occur most of the time at a pH around 7. In these conditions, ettringite is formed following the dissolution of monosulfate. The low pH also favors the dissolution of portlandite and C-S-H, which provide calcium to the pore solution and triggers the formation of gypsum. The degraded cement paste can be divided in the following zones, starting from the sound material toward the external surface [19]:

- The original paste not involved in the corrosion process,
- A zone in which ettringite had been formed in a reaction with monosulfate; the amount of calcium hydroxide is reduced,
- A zone containing gypsum; calcium hydroxide is absent, the C-S-H phase is partially decalcified (formation of horizontal cracks[13] preferentially in this region),
- A zone containing the C-S-H phase with a significantly reduced C/S ratio as its main constituent. Limited amounts of sulfates in adsorbed form may also be present.

In these conditions, many papers report losses in mechanical resistance [20] and expansions (see for instance reference [21]).

In the present case, the pH of the aggressive solution is around 13. As mentioned previously, the precipitation of gypsum was not observed in any simulations. The absence of gypsum from the results can be explained in part by the strong concentration in sodium, which tends to increase the solubility of this mineral [22], therefore limiting the precipitation process. Also, the strong OH^- concentration in the saltstone leachate limits the decalcification process. As reported in reference [3], the formation of gypsum is associated with the dissolution of portlandite, or C-S-H in the present case, which provides the necessary calcium for the precipitation. Limiting the amount of calcium in the pore solution thus hinders the formation of gypsum.

Very little research work was done to investigate the effect of sulfate attack at such pH values. Brown [20] and Cao [21] exposed cementitious materials to sulfate solutions without controlling the pH in solution containers. This resulted in a pH increasing to around 12.5 due

[13] For the geometry corresponding to Figure 4.

to the dissolution of portlandite. Cao [21] measured expansions that were more important for the high pH case (see Figure 9), where expansion is only caused by the formation of ettringite. Brown [20], on the contrary, measured more important expansions for low pH conditions, associated with more important drops in compressive strengths (Figure 10). It thus seems that the effect of a high pH on the damage sustained by concrete exposed to sulfate is not clear and will need additional research before it is settled.

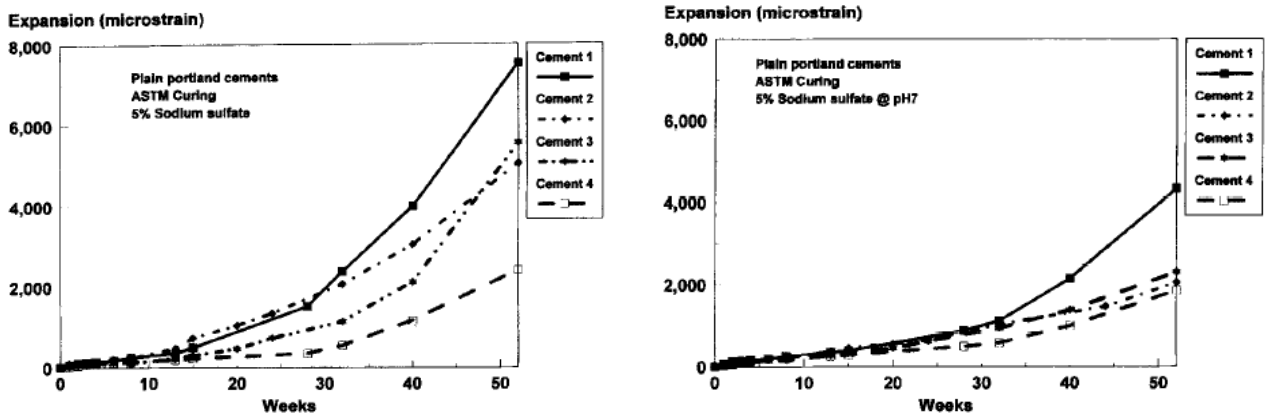

A: Uncontrolled (pH=12.5) Na_2SO_4 solution B: Controlled (pH=7) Na_2SO_4 solution

Figure 9 – Expansions of mortar bars made with different cements and immersed in 5% Na_2SO_4 solutions (taken from reference [21])

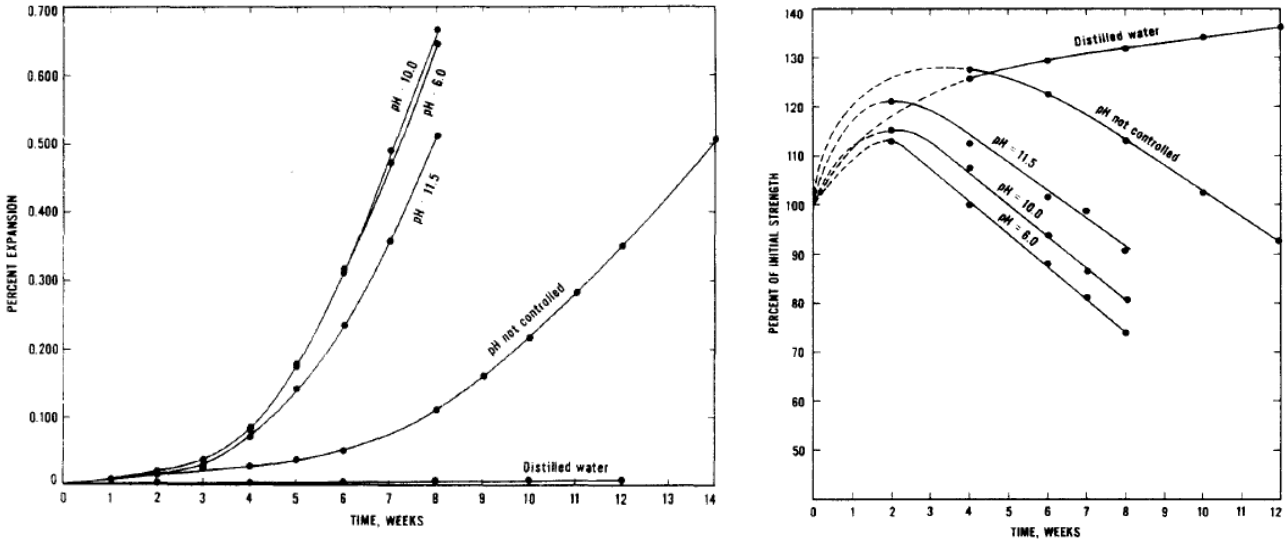

A: Expansions at different pH values B: Strengths at different pH values

Figure 10 – Mortar bars made with Type I cement and exposed to 5% Na_2SO_4 solutions. The "distilled water case" corresponds to pure water [20]

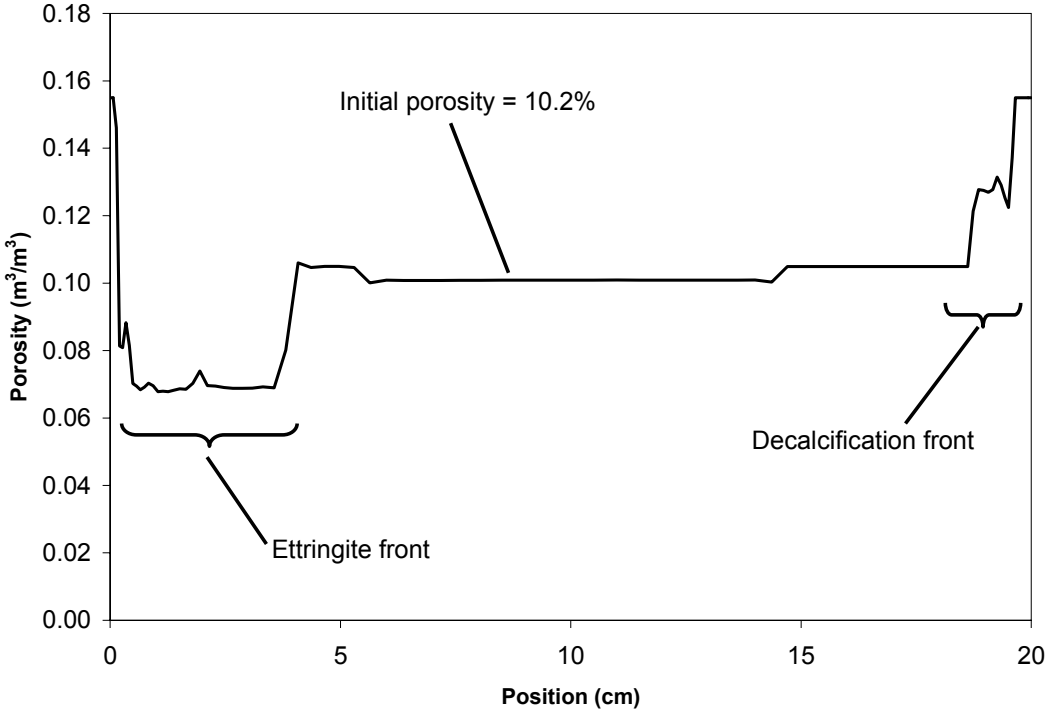

Figure 11 – Porosity distribution for the phase distribution presented in Figure 6

In the simulation results presented in this report, the dissolution and precipitation of phases locally modifies the porosity, which in turn affects the transport properties according to the function $M(\phi)$ in equation (6). Figure 11 shows the porosity distribution corresponding to the solid phase profiles in Figure 6. The formation of an ettringite front from the top surface of the slab reduces the porosity, which lowers the transport property values. According to Figure 11, the porosity goes from approximately 10% to 7%, which gives $M(\phi)$=0.6. This means that the transport properties are 60% lower in that area. It is important to emphasize that the calculations performed with STADIUM®® do not consider the possible effect of cracking that might be induced by this ettringite front. Tests results reported in reference [9] indicated that the damages resulting from a sulfate exposure could be associated with the presence of a gypsum peak behind the ettringite front. In the present study no such gypsum peaks were predicted by the model. Still, the formation of ettringite could damage the paste and increase the value of the transport parameters. In that case, the rate of ettringite ingress would be more important.

At the other end of the slab, Figure 11 indicates that despite the formation of a small ettringite peak, the decalcification of C-S-H leads to an increase in porosity from 10% to 15%. In that case, damage function $M(\phi)$ = 2.2. The decalcification of C-S-H at the soil/concrete boundary thus contributes to double the rate of degradation of the material. It should be noted that the porosity variation analysis gives similar result for both materials.

It is important to mention that one side effect of the absence of gypsum formation is that the amount of sulfur bound with the hydrated paste will be, for a given material, independent of the external sulfate exposure. This is due to the fact that the amount of ettringite formed is limited by the amount of alumina present in the material. Consequently, an ettringite front having a fixed height is formed. This is illustrated on Figure 12. In that case, the external sulfate concentration will only influence the rate of ingress of the ettringite front.

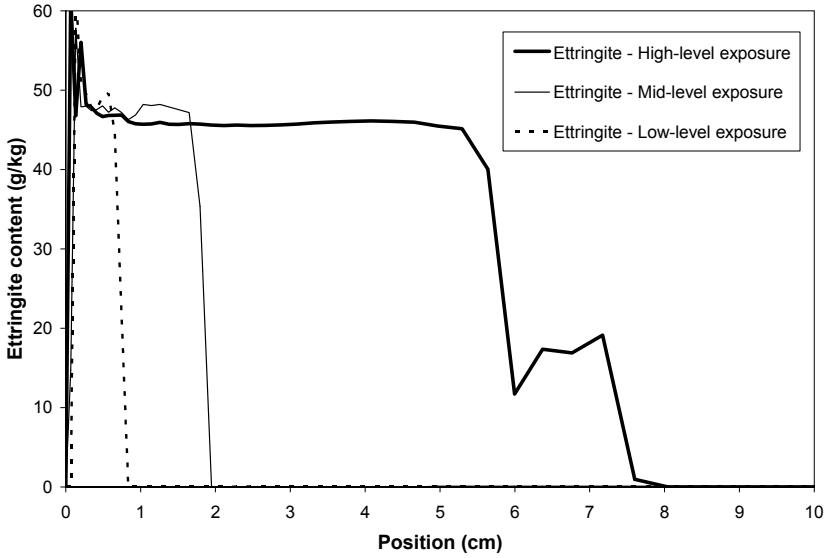

Figure 12 – Ettringite content in the ternary concrete after 50 years For different exposure conditions

Assuming that concrete sustains damage from sulfate exposure in high pH conditions, it is possible to provide a rough estimate of the increase in transport properties. Research work ongoing at SIMCO Technologies showed that microcracks (< ≈100μm) caused by cyclic load up to 90% of compressive strength have little effect on diffusion and drying rates. Diffusion coefficients and drying rates were shown to increase by approximately 50% in these conditions. However, recent results of chloride ingress in cracked samples [23] showed that for macrocracks (> ≈100μm), chloride diffuses at a velocity corresponding to its freewater value, which represents approximately a 50-fold increase in diffusion properties.

5. CONCLUSION

Simulations based on transport properties evaluated on two concrete mixtures with a water to binder ratio of 0.35 were performed to estimate the long-term durability of material exposed to saltstone waste leachate for an extended period of time. The simulations showed that the presence of sulfate in the leachate is responsible for the penetration of an ettringite front in the structure. No other sulfate-bearing minerals were predicted, including gypsum. According to the simulations, the exposure level (concentration of sulfate ions in the aggressive solution) is the parameter that has the strongest influence on the penetration kinetic.

The potential apparition of microcracks due to the formation of ettringite cannot be taken into account in STADIUM®®®. The simulations thus represent an optimistic situation where ettringite actually reduces the porosity of the material and reduces the rate of ingress of sulfate. In the presence of cracks, the transport properties would increase. Consequently, the rate of degradation would be worst than what was predicted by the model.

It was assumed that the other face of the concrete slab was exposed to pure water in the soil. According to the model, this particular boundary condition caused the decalcification of C-S-H, which could potentially affect the structural integrity of the waste vault. According to the simulations, the degradation could reach 4 cm after 10000 years of exposure.

Characterization of actual concretes exposed to high pH sulfate solutions are required to determine the consequences and damage resulting from exposure of these materials to these unique sulfate solution. Testing is underway in a separate task of this contract.

6. REFERENCES

1. Samson E., Marchand J., "Multiionic approaches to model chloride binding in cementitious materials", in: *2nd Int. Symp. on Advances in Concrete through Science and Engineering*, J. Marchand et al. eds., RILEM Proceedings PRO 51, Quebec City (Canada), 2006.

2. Samson E., Marchand J., "Modeling the effect of temperature on ionic transport in cementitious materials", *Cement and Concrete Research*, V. 37, 2007, pp. 455-468.

3. Samson E., Marchand J., "Modeling the transport of ions in unsaturated cement-based materials", *Computers and Structures*, V. 85, 2007, pp. 1740-1756.

4. Zhang G., Zheng Z., Wan J., "Modeling reactive geochemical transport of concentrated aqueous solutions", *Water Resources Research* V. 41, 2005, doi: 10.1029/2004WR003097.

5. Hall C., "Barrier performance of concrete: a review of fluid transport theory", *Materials and Structures*, V. 27, 1994, pp. 291-306.

6. Millington R.J., Quirk J.P., "Permeability of porous solids", *Transactions of the Faraday Society*, V. 57, 1961, pp. 1200-1207.

7. Zhang T., Samson E., Marchand J., "Effect of temperature on ionic transport properties of concrete", in Proceedings of the ConMAT Conference, N. Banthia et al. eds., Vancouver (Canada), 2005.

8. Xu T., Sonnenthal E., Spycher N., Pruess K., "TOUGHREACT – A simulation program for non-isothermal multiphase reactive geochemical transport in variably saturated geological media: applications to geothermal injectivity and CO_2 geological sequestration", *Computatioanl Geosciences*, V., 32, 2006, pp. 145-165.

9. Glasser F.P., Marchand J., Samson E., "Durability of concrete – Degradation phenomena involving detrimental chemical reactions", *Cement and Concrete Research*, V. 38, 2008, pp. 226-246.

10. Maltais Y., Marchand J., Samson E., "Predicting the durability of Portland cement systems in aggressive environments – Laboratory validation", *Cement and Concrete Research*, V. 34, no. 9, 2004, pp. 1579-1589.

11. Marchand J., Samson E., Maltais Y., Lee R.J., Sahu S., "Predicting the performance on concrete structures exposed to chemically aggressive environment – field validation" *Materials and Structures*, V. 35, 2002, pp. 623-631.

12. Maltais Y., Marchand J., Ouellet E., Samson E., Tourney P., "Service life prediction of high performance concrete mixture subjected to chloride penetration" *Proceedings of the Int. Conf. on Durability of HPC and Final Workshop of Conlife (Essen, Germany), M.J. Setzer & S. Palecki eds*., AEDIFICATIO Publishers (Freiburg, Germany), 2004, pp. 19-36.

13. Samson E., Marchand J., Snyder K.A., "Calculation of ionic diffusion coefficient on the basis of migration test results", *Materials and Structures*, V. 36, 2003, pp. 156-165.

14. Barneyback R.S., Diamond S., "Expression and analysis of pore fluid from hardened cement paste and mortars" *Cement and Concrete Research* V. 11, 1981, pp. 279-285.

15. Samson E., Maleki K., Marchand J., Zhang T., "Determination of the water diffusivity of concrete using drying/absorption test results", accepted for publication in *Journal of ASTM International*, 2008.

16. Glasser F.P., Marchand J., Samson E., "Durability of concrete – Degradation phenomena involving detrimental chemical reactions", *Cement and Concrete Research*, V. 38, 2008, pp. 226-246.

17. Alonso C., Andrade C., Castellote C., Castro P., "Chloride threshold values to depassivate reinforcing bars embedded in standardized OPC mortar", *Cement and Concrete Research*, V. 30, 2000, pp.1047-1055.

18. Berner U.R., "Modelling the incongruent dissolution of hydrated cement minerals", Radiochimica Acta, V. 44/45, 1988, pp. 387-393.

19. Skalny K., Marchand J., Odler I., "Sulfate attack on concrete", Modern Concrete Technology Series, Vol. 10, Spon Press (New-York, USA), 2002.

20. Brown P.W., "An evaluation of the sulfate resistance of cements in a controlled environment", *Cement and Concrete Research*, V. 11, 1981, pp. 719-727.

21. Cao H.T., Bucea L., Ray A., Yozghatlian S., "The effect of cement composition and pH of environment on sulfate resistance of Portland cements and blended cement", *Cement and Concrete Composites*, V. 19, 1997, pp. 161-171.

22. Marshall W.L., Slusher R., "Thermodynamics of calcium sulfate dehydrate in aqueous sodium chloride solutions, 0-110°C", The Journal of Physical Chemistry, V. 70, 1966, pp. 4015-4027.

23. Ismail M., Toumi A., François R., Gagné R., "Effect of crack opening on the local diffusion of chloride in cracked mortar samples", *Cement and Concrete Research*, V. 38, 2008, pp. 1106-1111.

12.0 ATTACHMENT 3

Saltstone Vaults 1 / 4 and Disposal Unit 2 Concrete Sample Tasks 2 & 4 – Experimental Results from Vault Concretes July 2009

Subcontract No. AC48992N Task 2 and 4

BLANK PAGE

Washington Savannah River Company

Subcontract no. AC48992N

Report
Tasks 2 & 4 – Experimental results from Vault Concretes

July 18, 2009

Prepared by:

SIMCO Technologies Inc.
203-1400 Boul. du Parc Technologique
Quebec QC G1P 4R7
Canada
(418) 656-0266 tel | (418) 656-6083 fax

LIMITED LIABILITY STATEMENT: THIS REPORT IS FOR THE EXCLUSIVE USE OF SIMCO'S CLIENT AND IS PROVIDED ON AN "AS IS" BASIS WITH NO WARRANTIES, IMPLIED OR EXPRESSED, INCLUDING, BUT NOT LIMITED TO, WARRANTIES OF MERCHANTABILITY AND FITNESS FOR A PARTICULAR PURPOSE, WITH RESPECT TO THE SERVICES PROVIDED. SIMCO ASSUMES NO LIABILITY TO ANY PARTY FOR ANY LOSS, EXPENSE OR DAMAGE OCCASIONED BY THE USE OF THIS REPORT. ONLY THE CLIENT IS AUTHORIZED TO COPY OR DISTRIBUTE THIS REPORT AND THEN ONLY IN ITS ENTIRETY. THE ANALYSIS, RESULTS AND RECOMMENDATIONS CONTAINED IN THIS REPORT REFLECT THE CONDITION OF THE SAMPLES TESTED EXCLUSIVELY, WHICH WERE MANUFACTURED FROM MATERIALS PROVIDED TO SIMCO BY THE CLIENT OR BY THIRD PARTIES. THE REPORT'S OBSERVATIONS AND TEST RESULTS ARE RELEVANT ONLY TO THE SAMPLES TESTED AND ARE BASED ON IDENTICAL TESTING CONDITIONS. FURTHERMORE, THIS REPORT IS INTENDED FOR THE USE OF INDIVIDUALS WHO ARE COMPETENT TO EVALUATE THE SIGNIFICANCE AND LIMITATIONS OF ITS CONTENT AND RECOMMENDATIONS AND WHO ACCEPT RESPONSIBILITY FOR THE APPLICATION OF THE MATERIAL IT CONTAINS.

THE STADIUM® MODEL IS A HELPFUL TOOL TO PREDICT THE FUTURE CONDITIONS OF CONCRETE MATERIALS. HOWEVER, ALL DURABILITY-MODELING PARAMETERS HAVE A STATISTICAL RANGE OF ACCEPTABLE RESULTS. THE MODELING USED IN THIS REPORT USES MEAN LABORATORY- OR FIELD-DETERMINED SINGLE VALUES AS INPUT PARAMETERS. THIS PROVIDES A SINGLE RESULT, WHICH PROVIDES A SIMPLE ANALYSIS EVALUATING CORROSION PROTECTION OPTIONS. PREVIOUS CONDITIONS ARE ASSUMED TO CARRY FORWARD IN THE PREDICTION MODEL; THERE ARE NO ASSURANCES THAT THE STRUCTURE WILL BE EXPOSED TO A SIMILAR ENVIRONMENT AS IN THE PAST.

Report update – July 2009

This report includes the latest results obtained on the Vault concrete mixtures. These results concern the porosity measurements and migration tests performed on the Vault 1/4 and Vault 2 mixtures hydrated one year in a fog room. Compressive strength measurements were also performed.

The most significant result came from the migration test performed on the Vault 2 concrete mixture. The diffusion coefficients obtained from the test result analysis showed a decrease of 67% from the coefficients estimated after 91 days of hydration. This means that the material will perform better than the long-term simulations of Task 3 indicated. These simulations were based on the test results obtained after 28 and 91 days of hydration.

Objective

This report presents the advancement of experimental Tasks 2 and 4. The objective of Task 2 is to evaluate transport properties for the mixtures used by SRNL for radioactive waste storage, while Task 4 consists in obtaining data on concrete samples exposed to aggressive solutions to validate modeled results.

The selected mixtures were:

A. Saltstone Vault 1/4 concrete with a w/b ratio of 0.38 prepared with an ASTM Type I/II cement and slag;
B. Saltstone Vault 2 concrete with a w/b ratio of 0.38 prepared with ASTM Type V cement, slag, fly ash, and silica fume.

This report is divided as follow. Section 2 presents the characteristics of raw materials. Section 3 details the formulations and the fresh properties of the mixtures. Section 4 presents the updated measurements performed on the mixtures. Finally, section 5 is concerned with the various ponding tests performed for this study.

Raw materials

This section presents the characteristics of the cements, supplementary cementing materials, aggregates, and admixtures used in the concrete mixtures.

Relative density and absorption of Foster sand and Rinker N°67 stone were determined based on CSA A23.2-6A *Relative density and absorption of fine aggregate* and CSA A23.2-12A *Relative density and absorption of coarse aggregate*, respectively.

Terminologies in previous CSA Standards have similar significances such as ASTM C127 *Standard Test Method for density, relative density (specific gravity), and absorption of coarse aggregates* and ASTM C128 *Standard Test Method for density, relative density (specific gravity), and absorption of fine aggregates*. The characteristics of aggregates are presented in Table 0-1.

Table 0-1 – Characteristics of fine and coarse aggregates

Raw materials		Absorption (%)	Relative density (SSD)	Apparent relative density
Sand	Foster	0.58	2.64	2.67
N° 67 Stone	Rinker	0.62	2.63	2.66

The relative density (specific gravity) of binders is useful to calculate mixture compositions. The data are given in Table 0-2.

Table 0-2 – Relative density of binders

	Type I/II cement	Type V cement	GGBFS	Force 10000 SF	Class F Fly Ash
	Lafarge	Lehigh	Holcim	Grace	SEFA
Relative Density	3.271	3.289	2.990	2.316	2.355

The chemical composition of binders is an input of the chemical equilibrium code in STADIUM® to estimate the composition of the hydrated cement paste. Data are given in Table 0-3. They were evaluated using the X-ray fluorescence technique.

Admixtures such as water reducers and entraining agents can affect the concrete performances and the workability of the fresh mixture. Depending on their dosage, admixtures can affect the setting of the binders, in particular the water reducing admixtures.

Table 0-3 – Chemical composition of binders (%)

Oxides	Type I/II cement	Type V cement	GGBFS	Force 10000 SF	Class F Fly Ash
	Lafarge	Lehigh	Holcim	Grace	SEFA
CaO	64.3	63.0	35.8	0.50	1.41
SiO_2	21.0	20.8	39.1	96.6	53.1
Al_2O_3	4.91	4.11	10.1	0.21	28.4
Fe_2O_3	3.50	4.32	0.36	0.18	7.99
SO_3	2.64	2.36	1.99	<0.1	<0.10
MgO	0.95	2.40	12.6	0.28	1.00
K_2O	0.37	0.57	0.27	0.50	2.99
Na_2O	0.09	0.07	0.22	0.07	0.44
LOI	1.32	1.73	0	1.21	2.39

According to ASTM C494/C494M *Standard specification for chemical admixtures for concrete*, water reducing admixtures can have a retarding effect. Type A water reducer requires that initial and final setting times are not extended by more than 1h30, compared to the same mixture prepared without the admixture. For type D water reducer, the additional setting time allowed is 3h30. The use and the dosage range of admixtures are presented in Table 0-4.

Table 0-4 – Dosage range of admixture for uses defined in ASTM C494/C494M

Admixture	use	Dosage range[1] for Type A use	for Type D use
MicroAir (BASF)	AEA[2]	-	-
Pozzolith 200N (BASF)	WR[3]	3 to 4 (195 to 260)	up to 6 (up to 390)
Polyheed 1020 (BASF)	MRWR[4]	3 to 5 (195 to 325)	-
Glenium 3030 NS (BASF)	HRWR[5]	up to 3 (up to 195)	-

(1) in fl oz / 100 lb of binder (in ml/100 kg of binder)
(2) AEA = Air Entraining Agent
(3) WR = water reducing admixture
(4) MRWR = mid-range water reducing admixture
(5) HRWR = high-range water reducing admixture

Concrete Mixtures

The mix designs of two Saltstone Vault concretes were provided by SNRL. Saltstone Vault 1/4 concrete was used to build Vault 1 in the late 1980's, while Saltstone Vault 2 concrete was designed to construct a pre-cast, reinforced, post tensioned water tank structure.

Samples of Saltstone Vault concretes were prepared based on ASTM C192/192M – 07 *Standard Practice for Making and Curing Concrete Test Specimens in the Laboratory*. Mixtures were cast in plastic cylinders (10 cm diameter, 20 cm length). Two batches of eighty liters (0.1 cubic yard) provided two sets of forty-two cylinders. Methods of consolidation and times of demolding differed between mixtures depending on the slump and on the setting time, respectively. Methods are detailed below. Once demolded, specimens were stored in moist room (100% RH) until testing.

Saltstone Vault 1/4 concrete

The Master Builders 300N reducing admixture was not available at the time of casting, so we used Pozzolith 200N, which is another BASF water reducing admixture. The air entraining admixture was BASF's MicroAir. Table 0-1 presents the properties of fresh and early age concrete for the two batches.

The Pozzolith 200N was not efficient enough to reach the specified consistency, i.e. a slump of 75 mm (3 inches). Because the amount of raw materials was limited, it was not possible to try another admixture. It was thus decided to cast this mixture. The concrete cylinders were consolidated on a vibrating table. Table 0-2 gives the final Saltstone Vault 1/4 concrete formulation prepared for this project.

Table 0-1 – Properties of fresh and early age Saltstone Vault 1/4 concrete for the two batches needed to make samples

Properties	Batch 1V2	Batch 1V3	Differences	
			actual	Allowed[1]
Slump (mm)	15	35	20	51
(in.)	5/8	1 3/8	6/8	2.0
Unit weigth (kg/m^3)	2,400	2,390	10	40
(lb/ft^3)	150	149	1	2.5
Air content (%)	2.5	3.0	0.5	0.8
Time at end of sampling (h:mm)	1:25	0:55		
f_c 7d (MPa) [2]	29.4	37.0	7.6	4.0
(psi)	4,264	5,366	1,102	574
Density at 7d (kg/m^3) [2]	2,370	2,390	20	
(lb/ft^3)	148	149	1	

([1]) based on ASTM C192/C192M
([2]) based on ASTM C39/C39M *Standard Test Method for Compressive Strength of Cylindrical Concrete Specimens*

Table 0-2 – Saltstone Vault 1/4 concrete formulation

Raw materials	Source	Formulation (kg/m^3)	(lb/yd^3)
Type I/II cement	Lafarge	255	430
GGBFS	Holcim	169	285
Sand	Foster	691	1,164
N° 67 Stone	Rinker	1,096	1,848
Water		162	273
w/b		0.38	0.38
Air content		3 %	3 %
Unit weight		2395 kg/m^3	149 lb/yd^3
Slump		35 mm	1 3/8 in.
		(ml / 100 kg of binder)	(fl oz / 100 lb of binder)
MicroAir	BASF	1.2	0.02
Pozzolith 200N	BASF	403	6.2

The differences in slump, unit weigh and air content between batches were lower than precision statement of ASTM C192/192M (Table 0-1). The difference in early strength was very high. The consolidation of samples does not seem to be the cause of the strength difference since unit weight values of specimen were in acceptable range. On the other hand, the delay before casting the samples of 1V2 batch was very long since we adjusted the water reducing admixture dosage on this batch with several iterations. For the 1V3 batch, we used

the total amount of water reducing admixture added in 1V2 batch. However, we added the full amount of admixture at the beginning of mixing and reduced time before casting samples within half an hour. The differences could affect the hardening at early time. We will check if strength development will be recovered at eighty days.

The dosage of the water reducing admixture was above the range for Type D use (Table 0-4). Concrete cylinders were too weak to be demolded without surface damage after three days. They were demolded after five days under wet burlap, and then cured in a fog room (100% relative humidity). The compressive strength at seven days was close to the required strength at twenty-eight days (i.e. 4,000 psi). The excess of water reducing admixture slowed the setting of concrete but seemingly did not affect its hardening.

The air content was lower than the specified value (i.e. 3% instead of 5%). The air entraining agent was less efficient due to poor workability of the mixture. Less air content than expected means a little more solid content in the formulation (Table 0-2). In this range, variation of entrained air content has little influence on the transport properties of concrete.

Saltstone Vault 2 concrete

The specified admixtures were not available at the time of casting. Consequently, we used admixtures for which we developed skills in the field of concretes containing supplementary cementing materials at low water to binder ratio.

Small trial batches were prepared to determine HRWRA dosage and check the air content without casting samples. As the effect of HRWRA diminished with time, we targeted higher slump value after ten minutes than required (7 ± 1 in.). The air content was high due to secondary effect of water reducing and HRWR admixtures. Table 0-3 presents the properties of fresh and early age concrete for the two batches needed to make cylindrical samples. The concrete cylinders were consolidated by rodding.

Table 0-3 – Properties of fresh and early age Saltstone Vault 2 concrete for the two batches needed to make samples

Properties	Batch 2V1	Batch 2V2	Differences	
			actual	allowed[1]
Slump (mm)	210	210	0	51
(in.)	8 ¼	8 ¼		2.0
Unit weigth (kg/m^3)	2,230	2,190	40	40
(lb/yd^3)	139.3	136.6	2.7	2.5

Air content (%)	7.4	8.5	1.1	0.8
Time at end of sampling (h:mm)	0:45	0:35		
f_c 8d (MPa)	21.0	19.2	1.8	
(psi)	3,040	2,785	261	
Density at 8d (kg/m^3)	2,260	2,230	30	
(lb/ft^3)	141	139	2	

([1]) based on ASTM C192/C192M

The differences in slump and early strength between batches were smaller than precision statement of ASTM C192/192M (Table 0-3). The precision statement of ASTM C192/192M should be used with caution for air-entrained concrete or concrete with slump over 6 in. (150 mm). The difference in air content between batches was slightly higher than standard precision statement. However, this gap was judged acceptable.

Table 0-4 gives the Saltstone Vault 2 concrete formulation. Dosage of WR was in the range for type A use. HRWR dosage was higher than type A use but in the mid-range use (3-6 fl oz / 100 lb of binder) defined by the producer. Concrete cylinders were demolded after two days under wet burlap, and then cured in a fog room (100% RH). We did not observe any important delay in concrete hardening, as observed on the previous mixture.

Table 0-4 – Saltstone Vault 2 concrete formulation

Raw materials	Source	Formulation (kg/m^3)	(lb/yd^3)
Type V cement	Lehigh	121	204
GGBFS	Holcim	162	274
Force 10000 SF	Grace	27	45
Class F Fly Ash	SEFA	95	159
Sand	Foster	548	923
N° 67 Stone	Rinker	1,111	1,873
Water		152	257
w/b		0.38	0.38
Air content		8 %	8 %
Unit weight		2110 kg/m^3	138 lb/yd^3
Slump after 10’		210 mm	8 ¼ in.
		(ml / 100 kg of binder)	(fl oz / 100 lb of binder)
MicroAir	BASF	3.1	0.05
Polyheed 1020	BASF	205	3.2
Glenium 3030 NS	BASF	232	3.6

Initial solid phases

Using the concrete formulations and the chemical composition of the cementitious materials, it is possible to estimate the mineral composition of the hydrated cement paste. The approach proposed by SIMCO Technologies assumes that the hydrated cement paste is composed of the following phases: C-S-H, portlandite, monosulfate (sulfate AFm) and C_4AH_{13} (hydroxy-AFm). The calculation is based on the total amount of calcium, silica, alumina and sulfur available to participate in the hydration process. This amount is the sum of the contribution of each component of the binder (cement, fly ash, slag …), for which a hydration degree is assumed. However, it is assumed that all SO_3 participates in the hydration process due to its high solubility.

Once the total amount of calcium, silica, alumina and sulfur is known, the various phases of the hydrated binder are calculated as follow:

- The amount of monosulfate is calculated from the SO_3 content. This removes calcium and alumina from the total amount.
- The amount of C-S-H is calculated from the silica content, if there is enough calcium left. If it's not the case, all the remaining calcium is used to form C-S-H and no portlandite and C_4AH_{13} is present.
- Depending on the amount of calcium and alumina remaining, C_4AH_{13} is formed.
- The remaining amount of calcium is used to calculate the initial portlandite content.

The initial solid phases were calculated using the binder chemical compositions and concrete formulations presented previously. The results, expressed in mass of mineral per total mass of concrete, are given in Table 0-5. Although the method is approximate and cannot reproduce the complexity of the hydration process, the results compare favorably with other methods presented in research papers[14] [15].

Table 0-5 – Initial solid phases in the concrete mixtures

Properties	Concretes	
	Vault 1/4	Vault 2
Hydration (%)		
Cement	80	80
Slag	50	60

[14] Nielsen E.P., Herfort D., Geiker M.R., Phase equilibria of hydrated Portland cement, Cement and Concrete Research 35 (2005) 109-115.
[15] Papadakis V.G., Experimental investigation and theoretical modeling of silica fume activity in concrete, Cement and Concrete Research 29 (1999) 76-86.

Fly Ash	-	30
Silica Fume	-	90
Mineral phases (g/kg)		
C-S-H	97.0	70.3
Portlandite	2.1	0.0
Monosulfate	33.1	21.5
C_4AH_{13}	13.2	0.0

Task 2 – Concrete Properties mesurements

To this date, Saltstone Vault concretes have been cured over ninety days in a fog room (100% RH). For a given mixture, the cylinders selected for testing were taken from separate batches. The mechanical properties of the mixtures were evaluated on the basis of compressive strength measurements. The following transport properties were evaluated:

- Porosity: evaluated according to the ASTM C642 standard procedure: *Standard Test Method for Density, Absorption and Voids in Hardened Concrete*,
- Diffusion coefficients: evaluated on the basis of migration test results, which is a modified version of the ASTM C1202 procedure: *Standard Test Method for Electrical Indication of Concrete's Ability to Resist Chloride Ion Penetration*,
- Water diffusivity: evaluated from the results of drying tests,
- Water storage: evaluated from small concrete disks equilibrated in boxes maintained at specific relative humidities using saturated salt solutions.

The test procedures to evaluate the diffusion coefficients, water diffusivity and water storage are described in the Task 5 report.

The following sections present the results obtained so far. All results are summarized in Table 16.

Compressive strength

Compressive strengths were tested based on ASTM C39/C39M *Standard Test Method for Compressive Strength of Cylindrical Concrete Specimens*. Two cylinders were taken from each batch. Four concrete specimens were thus tested for compressive strength. Table 0-1 presents the results of compressive strength results measured after 7, 29, 91 and 365 days of hydration on vault concretes.

Table 0-1 – Compressive strength for Saltstone Vault concretes

Properties	Saltstone Vault 1/4			Saltstone Vault 2		
	Actual average	CV (%)	Surrogate[1]	Actual Average	CV (%)	Surrogate[1]
f_c 7d (MPa) (psi)	32.1 4,656	13	42.7 6,193	20.1[2] 2,915	4.5	41.6 6,034
Density at 7d (kg/m^3) (lb/ft^3)	2,380 148	0.5	-	2,250[2] 140	0.7	-

f_c 28d (MPa) (psi)	59.8 8,673	3.8	54.0 7,832	35.2 5,105	2.8	56.7 8,224
Density at 28d (kg/m^3) (lb/ft^3)	2,390 149	0.1	-	2,250 140	1.0	-
f_c 90d (MPa) (psi)	63.3 9,181	15.8	65.3 9,471	47.2 6,846	2.8	62.1 9,007
Density at 90d (kg/m^3) (lb/ft^3)	2,400 150	0.18	-	2,240 140	0.16	-
f_c 365d (MPa) (psi)	64.4 9,340	4.5	65.7 9,529	47.0 6817	4.8	66.5 9,645
Density at 365d (kg/m^3) (lb/ft^3)	2,395 150	0.27	-	2,240 140	0.28	-

([1]) from data used in Task 1.
([2]) measured at 8 d.

The average compressive strength at twenty-eight days for Saltstone Vault 1/4 concrete was 8,673 psi, largely above the minimum strength (i.e. 4,000 psi) specified by design[16]. While compressive strengths at seven days were very different between separate batches, the results at 28 days were close enough to be considered independent of the origin of the batch as the low coefficient of variation (CV) showed.

The average compressive strength at twenty-eight days for Saltstone Vault 2 concrete was 5,105 psi, slightly above the minimum strength of 5,000 psi specified by design[1]. The dispersion of the results at twenty-eight days was low as shown by the low coefficient of variation.

Porosity measurements

The porosity measurements were performed according to the ASTM C642 standard procedure: *Standard Test Method for Density, Absorption and Voids in Hardened Concrete*. The porosity results are given in Table 0-2, Table 0-3 and Table 13. No significant changes in porosity values are measured between 29 and 91 days of hydration. Similarly, no significant changes were measured for the Vault 1/4 material after 365 days of hydration. However, a significant increase in porosity was measured on the Vault 2 mixture after 365 days of hydration, going from approximately 10% to 13%. The value of 13% is close to the porosity estimated from the desorption tests (see section 4.4). This may indicate that the measurements made at 28 and 91 days were performed on samples that were not fully saturated prior to testing. Recent measurements made by SIMCO Technologies showed that high quality mixtures may be sensitive to the initial saturation level when the ASTM C 642 procedure is performed (this is also discussed in section 4.4). Because of this, the analysis of migrations tests were performed using the porosity estimated from the desorption tests.

[16] Phifer, M. A., Millings, M. R., and Flach, G. P. 2006. Hydraulic Property Data Package for the E-Area and Z-Area Vadose Zone Soils, Cementitious Materials, and Waste Zones, WSRC-STI-2006-00198, Revision 0. Washington Savannah River Company, Aiken, SC. September 2006.

Table 0-2 – Porosity of Saltstone Vault concretes at 28 days

		Saltstone Vault 1/4	Saltstone Vault 2
Porosity at 28 days (%)	spec. 1	10.1	10.0
	spec. 2	9.9	10.7
	average	10.0	10.3
Absorption at 28 days (%)	spec. 1	4.4	4.6
	spec. 2	4.3	5.0
	average	4.4	4.8

Table 0-3 – Porosity of Saltstone Vault concretes at 90 days

		Saltstone Vault 1/4	Saltstone Vault 2
Porosity at 90 days (%)	spec. 1	10.4	10.7
	spec. 2	10.6	10.6
	average	10.5	10.6
Absorption at 90 days (%)	spec. 1	4.5	5.0
	spec. 2	4.7	5.0
	average	4.6	5.0

Table 13 – Porosity of Saltstone Vault concretes at 365 days

		Saltstone Vault 1/4	Saltstone Vault 2
Porosity at 365 days (%)	spec. 1	9.9	13.0
	spec. 2	10.1	13.1
	average	10.0	13.1
Absorption at 365 days (%)	spec. 1	4.3	6.1
	spec. 2	4.4	6.2
	average	4.4	6.2

Migration tests – Diffusion coefficients

The diffusion coefficients were evaluated on the basis of migration test, which is a modified version of the ASTM C1202 procedure: *Standard Test Method for Electrical Indication of*

Concrete's Ability to Resist Chloride Ion Penetration. The analysis of the migration test results provide the intrinsic diffusion coefficient of each ionic species, defined as:

$$D_i = \tau^s D_i^o$$

where τ^s is the intrinsic tortuosity of the material and D_i^o is the diffusion coefficient of the i^{th} species in freewater. The values in freewater can be found in textbooks[17].

The method used by SIMCO Technologies consists in accelerating the ions under an external potential and measure the electrical current across the sample over a 15-day period. The measured currents are analyzed to provide the diffusion coefficients following the method described in reference[18]. The results of the diffusion coefficient analyses are presented in Table 14.

The analysis requires the initial pore solution and the porosity of the material. The initial pore solution is strongly related to the current evolution between 0 and 100 hours of testing[5]. An algorithm in the migration test analysis module provides an estimation of the initial pore solution composition. The porosity values estimated form desorption test analyses (Table 5) were used for the analysis instead of the ASTM C642 results. As discussed later in the report, the ASTM standard procedure may have underestimated the porosity values.

The measured currents at 28, 91 and 365 days are presented in Figure 5 along with the simulation results. The measured current shown in Figure 5 exhibit a drop after 28 days, which can be caused by both a decrease in the pore solution concentration and a reduction of the transport properties as the hydration process continues in the materials. The diffusion coefficient analysis takes both factors into account. The experimental currents also show that the current values are lower for the Vault 2 concrete, which generally translates into lower diffusion coefficients.

[17] See for instance the Handbook of Chemistry and Physics from CRC Press. Values used for this study are (in E-9 m^2/s): OH-: 5.27, Na^+: 1.33, K^+: 1.96, SO_4^{2-}: 1.07, Ca^{2+}: 0.79, $Al(OH)_4^-$: 0.54, NO_3^-: 1.90, NO_2^-: 1.16.
[18] Samson E., Marchand J., Henocq P., Beausejour P., Recent advances in the determination of ionic diffusion coefficients using migration test results, Int. RILEM Symp. on Concrete Modelling – CONMOD08, 26-28 May 2008 (Delft, The Netherlands), 65-78.

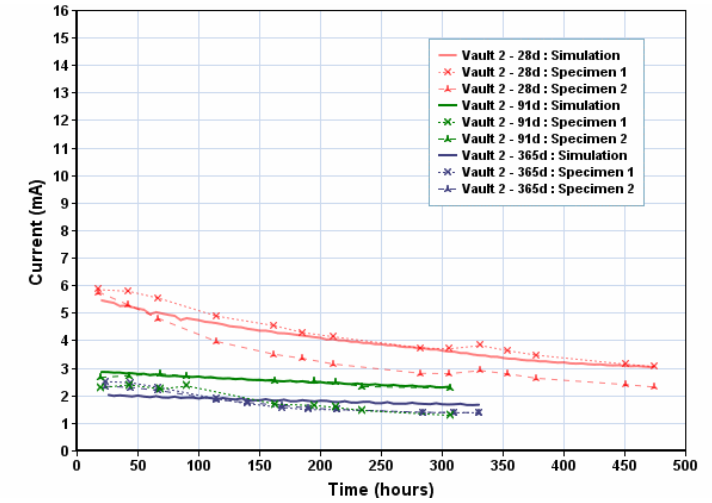

a) Vault 2 concrete

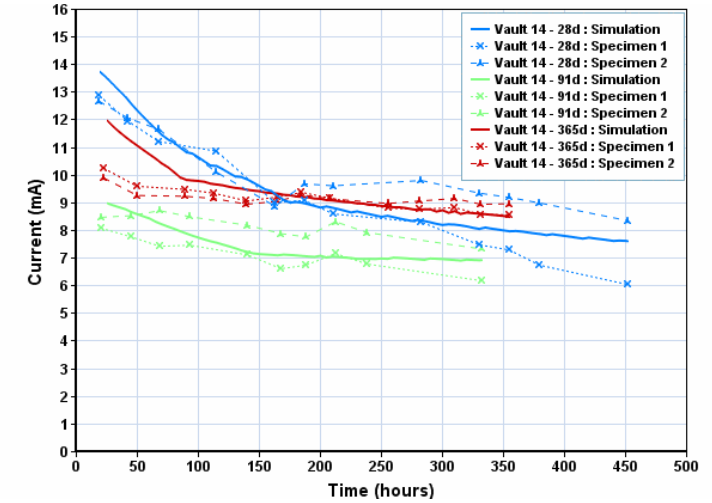

b) Vault 1/4 concrete

Figure 5 – Currents measured during the migration tests
at 28, 91 and 365 days for vault concrete mixtures

The results are given in Table 14. The Vault 1/4 results show a diffusion coefficient that is mostly constant through time. Based on tests performed on similar materials by SIMCO Technologies, this is not uncommon with slag concretes. On the other hand, the diffusion coefficients decrease with time for the Vault 2 concrete. The transport parameters drop by 14% between 28 and 91 days and by 67% between 91 and 365 days due to the hydration process. The reduction in transport properties is described in STADIUM® by the hydration function:

$$H(t) = \frac{a}{1 + (a-1)e^{-\alpha(t-t^{\text{ref}})}}$$

where t^{ref} is a reference time, in this case taken as 28 days. The parameter a represent the fraction of the diffusion coefficient at 28 days when the hydration process is completed ($t \rightarrow \infty$) and α [1/s] provides the rate of hydration. The time evolution of the diffusion coefficients is shown on Figure 6 for the Vault 2 mixture. The hydration parameters are: Vault 1/4 mixture: a=1.0, α=0.0 1/s (constant diffusion coefficients), Vault 2 mixture: a=0.30, α=0.0045 1/s.

Table 14 – Migration test results

Species	Self-diffusion (E-9 m^2/s)	Diffusion coefficients (E-11 m^2/s)					
		Saltstone Vault 1/4			Saltstone Vault 2		
		28d	91d	365d	28d	91d	365d
OH^-	5.273	3.63	3.71	3.50	1.40	1.20	0.40
Na^+	1.334	0.92	0.94	0.89	0.35	0.30	0.10
K^+	1.957	1.35	1.38	1.30	0.52	0.45	0.15
SO_4^{2-}	1.065	0.73	0.75	0.71	0.28	0.24	0.08
Ca^{2+}	0.792	0.55	0.56	0.53	0.21	0.18	0.06
$Al(OH)_4^-$	0.541	0.37	0.38	0.36	0.14	0.12	0.06
Cl^-	2.032	1.40	1.43	1.35	0.54	0.46	0.15
tortuosity		0.0069	0.0070	0.0066	0.0027	0.0023	0.00076

The evolution of the diffusion coefficients through time for the surrogate concretes tested by SIMCO Technologies and used in Task 1 are shown in Figure 7. The comparisons of surrogate and estimated D_i for this report can be considered to represent similar materials. The values are close enough and should not change the conclusions of the analysis presented in Task 1.

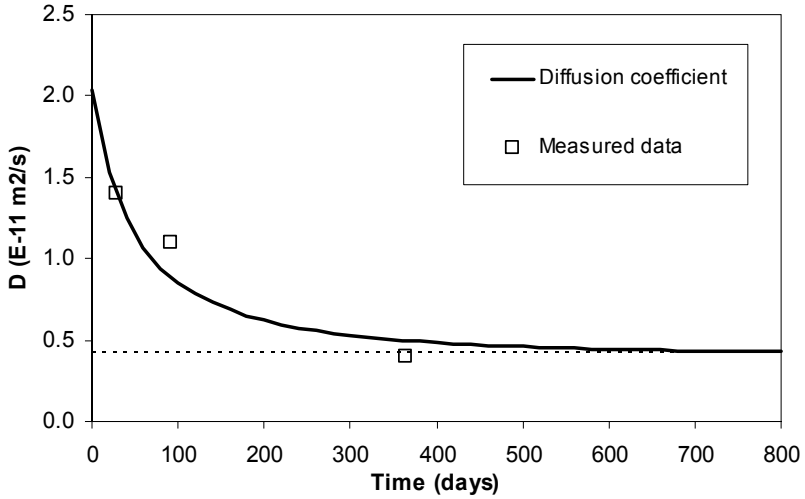

Figure 6 – Time evolution of the diffusion coefficient for the Vault 2 concrete mixture

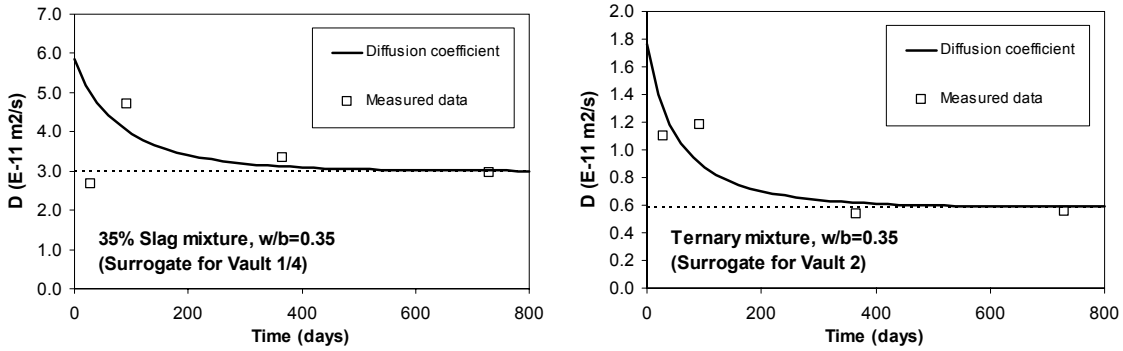

Figure 7 – Time evolution of the diffusion coefficient for the two surrogate concrete mixtures used in Task 1

It is worth mentioning that the values presented in Table 14 are high compared to most values of diffusion coefficients found in the literature (see for instance reference[19]). Published values for high performance mixtures are usually in the 10^{-13} m^2/s range. However, these are *apparent diffusion coefficients*, which hide the effect of the chemical reactions between the pore solution and the hydrated paste, and to a lesser extent the effect of the boundary conditions, within *D*. As mentioned previously, the diffusion coefficients estimated in this study are only a function of the material microstructure, which is characterized by the intrinsic tortuosity. In STADIUM®, the chemical reactions are considered in a separate module. As discussed in reference[20], the apparent diffusion coefficient is highly dependent on the test conditions from which it was evaluated. Using it to model ionic transport using other materials and boundary conditions is bound to provide erroneous durability predictions.

Moisture storage – Desorption/adsorption tests

The estimation of the permeability, discussed in the previous section, requires estimating the moisture capacity of the concrete mixtures. This material characteristic, also called desorption/adsorption isotherms, provides the water content in the material as a function of the external relative humidity. It is also used in STADIUM® to transform the relative humidity of the environment into a water content boundary condition.

Tests for desorption and adsorption isotherms were performed on thin 1-cm samples cut from cylinders after 21 days of hydration in the fog room. The samples were then immersed under water to improve hydration and saturation of the concrete.

For desorption tests, thin 28-days old samples were placed in different RH-controlled boxes: 11.3%, 33.1%, 54.4%, 75.5%, 85.1%, 91.0%, 94.6% and 97.3%. Eight disks per RH

[19] Leng F., Feng N., Lu X., An experimental study on the properties of resistance to diffusion of chloride ions of fly ash and blast furnace slag concrete, Cement and Concrete Research 30 (2000) 989-992.
[20] Marchand J., Samson E., Predicting the service-life of concrete – Limitations of simplified models, Canadian Conf. on Effective Design of Structures II, May 20-23, McMaster Univ. (Canada), 2008. To be published in a special issue of Cement and Concrete Composites.

conditions were prepared. The thin 28-days old samples for adsorption tests were first dried for two months in a 40°C chamber. Assuming that they were dry[21], they were then placed in other set of the RH-controlled boxes. The adsorption tests are still ongoing.

To determine the water content of individual samples after storage in RH-controlled box, their dry mass be known. The desorption test was thus stopped after three months for three of the eight samples. The dry mass of these samples was measured after they were kept for seven days at 105°C. Following this, the samples were immersed in water to get their saturated surface dry mass[22]. The desorption tests are still ongoing on the five remained samples per RH conditions.

The porosity determined on thin samples (Figure 8) is higher than the porosity estimated according to the ASTM C642 Standard Procedure (Tables 11 – 13), which may show the limitations of the standard method. Note 2 in the ASTM C642 Test Procedure says that: *"Hence, such pore space as may be present in the specimen that is not emptied during the* ***specified drying*** *or is not filled with water during the* ***specified immersion and boiling*** *or both is considered "impermeable" and is not differentiated from the solid portion of the specimen for the calculations, especially those for percent voids."*

"Depending on the pore size distribution and the pore entry radii of the concrete ***and on the purposes for which the test results are desired****, the* ***procedures*** *of this test method may be adequate, or they* ***may be insufficiently rigorous****. In the event that it is desired to fill more of the pores than will be filled by immersion and boiling, various techniques involving the use of vacuum treatment or increased pressures may be used. If a rigorous measure of total pore space is desired, this can only be obtained by determining absolute density by first reducing the sample to discrete particles, each of which is sufficiently small so that no impermeable pore space can exist within any of the particles."*

For the porosity estimation on the samples tested for desorption, we increased the precision to determine mass stabilization. The maximum allowable increase in mass for two successive values at intervals of 24 h was change from 0.5% (ASTM C642) to 0.01%. Reducing the thickness of the samples (from 50 to 10 mm) and increasing time of drying and immersion improved the saturation (filling more the pores) of the material. That can explain why the procedure applied for desorption tests shows higher porosity than the C642 ASTM Procedure.

The desorption results are presented in the Table 15. Figure 9 shows the relationship between water content and relative humidity after three months of desorption. Each data point is the average of three separate mass measurements.

The desorption tests at RH between 11.3 and 75.5 % are probably not yet stabilized. The desorption tests are still ongoing for five samples per RH conditions.

[21] Based on individual dry mass determined from ASTM C642 results
[22] Saturation is still ongoing. We used the saturated mass at the beginning of desorption tests to get the values presented in this report.

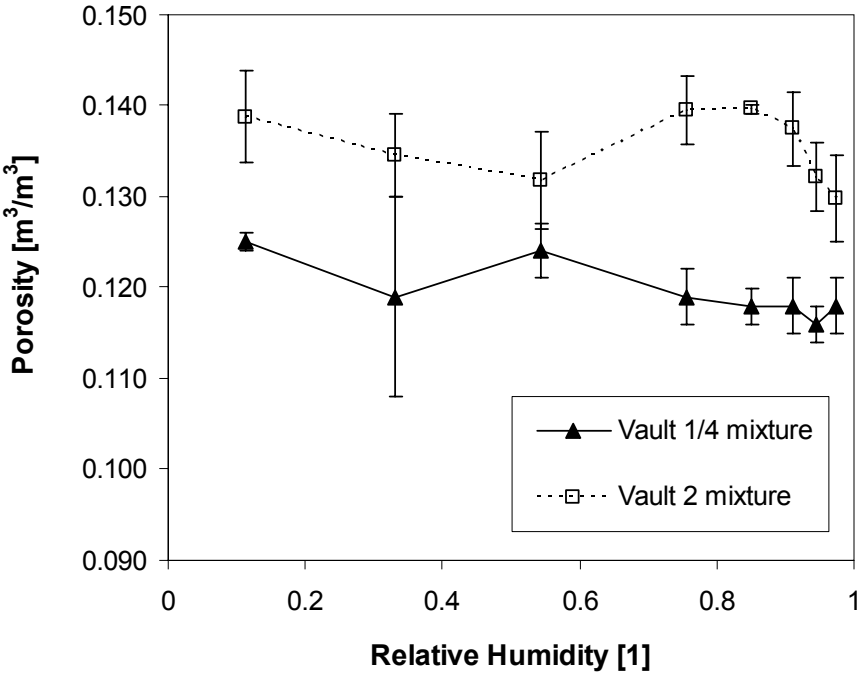

Figure 8 – Porosity for three companion samples after 3 months in RH-controlled boxes

Table 15 – Water content Desorption isotherms after 3 months in RH-controlled boxes

Salt	RH (%)	Water content (m^3/m^3 of concrete)			
		Saltstone Vault 1/4		Saltstone Vault 2	
		Average[1]	CV[1] (%)	Average[1]	CV[1] (%)
H_2O [2]	100.0	**0.120** [2]	4.6 [2]	**0.135** [2]	4.1 [2]
K_2SO_4	97.3	0.112	2.8	0.121	4.0
KNO_3	94.6	0.108	1.9	0.122	3.7
$BaCl_2.2\ H_2O$	91.0	0.108	3.2	0.125	3.9
KCl	85.1	0.106	2.2	0.122	0.2
NaCl	75.5	0.099	1.2	0.111	3.1
$Mg(NO_3)_2.6\ H_2O$	54.4	0.081	0.3	0.075	3.8
$MgCl_2.6\ H_2O$	33.1	0.051	9.1	0.038	6.3
$LiCl.H_2O$	11.3	0.031	2.2	0.021	3.1

Note 1: determined on 3 thin samples for a total concrete volume of about 250 cm^3.

Note 2: Porosity measured on 24 thin samples for a total concrete volume of about 2,000 cm^3.

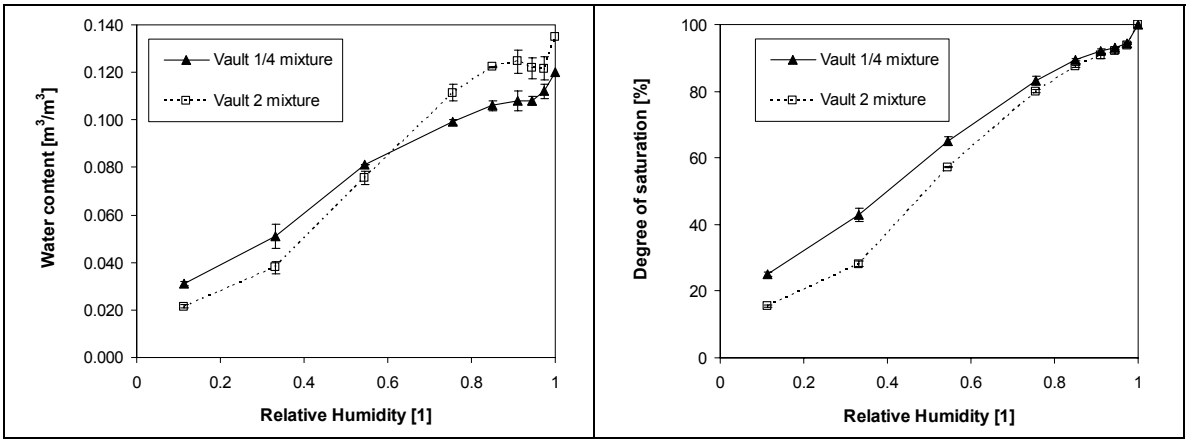

Figure 9 – Desorption isotherms after 3 months in RH-controlled boxes

Water contents obtained between 85.1 to 97.3 % RH are nearly equal (Figure 9). For Vault 2 mixture, isotherm curve decreases from 91.0 to 97.4 % RH. Using the degree of saturation (ratio of the water content over the porosity value) of individual samples to present these results corrects the slope of the isotherm curve in this range (Figure 9). This confirms that actual porosity of individual sample was affected during the test depending on the RH condition.

After 3 months of desorption, the samples in low RH-controlled boxes (at 75 % and lower) still show a reduction in mass. However, the situation is different for the high-humidity boxes. In that case, the last measurements show an increase in the mass of samples. Above 75 % RH, sample began to loose weight, reach a minimum mass and then gain in mass. Figure 10 illustrates the time line of mass measurement during desorption tests. Time to reach minimum mass is short relatively to delay between measurements. So, minimum masses were probably not precisely detected.

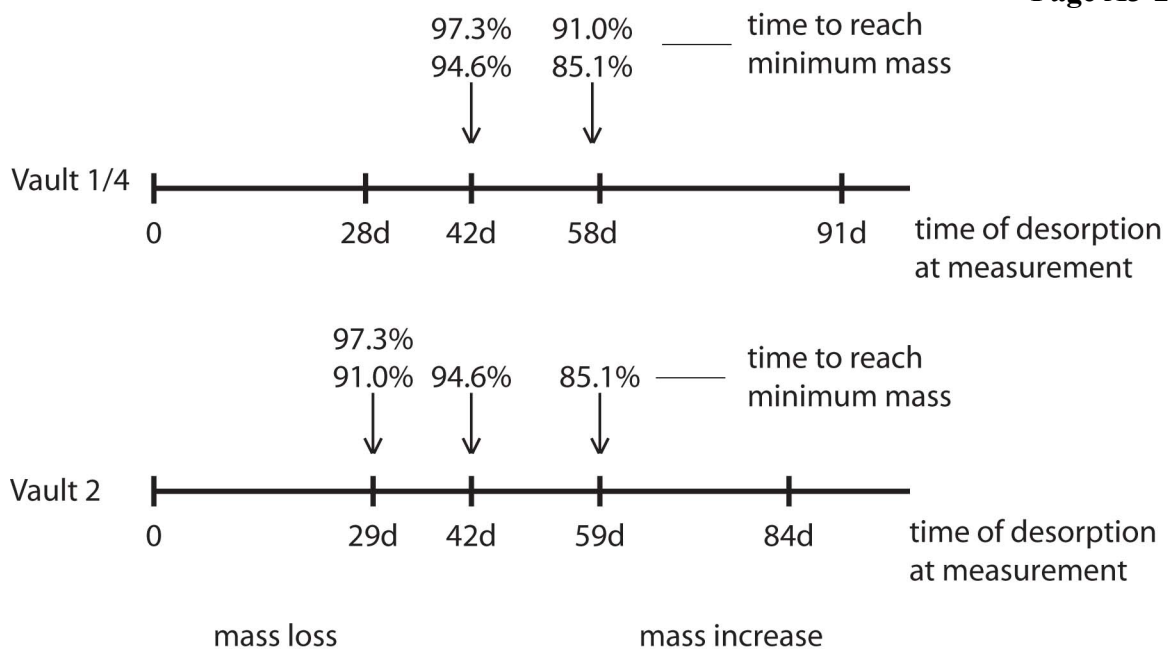

Figure 10 Time line of mass measurement – Time to reach sample minimum mass for desorption isotherms in high RH-controlled boxes

In cementitious materials, 76 % RH corresponds to the equilibrium moisture between empty capillary pores and saturated gel pores[23]. Below 76 % RH, drying begins to empty the gel pores. As water that remains in cement paste below 76 % RH is physically bound within C-S-H, no free water (water in capillaries) is still available for new reaction: hydration of remaining unhydrated Portland cement is stopped[24].

Above 76 % RH, the remaining water in capillary pores can contribute to hydration of cement and reaction of pozzolans (silica fume, fly ash, slag). New hydration products increase the density of the material by chemically and physically bounding water. Moreover, the new products can reduce the size of capillaries.

Desorption tests done above 76 % RH are thus affected by the aging of cementitious materials. Due to aging, the minimum mass obtained is overestimated and the porous volume is underestimated. Desorption tests done below 76 % RH should be less affected by the aging. Since the samples are relatively thin, the internal humidity should drop below 76 % RH rapidly and stop the hydration process.

The water content of samples after 2 month in adsorption conditions is determined assuming porosity similar to the average total water content determined on 24 thin samples for desorption test. Following the initial drying procedure at 40°C, the water content of samples was below the moisture equilibrium reached in desorption test at lowest RH (11.3 %).

[23] Baroghel-Bouny, V. 'Characterization of cement pastes and concretes – Methods, analysis, interpretations', (Laboratoire Central des Ponts et Chaussées, Paris, 1994).
[24] Neville A.M., Properties of concrete, 4th Edition, 1995

Figure 11 shows the relationship between water content and relative humidity after two months of adsorption. Each data point is the average of 5 separate mass measurements. The error bars indicate standard deviation of the five values. Figure 12 and Figure 13 show preliminary adsorption/desorption.
The mass of samples exposed to high RH is not yet stabilized. Moreover, results must be corrected by the actual porosity of each sample. So, the adsorption test results presented in this report must be considered as preliminary.

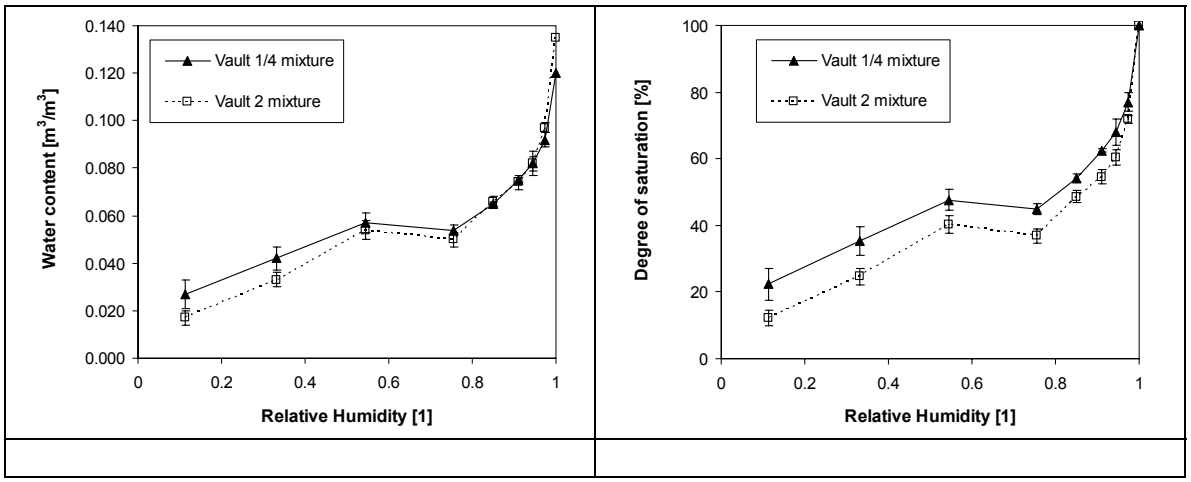

Figure 11 – Preliminary adsorption isotherms after 2 months in RH-controlled boxes

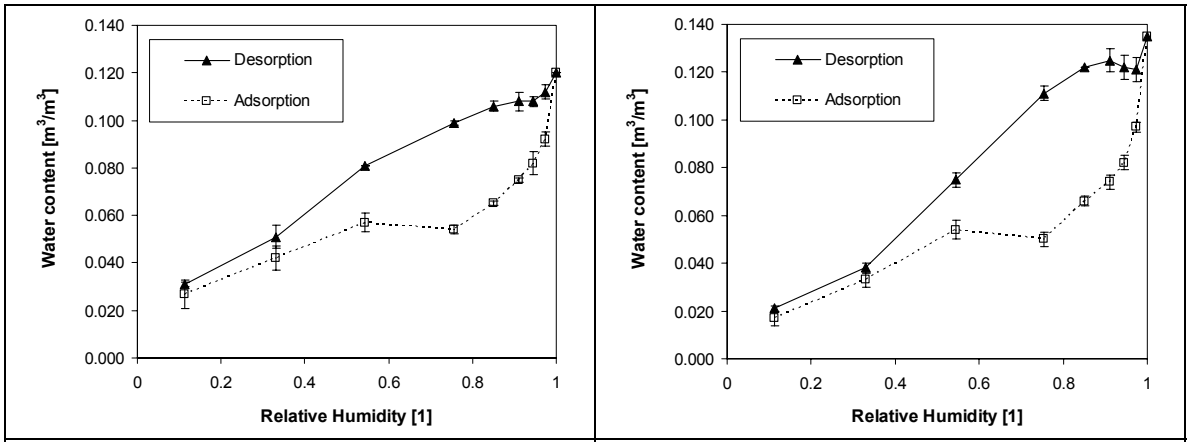

a) Vault 1/4 mixture | b) Vault 2 mixture

Figure 12 – Adsorption/desorption isotherms – preliminary results

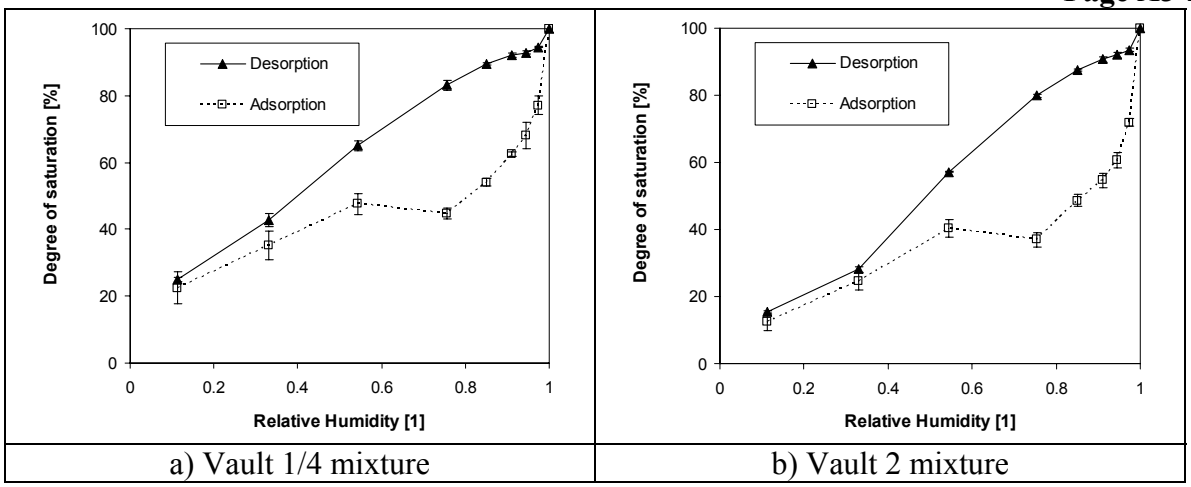

a) Vault 1/4 mixture | b) Vault 2 mixture

Figure 13 - Adsorption/desorption isotherms – preliminary results

Drying tests – Moisture diffusivity

The moisture diffusivity of the concrete mixtures is evaluated on the basis of drying tests results. The analysis of the mass loss curves provides the empirical water diffusivity $D_w = Ae^{Bw}$ based on the method described in reference[25]. It consists in adjusting *A* and *B* to reproduce the measured mass loss during the drying test. The mass loss is modeled according to Richards' model:

$$\frac{\partial w}{\partial t} - \mathrm{div}\left(Ae^{Bw}\,\mathrm{grad}(w)\right) = 0$$

where w is the volumetric water content [m^3/m^3].

The tests were started after 28 days of hydration in a fog room. The measured mass losses are presented in Figure 14 and Figure 15 along with the simulation results. The results of the water diffusivity analyses are presented in Figures 10-11 and in Table 16. For the Vault 1/4 concrete, A=0.02E-14 m^2/s and B=112, which gives D_w=1.4E-10 m^2/s at saturation ($w=\phi$). For the Vault 2 concrete, A=1.20E-14 m^2/s and B=67.6, which gives D_w=1.1E-10 m^2/s at saturation. The simulations were performed with the porosity determined on desorption samples (Table 5). The water contents (ω_∞) of the thin (1 cm) samples when their mass is stable (shown in Figure 14 and Figure 15) are close to the results of desorption at 54.4 % RH (Table 5) for the two mixtures. That confirms that the procedure used to determine porosity on desorption samples is more accurate than ASTM C642 procedure in the case of water diffusivity.

[25] Samson E., Maleki K., Marchand J., Zhang T., Determination of the water diffusivity of concrete using drying/absorption test results, Journal of ASTM Int. 5 (2008) JAI101322.

Both water diffusivity values at saturation are very similar and indicate a similar resistance to drying and water ingress. It should be noted that the fitting shown on Figure 14 and Figure 15 is adequate at most, showing the limits of the simplified Richards' approach to model moisture flow. This prompted the use of a more refined approach to assess the resistance to moisture flow of the vault concretes.

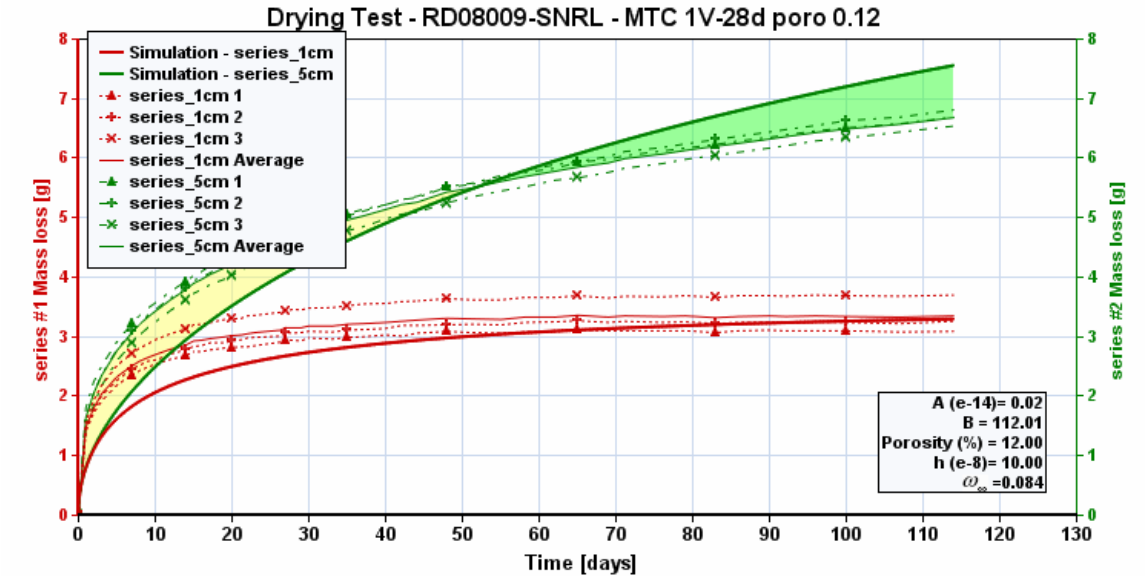

Figure 14 – Mass loss measured during the drying test for Vault 1/4 concrete

and simulation results with A=0.02E-14 m^2/s and B=112

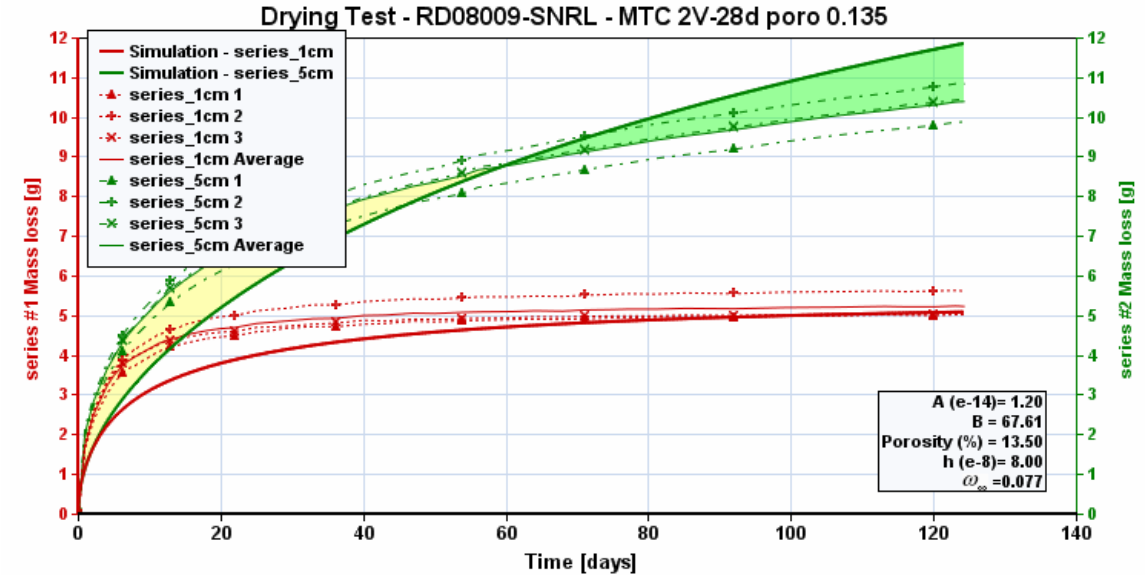

Figure 15 – Mass loss measured during the drying test for Vault 2 concrete

In the second approach, the drying test results were used to estimate the intrinsic permeability of the concrete mixtures. The mass loss profiles were reproduced using a moisture transport model that separately considers the liquid and water vapor transport. It is assumed that the liquid flow $\mathbf{v_l}$ follows Darcy's law:

$$\mathbf{v_l} = -\frac{k_l}{\mu}\,\mathrm{grad}(p_l)$$

where k_l is the permeability [m^2]. It can be portioned according to $k_l = k_r\ k_s$, where k_r is the relative permeability and k_s is the intrinsic permeability. The water vapor flow $\mathrm{v_v}$ follows the generalized Fick's law of diffusion:

$$\mathbf{v_v} = -D_v\,\mathrm{grad}\Big(\frac{\rho_v}{\rho_g}\Big)$$

where the diffusion coefficient D_v [m^2/s] can also be partitioned according to $D_v = \tau D_v^o$, where τ is the tortuosity and D_v^o is the water vapor self-diffusion coefficient. These two expressions can be combined, into a single mass conservation equation to yield:

$$\frac{\partial w}{\partial H}\frac{\partial H}{\partial t} - \mathrm{div}\Big(\underbrace{\Big[\frac{\rho_L RT}{M_w \mu}k_s S^n \frac{1}{H}}_{\text{liquid contribution}} + \underbrace{D_v^o \tau_s (1-S)^{7/3}\Big(\frac{M_w}{\rho_L RT}\Big)p_v^s\Big]}_{\text{water vapor contribution}}\mathrm{grad}(H)\Big) = 0$$

where w [m^3/m^3] is the volumetric water content, H [1] is the relative humidity, S [1] is the saturation, k_s [m^2] is the intrinsic permeability of the material, τ_s [1] is the intrinsic tortuosity (estimated from the migration tests), μ [Pa.s] is the dynamic viscosity of the liquid phase, ρ_l [Pa] is the density of the liquid phase, M_w [0.018 kg/mol] is the molar mass of water, R is the ideal gas constant [8.3143 J/mol/°K], T is the temperature [°K], D_v^o [m^2/s] is the water vapor self-diffusion coefficient and p_v^s [Pa] is the saturation vapor pressure. The term $\partial w/\partial H$ is estimated from the desorption results obtained in section 4.4.

The intrinsic permeability is the only unknown parameter in the model. Similar to the previous approach based on Richards' mass conservation equation, the model is used to reproduce the drying tests by adjusting the intrinsic permeability.

The results are shown on Figure 16 and Figure 17 and show a better fit with the measured mass losses. The estimated intrinsic permeabilities are 5E-22 m^2 for Vault 1/4 concrete and 18E-22 m^2 for Vault 2 concrete. While the difference between the two values seems important, it should be noted that the permeability can vary by several order of magnitude between good concretes and poor quality concretes. For instance, measurements performed by SIMCO Technologies using the same methodology gave 3E-21 m^2 for an ordinary Portland cement concrete made at a w/c ratio of 0.5 and 140E-21 m^2 for a poor quality mixture made at a 0.75 w/c ratio.

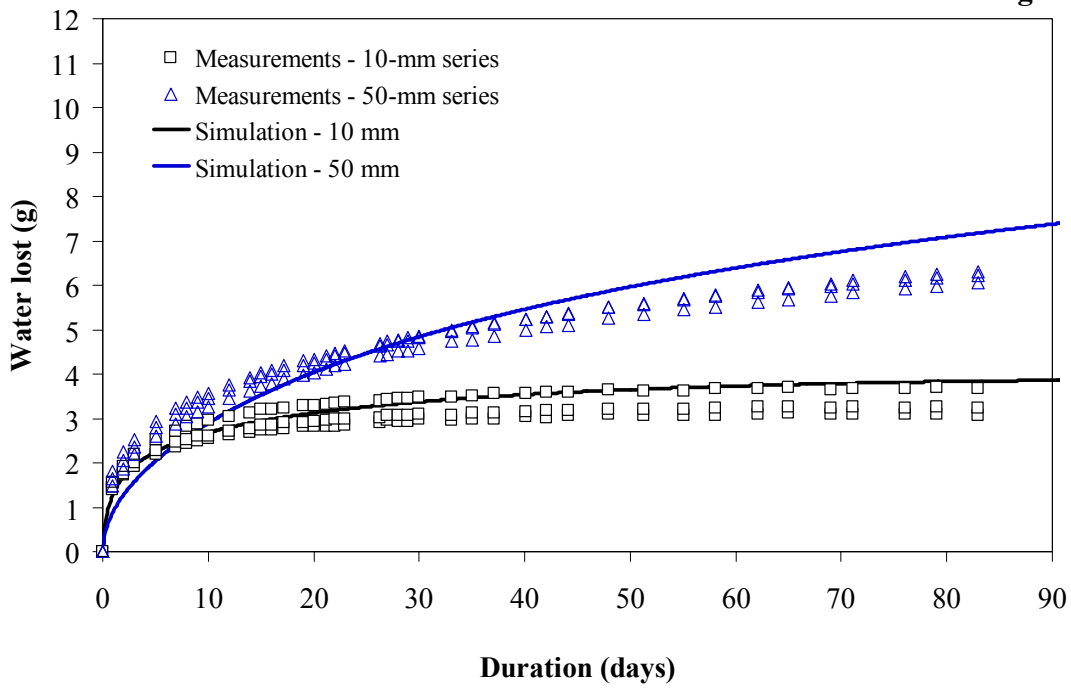

Figure 16 – Mass loss measured during the drying test for Vault 1/4 concrete and simulation results with k_s=5E-22 m^2

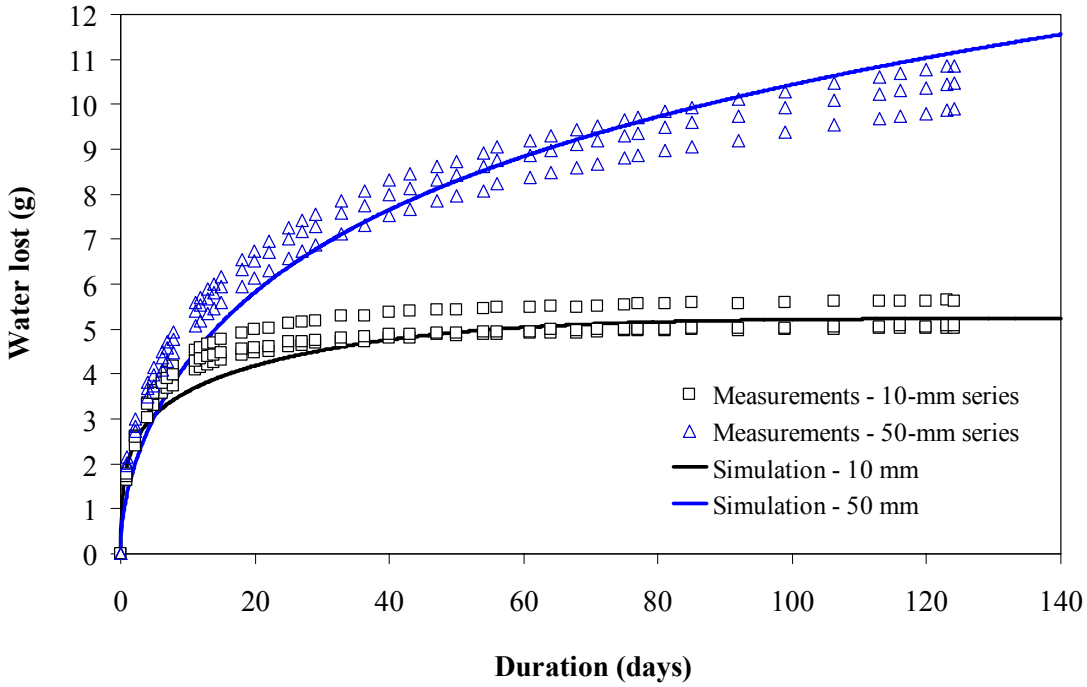

Figure 17 – Mass loss measured during the drying test for Vault 2 concrete and simulation results with k_s=18E-22 m^2

Properties summary

Table summarizes all the transport properties measured so far on the vault concrete mixtures.

Table 16 – Transport properties for Saltstone Vault concretes

Properties	Units	Concrete mixtures	
		Vault 1/4	Vault 2
Water/binder ratio		0.38	0.38
Cement type	(-)	I/II	V
Cement	(kg/m^3)	255	121
Mineral admixture	(kg/m^3)		
GGBFS		169	162
Fly ash (F)			95
Silica fume			27
Water	(kg/m^3)	162	152
Fine aggregate	(kg/m^3)	691	548
Coarse aggregate	(kg/m^3)	1096	1111
Compressive strength	(MPa)		
7d		32.1	20.1
28d		59.8	35.2
91d		63.3	47.2
365d		64.4	47.0
Porosity (ASTM C642)	(% vol.)		
28d		10.0	10.3
91d		10.5	10.6
365d		10.0	13.1
Porosity (from desorption tests)	(% vol.)	12.0	13.5
OH- diffusion coef.	(E-11 m^2/s)		
28d		3.63	1.40
91d		3.71	1.20
365d		3.50	0.40
Tortuosity	(-)		
28d		0.0069	0.0027
91d		0.0070	0.0023
365d		0.0066	0.00076
Water diffusivity (28d)			
A	(E-14 m^2/s)	0.02	1.2
B	(-)	112.0	67.6
Permeability	(E-22 m^2)	5.0	18.0

Task 4 – Immersion (ponding) test

This test series consists of immersing concrete specimens in a salt solution and evaluating the ions profiles after a certain exposure time. The experimental results - the concentration in cementitious material of acid soluble ionic species versus penetration depth provides information to validate the transport properties measured on the concrete.

Vault concretes were exposed to a NaCl reference solution in addition to exposure solutions similar to saltstone pore solution. Immersion test in chloride solution allows validating the hydration parameters of concretes used in the model since chloride can easily be tracked in cementitious materials. However, the chemical element of interest in saltstone pore solution exposure cases is sulfate.

Immersion in NaCl reference solution

After 56 days of curing, specimens for ponding tests were prepared following the procedure detailed in the Task 5 report. For each Vault concrete mixture, two specimens were immersed in 20 liters of 0.5 N NaCl solution. The solution was renewed on a regular basis to maintain pH under 10.5. The ionic penetration was determined after 90 days of exposure. Two samples were pulled out of the testing solution and were analyzed for chloride content. This was achieved by dry-milling the samples from the exposed surface over 2 mm depth increments. The powder collected over each depth was dissolved in acid and analyzed for chloride. The procedure is similar to the ASTM 1152 test method.

The results are shown in Figure 18 and Figure 19. The chloride penetration is weak for both materials, which corresponds to the low diffusion coefficients estimated with the migration tests. The Vault 2 concrete shows a slightly weaker chloride ingress rate, which follows the diffusion coefficient results. The materials exhibit very different chloride binding capacity. Near the exposure surface, the total amount of chloride almost reaches 6 g/kg for the Vault 1/4 concrete while it barely goes over 3 g/kg for the Vault 2 material. One of the reasons for this discrepancy is the presence of more SO_3 in the Vault 1/4 binder, which yields more monosulfates in the hydrated paste. Chloride binds with the paste by exchanging SO_4^{2-} with the monosulfate to form a chloride-AFm phase called Friedel's salt, according to:

$$\text{Monosulfate} + 2Cl^- \leftrightarrow \text{Friedel's salt} + SO_4^{2-}$$

Accordingly, more monosulfate translates into more chloride binding. Also, the presence of C_4AH_{13} in the hydrated paste of the 1/4 concrete contributes to increase the chloride binding capacity. Upon chloride penetration, C_4AH_{13} dissolves and additional monosulfate is precipitated from the SO_4^{2-} in the pore solution. This additional amount of monosulfate then exchanges chloride to form Friedel's salt.

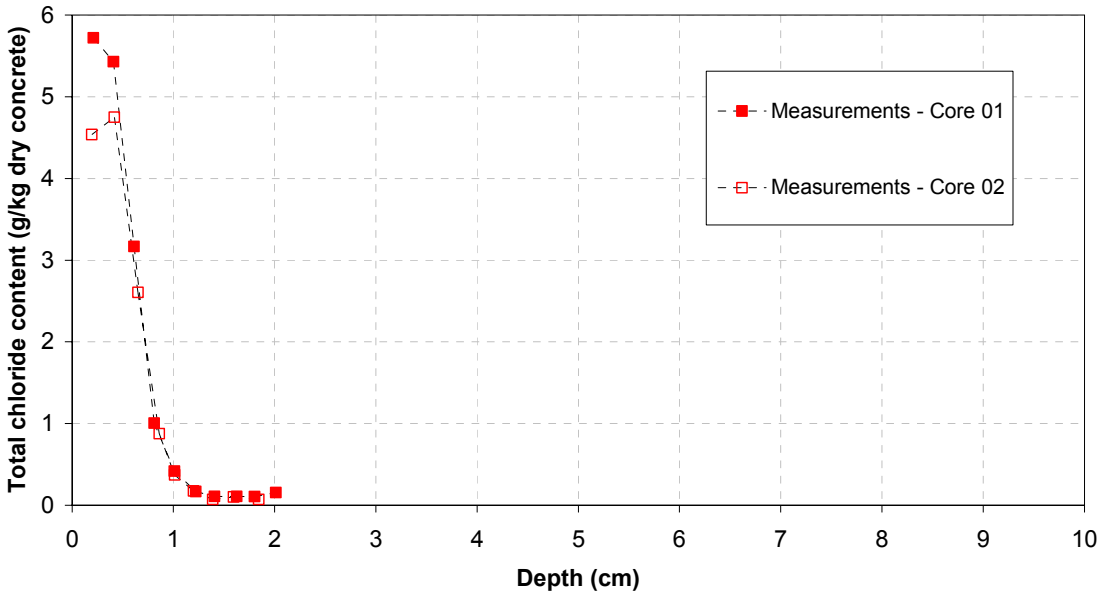

Figure 18 – Chloride profiles after 90 days of immersion in 0.5 N NaCl solution for Vault 1/4 concrete

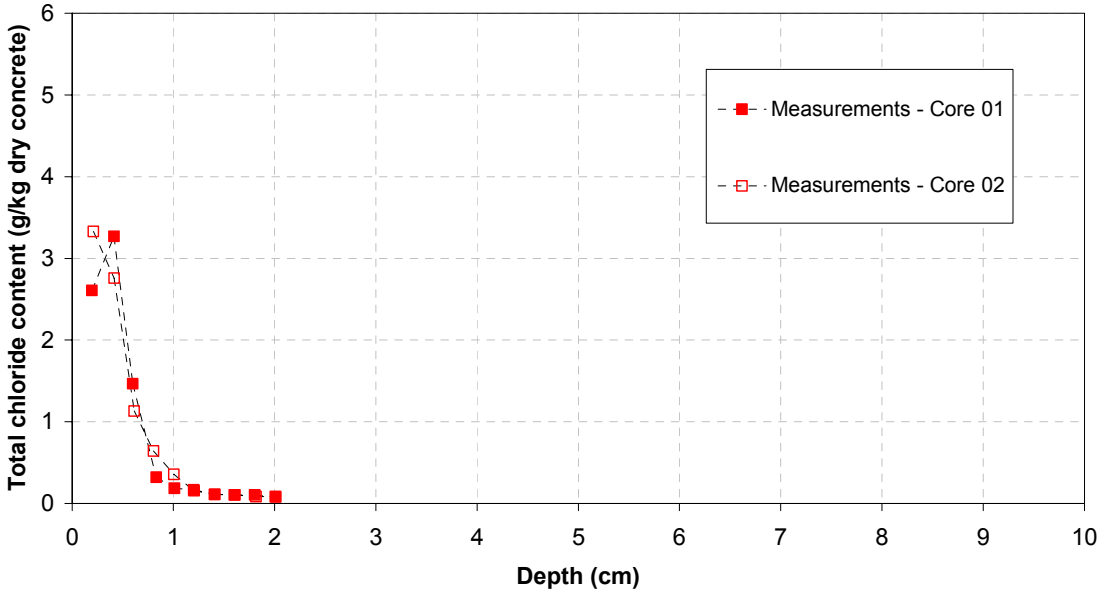

Figure 19 - Chloride profiles after 90 days of immersion in 0.5 N NaCl solution for Vault 2 concrete

Immersion in a solution similar to saltstone pore solution

The composition (make up chemicals per L of DI water) of undiluted exposure solution for immersion tests (CASE 1) is presented in Table 0-1.

Table 0-1 – Chemicals content for undiluted saltstone-like exposure solution

Chemicals	M.M.	(mmol/L of DI water)	(g/L of DI water)
NaOH	39.99734	959.31	38.37
$NaNO_3$	84.9949	3306.19	281.01
$NaNO_2$	68.9955	934.67	64.49
Na_2CO_3	105.9889	16.66	1.77
Na_2SO_4	142.0426	260.25	36.97
$Al_3(NO_3)_3$ ($9H_2O$)	429.09522	0.04	0.02
Na_3PO_4 ($12H_2O$)	388.124721	1.58	0.6

The exposure solution for cases 2 and 3 of immersion tests consist of the previous solution diluted in lime water at rate of 10:1 and 100:1, respectively. Lime water was obtained by dissolving 1.5 g $Ca(OH)_2$ in 1 kg of DI water. For a 1 liter volume of CASE 2 exposure solution, a volume of 100 mL of undiluted solution was mixed with 900 mL of lime water. For a 1 liter volume of CASE 3 exposure solution, a volume of 10 mL of undiluted solution was mixed with 990 mL of lime water.

For modeling purposes, the concentrations must be expressed on a L of solution basis. We obtain these values by dividing the contents per L of DI water (Table 0-1) by the volume of solution obtained from this mixture, given by following equation:

$$V_s = \frac{M_{salts} + M_w}{\delta_s}$$

with V_s = volume of solution obtained from Table 15 with 1 L of DI water (L)
δ_s = density of solution (g/L)
M_{salts} = Mass of all the salts in 1 L of DI water (g), Table 15
M_w = Mass of 1 L of DI water (g).

The density of the salt solution prepared from Table 0-1 is 1232.2 kg/m^3. The chemical compositions (make up chemicals per L of solution) of exposure solutions for immersion tests are presented in Table .

After 56 days of curing, specimens for ponding tests were prepared following the procedure detailed in the Task 5 report. For each Vault concrete mixture, eight specimens were immersed in 30 liters of solution for each exposure solution. These solutions were not renewed during the exposure period. The sulfur penetration was determined after 90 days of exposure. Two samples were pulled out of the testing solution and were analyzed for sulfur content. This was achieved by dry-milling the samples from the exposed surface over 2 mm depth increments. The powder collected over each depth was dissolved in acid and analyzed

for sulfate. The procedure is similar to the ASTM 1152 test method. Other samples will be tested after longer exposure durations.

Table 18 – Chemical composition of exposure solutions (mmol/L of solution)

Chemicals	CASE 1 undiluted	CASE 2 1:10	CASE 3 1:100
OH^-	832	119.7	40.9
Na^+	4995	499.5	5.0
Ca^{2+}	0	18.2	20.0
SO_4^{2-}	226	22.6	0.2
NO_3^-	2868	286.8	2.9
NO_2^-	811	81.1	0.8
CO_3^{2-}	14	1.4	0.0
AlO_2	0	0.0	0.0
PO_4^{3-}	1	0.1	0.0

The results are presented in Figure 20 and Figure 21. For both materials, all measurements gave mostly flat sulfur profiles, whatever the type of exposure solutions. In some cases, there seems to be a trend downward, especially for the Vault 1/4 material. But the slope of the profiles is so weak that it could be attributed to the experimental error. Simple calculations show that the measured sulfur content roughly corresponds to the total sulfur content found in the SO_3 of the unhydrated binder materials: 1.7 $g/kg_{concrete}$ for the Vault 1/4 concrete and 1.1 $g/kg_{concrete}$ for the Vault 2 concrete (see Table 0-3 for the chemical composition of the binders).

The absence of any indication of sulfate ingress is not surprising for CASE 3 since the exposure solution contains a very weak sulfate concentration, but could have been expected for the other cases. It most probably has to do with the low transport properties of the concrete mixtures, coupled with the fact that sulfate has a very low self-diffusion coefficient. It is also possible that the low transport properties have limited the chemical reactions involving sulfate in a very narrow region near the exposure surface. In that case, the method used to measure the sulfur content may be to imprecise to catch these fine details. Longer exposure periods may provide more indication on the sulfate ingress rate.

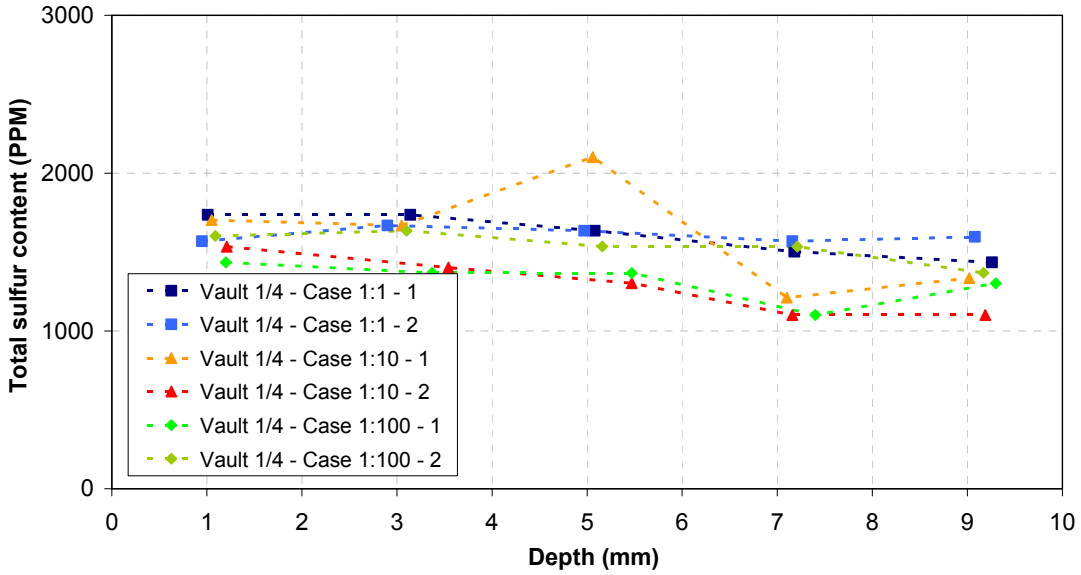

Figure 20 - Sulfate profiles after 92 days of immersion in salt solution for Vault 1/4 concrete

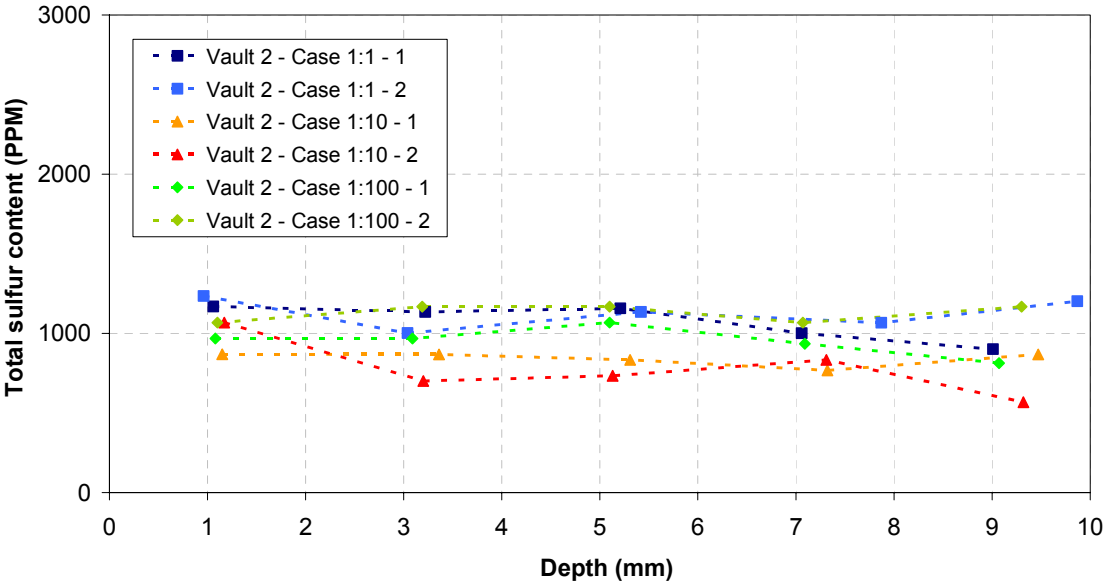

Figure 21 - Sulfate profiles after 92 days of immersion in salt solution for Vault 1/4 concrete

Ponding experiment simulations

The model STADIUM® was used to simulate the ponding experiments using the transport properties estimated in Task 2 (see the summary in Table 16). The porosities estimated on the basis of the desorption tests were used for the calculations. The simulations were performed with the following set of ionic species: OH^-, Na^+, K^+, SO_4^{2-}, Ca^{2+}, $Al(OH)_4^-$, Cl^-, $H_2SiO_4^{2-}$, CO_3^{2-}, NO_3^- and NO_2^-. The presence of Al-oxide and PO_4^{3-} in the exposure solution was not considered in the calculations, since their concentration is very low. The initial solid phases present in the material were described in section 3.3 of this report. The basic set is: C-S-H, portlandite, monosulfate and C_4AH_{13}. The equilibrium of C-S-H is modeled according to Berner's approach[26] (Figure 22), where C-S-H is assumed to be formed by a mixture of portlandite and CaH_2SiO_4, and where the Ksp of portlandite depends on the C/S ratio of the phase.

Upon contaminant ingress, interactions with the pore solution species can lead to the formation or dissolution of other phases. The minerals considered for the simulation are summarized in Table 19. For the saltstone leachate cases, the presence of sulfate can lead to the formation of ettringite and gypsum while the presence of CO_3^{2-} in solution can potentially lead to the precipitation of calcite, monocarboaluminate and thaumasite. These minerals were considered in the simulations.

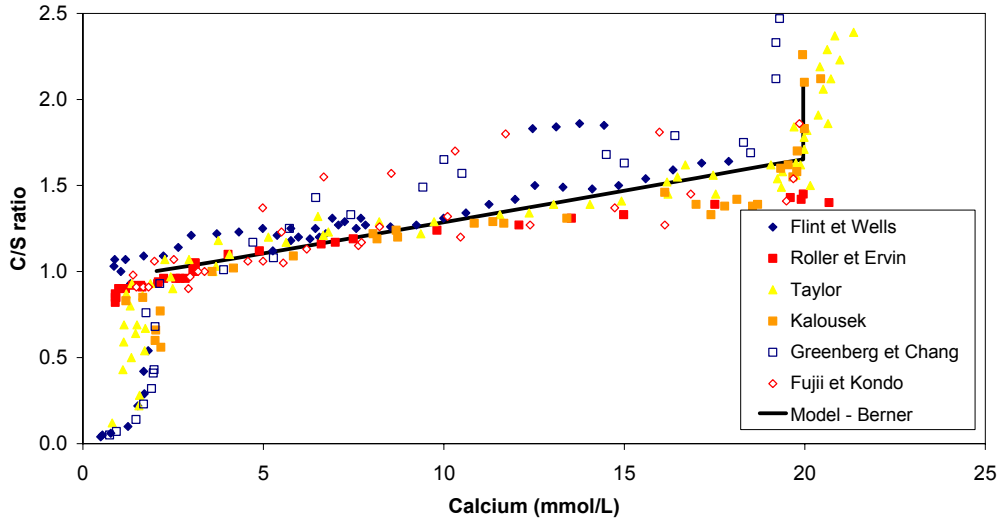

Figure 22 – C/S vs. calcium relationship for C-S-H

[26] Berner U.R., Evolution of pore water chemistry during degradation of cement in a radioactive waste repository environment, Waste Management 12 (1992) 201-219.

Table 19 – Mineral phases considered in the simulations

Minerals	Composition	log(K_{sp}) @ 25°C
Portlandite[†]	$Ca(OH)_2$	-5.15 if C/S > 1.65 f(C/S) if 1≤ C/S ≤ 1.65
C-S-H [†]	CaH_2SiO_4	-8.16
Monosulfates	$3CaO.Al_2O_3.CaSO_4.12H_2O$	-29.4
Ettringite	$3CaO.Al_2O_3.3CaSO_4.26H_2O$	-44.0
Friedel's salt[*]	$3CaO.Al_2O_3.CaCl_2.12H_2O$	2.5
Hydroxy-AFm	$4CaO.Al_2O_3.13H_2O$	-25.4
Gypsum	$CaSO_4.2H_2O$	-4.58
Thaumasite	$2CaO.2SiO_2.2CaSO_4.2CaCO_3.26H_2O$	-44.7
Calcite	$CaCO_3$	-8.48
Monocarboaluminate	$3CaO.Al_2O_3.\ CaCO_3.11H_2O$	-31.47

[†] C-S-H → 0.65 $Ca(OH)_2$ + CaH_2SiO_4
[*] Ionic exchange mechanism: Monosulfate + $2Cl^-$ ↔ Friedel's salt + SO_4^{2-}

The simulation results for the chloride ingress cases are shown on Figure 23 and Figure 24. In both cases, the model correctly reproduces the binding of chloride with the paste by matching the chloride contents measured near the exposed surfaces. For both materials, the model predictions are slightly behind the measured chloride profiles, which may be caused by an underestimation of the transport properties. Chloride profiles after one year of exposure to NaCl will provide additional data to support the transport parameter estimations.

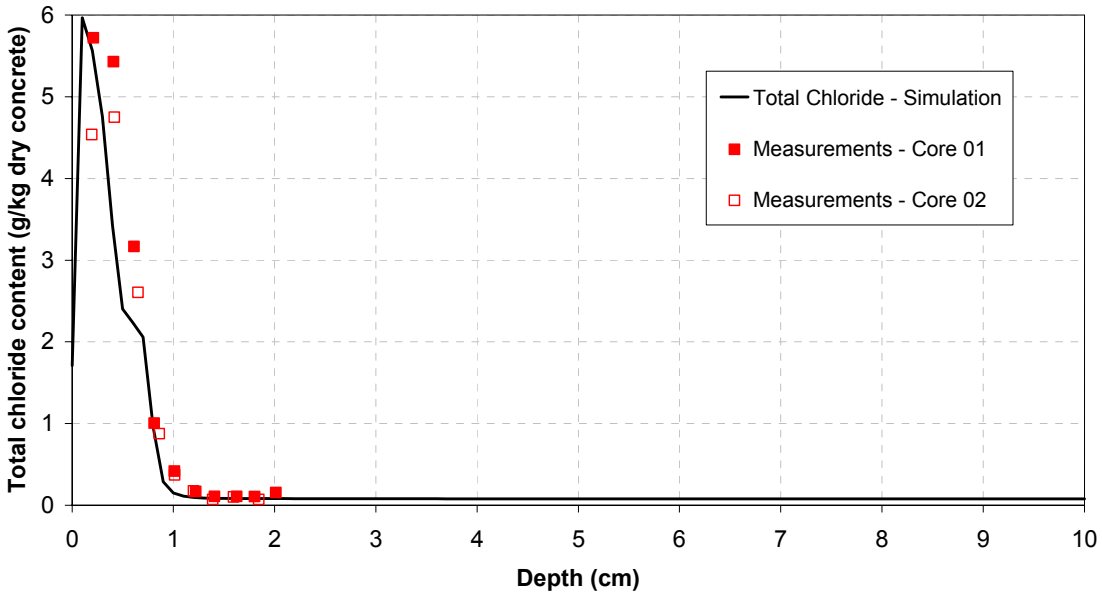

Figure 23 – Chloride ponding simulation of the Vault 1/4 concrete after 90 days of exposure to NaCl

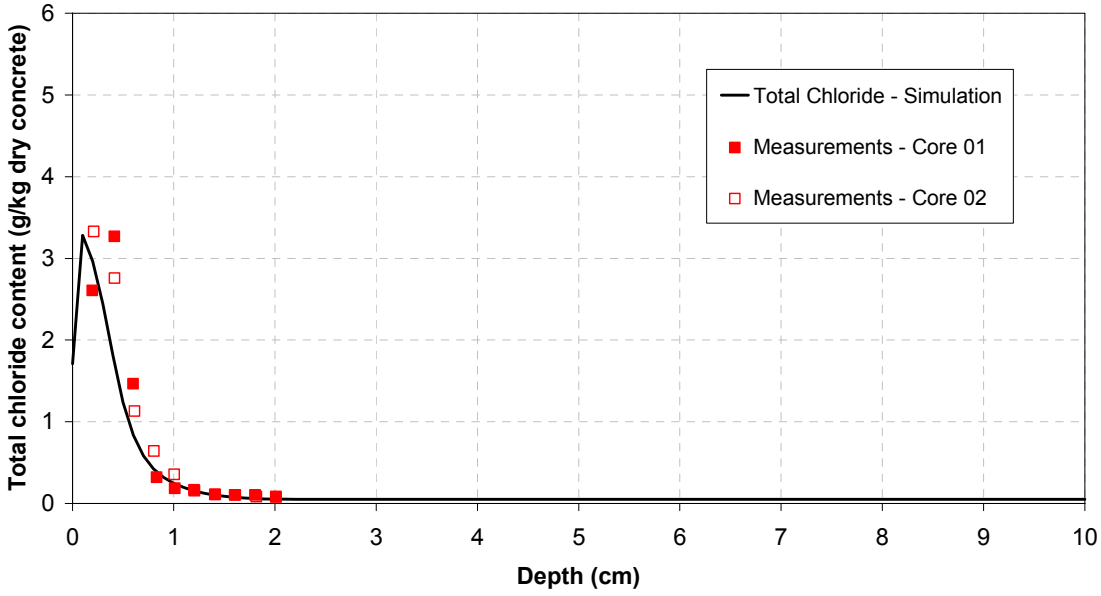

Figure 24 – Chloride ponding simulation of the Vault 2 concrete after 90 days of exposure to NaCl

The simulation results with the saltstone-leachate exposure conditions are presented in the following paragraphs. The analysis starts with the Vault 1/4 simulation results. The simulated mineral distribution for the Vault 1/4 concrete exposed to the 1:1 (Case 1) solution is showed on Figure 25. The numerical results show that upon contact with this solution, hydroxy-AFm

dissolves and is replaced by monosulfate. Near the exposed surface, the presence of sulfate and carbonate lead to the precipitation of ettringite, monocarboaluminate and calcite. The formation of these phases is accompanied by the dissolution of AFm. The model does not predict the formation of gypsum and thaumasite. However, the loss of CaH_2SiO_4 near the surface may indicate the formation of thaumasite in the earliest stage of the ponding test. Due to the high pH of the contact solution, no significant dissolution of portlandite is observed.

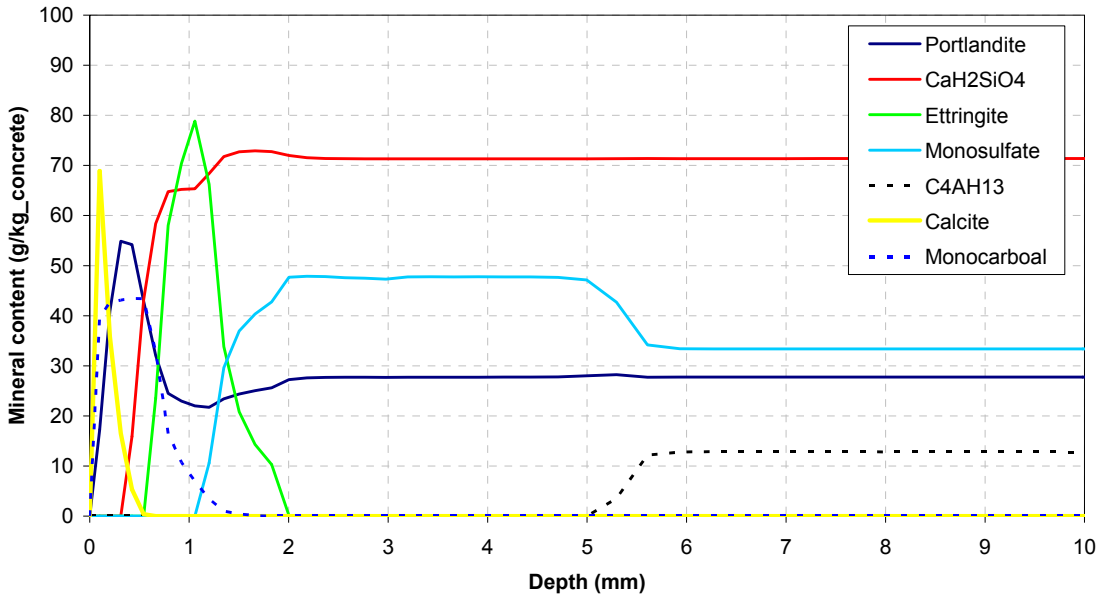

Figure 25 – Simulated mineral phase distribution for the Vault 1/4 concrete exposed 91 days to the 1:1 (Case 1) solution

The solid phase distribution for the 1:10 (Case 2) contact solution is presented on Figure 26. Compared to the previous case, the ettringite peak is not as deep but it reaches a higher content value. Also, the model predicts the formation of a small thaumasite peak near the surface. The combination of these two factors indicates that this case may be more detrimental to the material over a long period of time even if the sulfate concentration in the contact solution is lower because it could potentially lead to more cracking in the hydrated cement paste. Finally, only trace amounts of carbonate phase are formed due to the weak concentration of CO_3^{2-} in the contact solution.

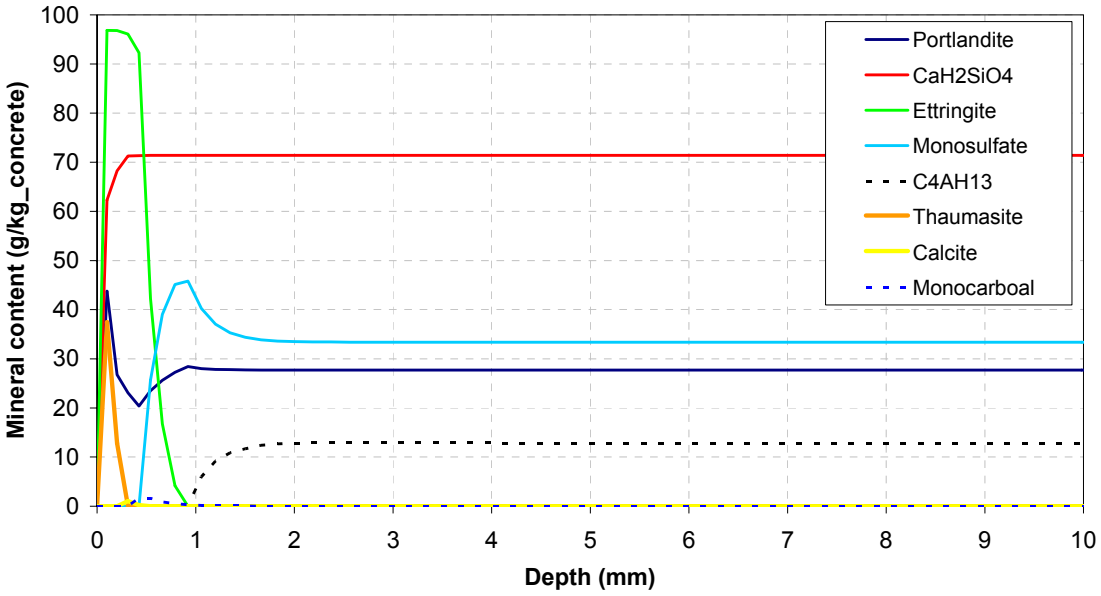

Figure 26 – Simulated mineral phase distribution for the Vault 1/4 concrete exposed 91 days to the 1:10 (Case 2) solution

The last case corresponds to the 1:100 contact solution. The results are shown on Figure 27. The simulations indicate only minor modification to the solid phase distribution in the paste, as a portion of the hydroxy-AFm is replaced by monosulfate. According to the model, the sulfate concentration in the contact solution is too weak to yield ettringite formation in the material. Also, since the contact solution is around pH 12.5, there is no dissolution of portlandite and decalcification of C-S-H.

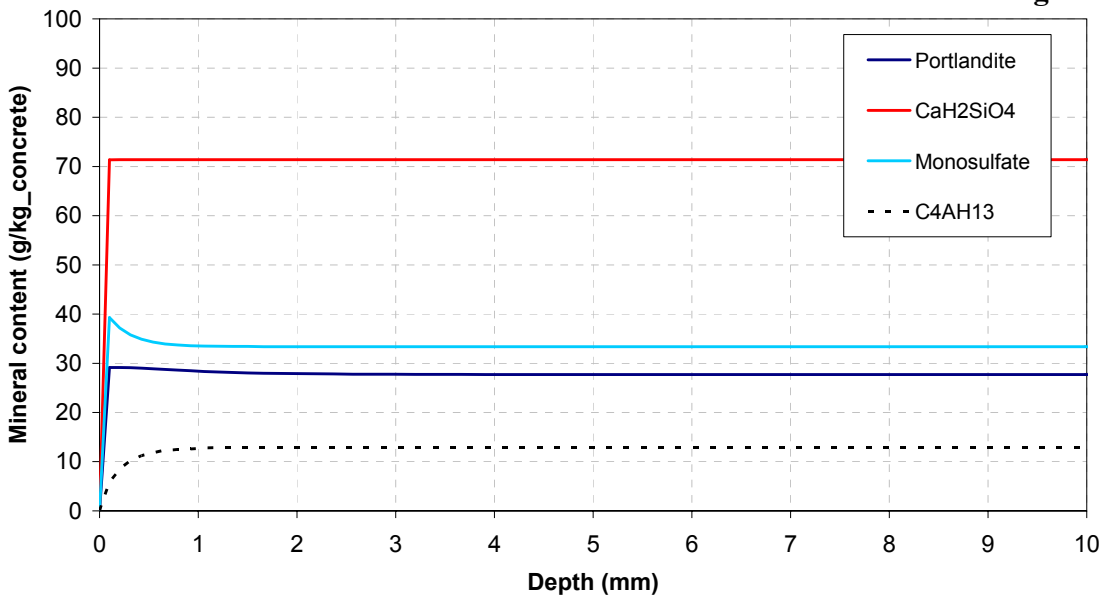

Figure 27 – Simulated mineral phase distribution for the Vault 1/4 concrete exposed 91 days to the 1:100 (Case 3) solution

These results are compared to the experimental sulfur profiles on Figure 28. The numerical sulfur content was obtained by adding the contribution of all minerals containing this element. The overall sulfur level is correctly reproduced by the model. However, the model predicts an increase in the level of sulfur between the surface and 6 mm for the Case 1 exposure and this was not observed experimentally. This increase in sulfur content is directly linked to the transformation of C_4AH_{13} into monosulfate. It is possible that the amount of C_4AH_{13} estimated from the chemical composition of the cement and slag is too important. Lowering the initial amount of this phase would decrease this sulfur level observed between 2 and 6 mm on the numerical simulations. For cases 1 and 2 (1:1 and 1:10 contacting solutions), the peak of ettringite near the surface translates into an increase of sulfur covering the first depth increment. Again this is not observed experimentally. As mentioned previously, it is possible that the sulfur peak is too narrow and the measurement method cannot catch its presence. A longer exposure period could validate the presence of this sulfur peak.

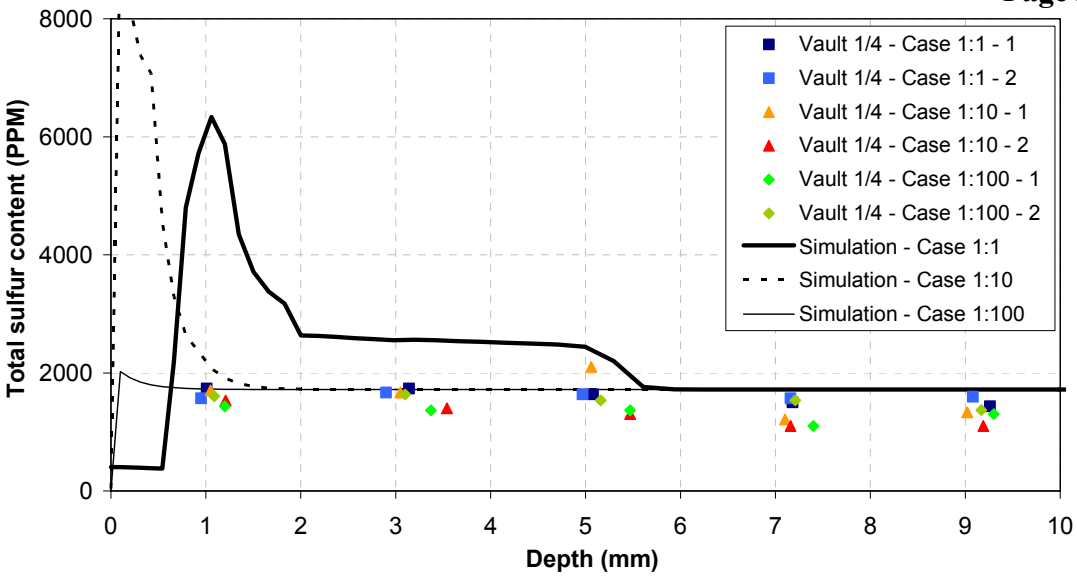

Figure 28 – Comparison of the simulated and measured sulfur profiles for the Vault 1/4 concrete

Globally, the same observations can be made on the simulation results for the Vault 2 concrete, as shown on Figure 29 and Figure 30. The main difference between the two materials is related to the absence of hydroxy-AFm in Vault 2 concrete. The increase of the monosulfate content due to the dissolution of C_4AH_{13} is thus not observed. This yield a better fit with the measured sulfur profiles, as shown on Figure 31. But again, the sulfur peak corresponding to ettringite close to the exposure surface predicted by the model is not observed experimentally.

The comparison between the measurements and the simulations emphasize the difficulty of quantifying fine modifications to the microstructure of cementitious materials. The layer-by-layer technique is well adapted to chloride since it penetrates rapidly and reacts extensively with the paste. This leads to profiles that are easily measured, even for high performance materials. In the case of sulfur, the contrast is not as important and this makes the observation more difficult. Preparing hydrated pastes with the same water to binder ratio and with the same cement and admixtures could be a way to resolve this. Removing the aggregates would

allow using more precise technique such as XRD and microprobe, which would make the quantification of microstructure alterations easier.

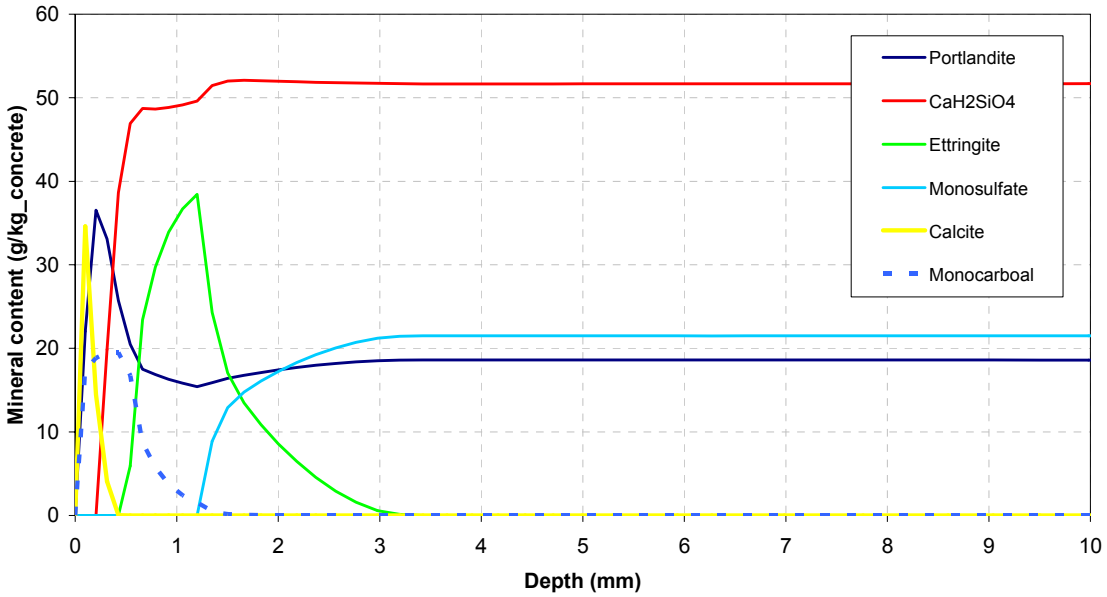

Figure 29 – Simulated mineral phase distribution for the Vault 2 concrete exposed 91 days to the 1:1 (Case 1) solution

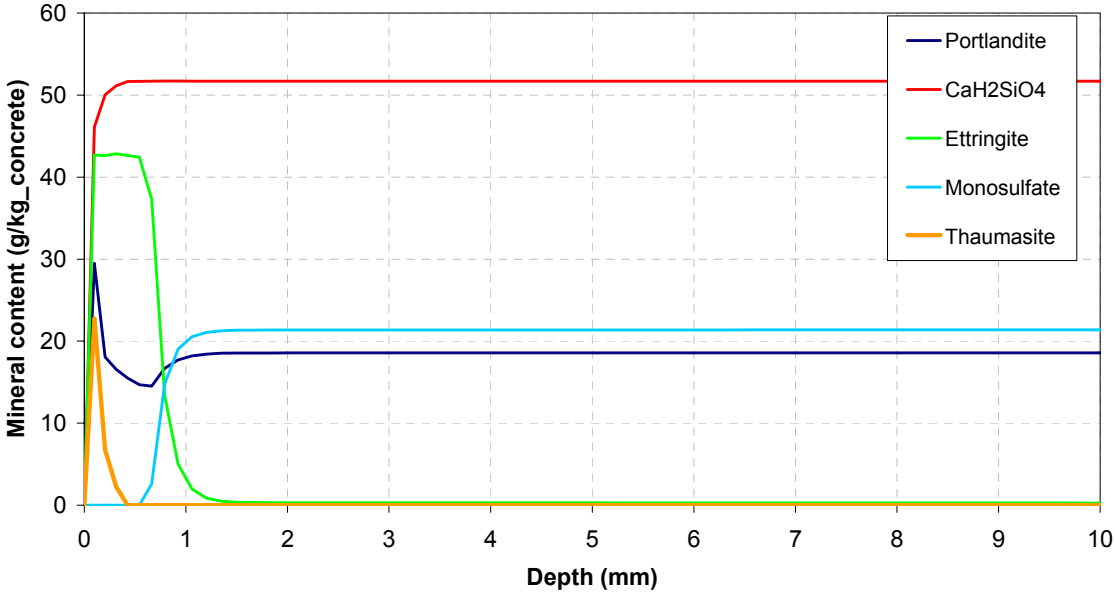

Figure 30 – Simulated mineral phase distribution for the Vault 2 concrete exposed 91 days to the 1:10 (Case 2) solution

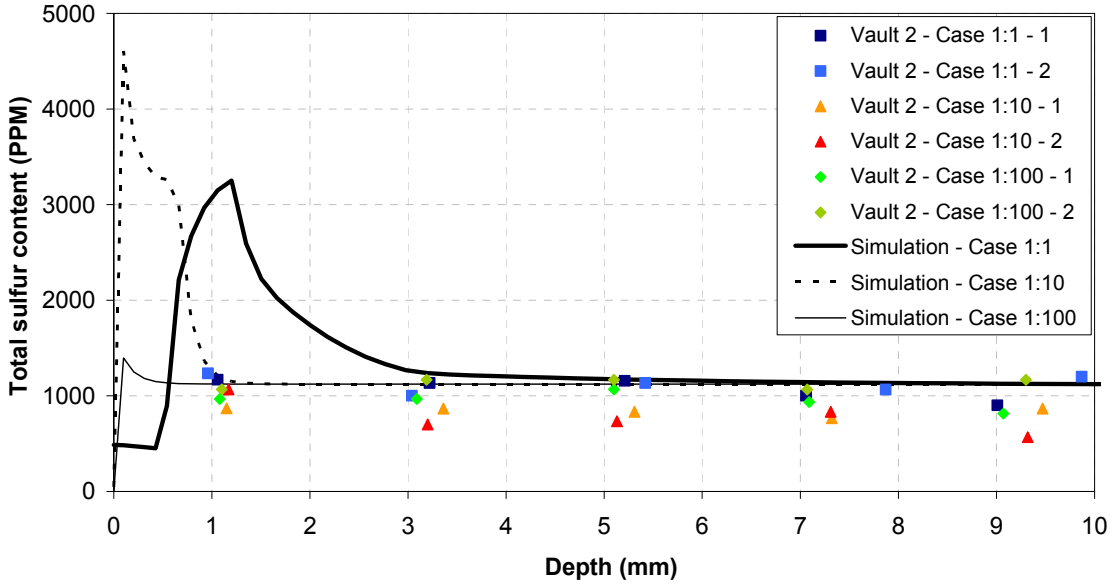

Figure 31 – Comparison of the simulated and measured sulfur profiles for the Vault 2 concrete

Appendix A – Samples

Table 20 – Use of cylinders for Vault 1/4 concrete

Batch 2		Batch 3	
1V 201	Imm 56d	1V 301	fc 7d
1V 202		1V 302	iso 28d
1V 203		1V 303	fc 90d
1V 204		1V 304	fc 90d
1V 205		1V 305	Imm 56d
1V 206		1V 306	
1V 207		1V 307	fc 90d
1V 208		1V 308	
1V 209		1V 309	
1V 210		1V 310	Imm 56d
1V 211	poro-mig 28d	1V 311	iso 28d
1V 212		1V 312	iso 28d
1V 213	fc 7d	1V 313	iso 28d
1V 214		1V 314	
1V 215	poro-mig 90d	1V 315	
1V 216	Imm 56d	1V 316	Imm 56d
1V 217	Imm NaCl	1V 317	
1V 218	fc 7d	1V 318	
1V 219		1V 319	
1V 220		1V 320	dry 28d
1V 221	iso 28d	1V 321	iso 28d
1V 222	iso 28d	1V 322	
1V 223	Imm 56d	1V 323	fc 28d
1V 224		1V 324	
1V 225		1V 325	Imm 56d
1V 226		1V 326	
1V 227		1V 327	
1V 228		1V 328	
1V 229		1V 329	
1V 230		1V 330	iso 28d
1V 231	Imm 56d	1V 331	Imm 56d
1V 232	fc 28d	1V 332	fc 28d
1V 233	Imm 56d	1V 333	
1V 234	Imm 56d	1V 334	
1V 235	iso 28d	1V 335	
1V 236	dry 28d	1V 336	
1V 237	iso 28d	1V 337	
1V 238		1V 338	
1V 239		1V 339	
1V 240	iso 28d	1V 340	Imm 56d
1V 241	fc 28d	1V 341	poro-mig 90d
1V 242	iso 28d	1V 342	poro-mig 28d
1V 243		1V 343	
1V 244		1V 344	

Table 21 – Use of cylinders for Vault 2 concrete

Batch 1		Batch 2	
2V 101		2V 201	
2V 102		2V 202	
2V 103		2V 203	
2V 104		2V 204	
2V 105		2V 205	
2V 106	lmm 56d	2V 206	
2V 107		2V 207	
2V 108		2V 208	
2V 109	iso 28d	2V 209	
2V 110		2V 210	
2V 111		2V 211	
2V 112	lmm 56d	2V 212	fc 90d
2V 113		2V 213	
2V 114	lmm NaCl	2V 214	
2V 115	iso 28d	2V 215	
2V 116		2V 216	iso 28d
2V 117	iso 28d	2V 217	
2V 118		2V 218	
2V 119		2V 219	
2V 120		2V 220	
2V 121	iso 28d	2V 221	lmm 56d
2V 122	lmm 56d	2V 222	
2V 123	iso 28d	2V 223	
2V 124		2V 224	iso 28d
2V 125		2V 225	
2V 126	fc 8d	2V 226	
2V 127		2V 227	
2V 128		2V 228	lmm 56d
2V 129		2V 229	dry 28d
2V 130	dry 28d	2V 230	lmm 56d
2V 131	lmm 56d	2V 231	lmm 56d
2V 132		2V 232	iso 28d
2V 133		2V 233	fc 90d
2V 134		2V 234	
2V 135		2V 235	
2V 136		2V 236	lmm 56d
2V 137	fc 8d	2V 237	iso 28d
2V 138	fc 28d	2V 238	poro-mig 28d
2V 139	fc 28d	2V 239	fc 28d
2V 140	lmm 56d	2V 240	iso 28d
2V 141	lmm 56d	2V 241	lmm 56d
2V 142	poro-mig 28d	2V 242	fc 28d
2V 143	iso 28d	2V 243	iso 28d
2V 144		2V 244	fc 8d

DISTRIBUTION:

A. B. Barnes, 999-W
H. H. Burns, 999-W
T. W. Coffield, 705-1C
A. D. Cozzi, 999-A
M. E. Dehnam, Jr., 773-42A
K. L. Dixon, 773-42A
G. P. Flach, 773-42A
J. C. Griffin, 773-A
E. K. Hansen, 999-W
J. R. Harbour, 999-W
C. C. Herman, 999-W
M. H. Layton, 705-1C
J. E. Marra, 773-A
S. L. Marra, 773-A
M. A. Phifer, 773-42A
T. C. Robinson, 705-1C
L. B. Romanowski, 705-1C
K. H. Rosenberger, 705-1C
R. R. Seitz, 773-43A
E. L. Wilhite, 773-43A